ISSN: 2707-1146
e-ISSN: 2709-4189

Nature & Science

International Scientific Journal

THE REPUBLIC OF AZERBAIJAN

NATURE & SCIENCE

International Online Scientific Journal

Volume: 6 Issue: 8

Baku

2024

The journal is included in the register of Press editions of the Ministry of Justice of the Republic of Azerbaijan on 04.07.2019.
Registration No. 4243

International Indices

ISSN: 2707-1146
e-ISSN: 2709-4189
DOI: 10.36719

Editorial address
AZ1073, Baku,
Matbuat Avenue, 529,
"Azerbaijan" Publishing House,
6-th floor

Tel.: +994 50 209 59 68
+994 99 805 67 68
+994 99 808 67 68
+994 12 510 63 99

e-mail:
nature.science2000@aem.az

CHEMISTRY

Prof. Dr. Vagif ABBASOV, Y. H. Mamedaliyev's Institute of Petrochemical Processes of the MSERA / Azerbaijan
Prof. Dr. Nazim MURADOV, University of Central Florida / USA
Prof. Dr. Georgi DUKA, Moldovan Academy of Sciences / Moldova
Prof. Dr. Vagif FARZALIYEV, Institute of Chemistry of Additives named after M. Guliyev of the MSERA / Azerbaijan
Prof. Dr. Dunya BABANLI, Azerbaijan State Oil and Industry University / Azerbaijan
Prof. Dr. Shahana HUSEYNOVA, Technical University of Berlin / Germany
Assoc. Prof. Dr. Mahiyaddin MEHDIYEV, Mingachevir State University / Azerbaijan
Assoc. Prof. Dr. Fizza MAMMADOVA, Institute of Natural Research, Nakhchivan Branch of the MSERA / Azerbaijan
Assoc. Prof. Dr. Bilal BUSHRA, Muhammad Ali Jinnah University / Pakistan

PHYSICS AND ASTRONOMY

Prof. Dr. Hamzaagha ORUJOV, Baku State University / Azerbaijan
Prof. Dr. Yalchin AFANDIYEV, The University of Texas at Austin / USA
Prof. Dr. Eldar VALIYEV, National Technical University / Ukraine
Ph. D. Adalet ATAYI, Shamakhi Astrophysics Observatory named after Nasiraddin Tusi of the MSERA / Azerbaijan

BIOLOGICAL SCIENCES AND AGRARIAN SCIENCES

Prof. Dr. Irada HUSEYNOVA, Institute of Molecular Biology and Biotechnology of MSERA / Azerbaijan
Prof. Dr. Ibrahim JAFAROV, Scientific Research Institute of Plant Protection and Technical Plants of the MARA / Azerbaijan
Prof. Dr. Mehmet KARATASH, Nejmettin Erbakan University / Turkey
Prof. Dr. Shaig IBRAHIMOV, Institute of Zoology of MSERA / Azerbaijan
Prof. Dr. Alovsat GULIYEV, Institute of Soil Science and Agro Chemistry of MSERA / Azerbaijan
Prof. Dr. Elshad GURBANOV, Baku State University / Azerbaijan
Prof. Dr. Panah MURADOV, Institute of Microbiology of MSERA / Azerbaijan
Prof. Dr. Ilham SHAHMURADOV, Institute of Botany of MSERA / Azerbaijan
Prof. Dr. Ulduz HASHIMOVA, Institute of Physiology of MSERA / Azerbaijan
Prof. Dr. Sayyara IBADULLAYEVA, Institute of Botany of MSERA / Azerbaijan
Prof. Dr. Rajes KUMAR, Ministry of Textile / India
Prof. Dr. Duygu KILICH, Amasya University / Turkey
Prof. Dr. Dashgin GANBAROV, Nakhchivan State University / Azerbaijan
Assoc. Prof. Aladdin EYVAZOV, Institute of Zoology of MSERA / Azerbaijan
Assoc. Prof. Akif AGHBABALI, Baku State University / Azerbaijan
Assoc. Prof. Abulfaz TAGHIYEV, Baku State University / Azerbaijan
Assoc. Prof. Dr. Mahir HAJIYEV, Cattle-breeding Scientific Research Institute of the MARA / Azerbaijan
Assoc. Prof. Mahir MAHARRAMOV, Nakhchivan State University / Azerbaijan
Assoc. Prof. Tarana AKBARI, Azerbaijan State Pedagogical University, Shamakhi / Azerbaijan
Assoc. Prof. Dr. Arif HUSEYNOV, Azerbaijan State Agricultural University / Azerbaijan
Assoc. Prof. Dr. Sevda TAHIRLI, Baku State University / Azerbaijan
Assoc. Prof. Azarchin MURADOV, Ilisu State Nature Reserve / Azerbaijan
Assoc. Prof. Dr. Aytakin AKHUNDOVA, Baku Slavic University / Azerbaijan
Dr. Svetlana GORNOVSKAYA, Beloserkovsk National Agrarian University / Ukraine
Dr. Fuad RZAYEV, Institute of Zoology of MSERA / Azerbaijan

EARTH SCIENCES AND GEOGRAPHY

Prof. Dr. Elkhan NURIYEV, Baku State University / Azerbaijan
Prof. Dr. Salih SHAHIN, Gazi University / Turkey
Prof. Dr. Mehmet UNLU, Marmara University / Turkey
Prof. Dr. Shakar MAMMADOVA, Baku State University / Azerbaijan
Assoc. Prof. Dr. Anvar ALIYEV, Institute of Geography named after academician Hasan Aliyev of MSERA / Azerbaijan
Assoc. Prof. Dr. Ramiz AHLIMANOV, Baku State University / Azerbaijan

ISSN: 2707-1146
e-ISSN: 2709-4189

MEDICINE AND PHARMACEUTICAL SCIENCES

https://doi.org/10.36719/2707-1146/47/5-9

Gulnar Bandalizada
Scientific Research Institute of Medical Prevention
named after V. Y. Akhundov
gulnarbendelizade@gmail.com
Gulnara Aliyeva
Scientific Research Institute of Medical Prevention
named after V. Y. Akhundov
gulnarealiyeva555@gmail.com
Yegana Abbasova
Scientific Research Institute of Medical Prevention
named after V. Y. Akhundov
yegane.bagirova@inbox.ru
Solmaz Aghayeva
Scientific Research Institute of Medical Prevention
named after V. Y. Akhundov
solmazagayeva645@gmail.com
Sakina Bakhshiyeva
Scientific Research Institute of Medical Prevention
named after V. Y. Akhundov
sekinebaxsiyeva001@gmail.com

Basic Principles of its Diagnosis and Prevention of Ascaridosis in the Modern Era

Abstract

Human helminthiasis is one of the urgent problems of medical science and practical healthcare. More than 90 % of parasitic diseases in humans are caused by helminthiasis. Among helminths, soil-transmitted helminths are of particular importance due to their widespread distribution and the role they play in human pathologies.

Ascaris lumbricoides is the most widespread helminth among soil-transmitted helminths. Ascariasis is widespread in all countries, as well as in Azerbaijan, according to the WHO, about 15 % of the world's population is infected with it. WHO has prepared a program for the control and prevention of soil-transmitted helminths for 2016-2020, taking into account the negative impact of this ascariasis on human pathology, especially in children and their widespread distribution not only in developing countries, but also in developed European regions. One of the main goals of this program is to eliminate ascariasis among schoolchildren in the European region by 2020.

The Republic of Azerbaijan is one of the regions where soil-transmitted helminths is widespread. Many scientific-research works on various aspects of ascariasis have been carried out at the Scientific-Research Institute of Medical Parasitology and Tropical Medicine in Azerbaijan.

Ascariasis infection causes nervous system and cognitive impairment, mental and physical weakness and growth retardation in children. In adults, in most cases, irritability, reduced work capacity, and sleep disturbances occur.

Even if children and adults do not have any clinical symptoms, ascariasis causes weight loss and some infectious diseases (dysentery, typhoid fever, etc.). Ascariasis leads to complications of pregnancy and other pathological changes. Mechanical or parenchymal jaundice can be observed in 65 % of patients with ascariasis. Therefore, it is very important to study the current situation of the and to implement effective prevention and control measures against it.

Keywords: *helminthoses, soil-transmitted helminths, ascariasis, larvae, prevention*

ISSN: 2707-1146
e-ISSN: 2709-4189

Introduction

Human helminthiasis is one of the urgent problems of medical science and practical healthcare. More than 90 % of parasitic diseases in humans are caused by helminthiasis.

Among helminths, soil-transmitted helminths are of particular importance due to their widespread distribution and the role they play in human pathologies. More than a quarter of the world's population is infected with soil-transmitted helminths. Humans are infected with soil-transmitted helminths mainly through external environmental factors (contaminated water, soil, vegetation, etc.).

Soil-transmitted helminths are found in developing countries with low sanitary-hygienic conditions in most countries of the world. On the other hand, since the development of the causative agent of soil-transmitted helminths is related to the external environment, they are mostly found in countries with tropical and subtropical climates.

Ascaris lumbricoides is the most widespread helminth among soil-transmitted helminths. Ascariasis is a widespread helminth in all countries, as well as in Azerbaijan. According to WHO, about 15 % of the world's population is infected with this helminth. Taking into account the negative impact of ascariasis on human pathology, especially in children, it has prepared a program for 2016-2020 on the control and prevention of soil-transmitted helminths in the countries of the European region. One of the main goals of this program is to eliminate ascariasis among schoolchildren in the European region by 2020 (VOZ, 2016-2020).

The Republic of Azerbaijan is one of the regions where soil-transmitted helminths is widespread. The study of these helminthoses on a scientific basis in the Republic began dynamically and intensively in 1931, after the establishment of the Scientific Research Institute of Medical Parasitology and Tropical Medicine in Azerbaijan. During these years, a lot of scientific and research work has been carried out on various aspects of the disease. As a result of these studies, the prevalence level, risk groups, epidemiological characteristics of ascariasis among the population in different regions and settlements were studied, efficient diagnostic methods, effective treatment schemes were developed, and some achievements were made in the fight against them. It should be noted that most of these research works were carried out 25-30 years ago.

Chobanov R. A. in his researches, it was shown that ascariasis was found on average in 22.1 % of the population in the republic until 1985. However, ascariasis is not evenly distributed in different regions, and according to the level of infection of this helminthosis, their foci are divided into 5 types. It is shown that ascariasis is 10 % in type I and II foci, 10-24.9 % in type III foci, 25-30.9 % in type IV foci, and more than 40 % in type V foci. Apparently, as part of the development of ascariasis takes place in the soil, their foci are divided into 3 groups according to contamination with helminth eggs:

- Type I slightly contaminated soil – with 11 ascariasis eggs in 1 kg of soil,
- Type II relatively contaminated – with 11 to 35 ascariasis eggs per 1 kg of soil,
- Type III heavily contaminated – soils with more than 35 ascariasis eggs per 1 kg of soil.

In the conducted studies, the authors show that 4-11 year-old children and housewives are mostly infected with these helminthoses (Chobanov, 1985, p. 46).

Examinations carried out on the Absheron peninsula, which is not favorable for ascariasis infection, revealed that 9.73 ± 0.7 % of the population was infected with ascariasis on average. These examinations show that ascariasis infects mostly 4-11-year-old children (Salehov, Fatullayeva, 2018, p. 140-144; Salehov, Khanmirzayev, 2020, p. 89-94).

In most studies, one method was used during examinations. In some cases, the parasite does not secrete eggs, and in other cases, only the male species of the parasite is present in the intestines, in which case the correct result of the examination cannot be obtained. Therefore, the infection rates shown in these studies do not fully reflect the real situation.

In recent years, some researchers have studied the incidence of ascariasis in children, its migration and intestinal stage. Ascariasis was detected in 21.0 ± 1.1 % of children. Here, ascariasis is the least common in children aged 1-3 years (13.6 ± 2.3 %), and the most common in children

ISSN: 2707-1146
e-ISSN: 2709-4189

aged 4-7 (24.5 ± 2.1 %) and 8-11 years old (25.8 ± 2.1 %) found in children. Apparently, ascariasis has been spreading among children at a high level in recent years (Ibrahimova, 2014, p. 21; Salehov, 2015, p. 207-210; Salehova, 2017, p. 21; Salehov, Ibrahimova, 2013, p. 94-95; Salehov, Ibrahimova, Salehova, 2013, p. 156-158).

Ascariasis infection peaks in pre-school and school-aged children and gradually decreases with age. Immunity occurs after infection with ascariasis, but this immunity does not prevent re-invasion. About 2,090 deaths are recorded worldwide as a result of ascariasis infection every year, with the highest percentage of deaths occurring in children aged 1-4 years. Although mortality is low compared to other infectious diseases, ascariasis causes disability, with disability peaking in children aged 5-9 years.

Ascariasis is not transmitted from person to person. The disease is transmitted to humans through fecal-oral route. Infection occurs when invasive eggs from contaminated soil fall into the human body (soil, water, greens, etc.). Invasion stage 3 larvae (L3) hatch, penetrate the intestinal mucosa and enter the bloodstream. Larvae are carried from the liver to the lungs by human blood. While in the lungs, the larvae grow significantly. Subsequently, the larvae reach the pulmonary airways, ascend the bronchotracheal tract, are swallowed, and fully developed L4 stage larvae enter the human small intestine, completing the migration cycle. Larvae turn into adult helminths up to 35 cm long in the intestine (Prevention, 2015). Adult helminths subsequently live in the intestine for 1-2 years. Although adult female helminths shed up to 400,000 eggs per day in human feces, the eggs must embryonate in moist, warm soil before they become infective to humans (Prevention, 2015). The presence of soil is essential for the completion of the life cycle, which is why the ascaris is called a soil-transmitted helminth (STH).

Ascariasis infection causes nervous system and cognitive impairment, mental and physical weakness and growth retardation in children. In adults, in most cases, irritability, reduced work capacity, and sleep disturbances occur. Even if children and adults do not have any clinical symptoms, ascariasis causes weight loss and some infectious diseases (dysentery, typhoid fever, etc.) Ascariasis leads to complications of pregnancy and other pathological changes. Mechanical or parenchymal jaundice can be observed in 65 % of patients with ascariasis.

In the migration phase of ascariasis, allergic symptoms are manifested in the body. During instrumental examinations, focal infiltrates are detected in the lungs, the amount of eosinophils in the blood increases and fluctuates between 15-30 %, in some cases this indicator is 60 % and more. In ascariasis, such a situation is called Löffler symptom complex.

In the intestinal phase of ascariasis, the clinical symptoms are different: usually these symptoms are weak, sometimes they are moderate, and in most cases, no symptoms are observed. In rare cases, the clinical symptoms are so severe that the patient's life is in danger and urgent treatment is required. This situation is more dangerous for children and can result in death. In the second phase, gastrointestinal or nervous system symptoms come to the fore in patients.

In the diagnosis of the first phase of ascariasis, IFA is also used from serological reactions.

Parasitological (coprological) examination methods are based on the finding of ascariasis eggs in feces.

Among these methods, the Fylborn method (enrichment method) is based on the principle of collecting eggs in the upper layer of the used liquid. When the patient's stool is examined by the Kato-Miuri method, the mixture proposed by the author is prepared in advance: 500 ml of glycerin + 500 ml of 6 % phenol solution + 6 ml of 3 % aqueous solution of malachite. Hydroscopic cellophane sheets cut into strips 20-30 mm thick with a thickness of 40-50 μM are kept (soaked) in this mixture for 24 hours before use, and after being covered with faeces on the object glass, they are examined with a microscope. It should be noted that the Kato-Miura method is a simple, hygienic and effective method that is not inferior to other methods (Najafov, 2014, p. 134).

Reducing or eliminating ascariasis remains a global challenge. Application of preventive chemotherapy is carried out by regular and repeated administration of anthelmintic drugs to risk groups. The goal of these programs is to reduce infestation. Prophylactic chemotherapy is

administered once a year or two years to young children (12-23 months), preschool children (24-59 months), school-age children and women of reproductive age by giving anthelmintic drugs.

However, as a result of regular treatments, sometimes, the formation of resistance to these anthelmintic preparations is observed. Thus, in ascariasis, the occurrence of persistence in anthelmintic treatment has been determined. This factor can create additional obstacles in the fight against ascariasis.

Implementation of hygiene (WASH) programs can also be beneficial in controlling ascariasis. Observance of sanitation rules can significantly reduce Ascariasis infestation (Strunz et al., 2014). However, the effects of WASH programs are not immediate and require long-term financing (Vaz Nery et al., 2019). Although the implementation of WASH programs has been carried out on a global scale in recent years, it is not possible to achieve control and high results using these programs alone.

Ascariasis eggs are resistant to the environment (Jourdan et al., 2018). People living in endemic areas are repeatedly infected with ascariasis and can be re-infected usually 3 months after treatment. The response of the human body to ascariasis can be either inflammatory processes or immunomodulation. The destruction of larvae in the human body depends on the immune response.

From this point of view, it is very important to study the current situation of ascariasis and implement effective prevention and control measures against them.

Conclusion

Ascariasis infection causes nervous system and cognitive impairment, mental and physical weakness and growth retardation in children. In adults, in most cases, irritability, reduced work ability, and sleep disturbances occur. Even if children and adults do not have any clinical symptoms, ascariasis causes weight loss and some infectious diseases (dysentery, typhoid fever, etc.). Ascariasis leads to complications of pregnancy and other pathological changes. Mechanical or parenchymal jaundice can be observed in 65 % of patients with ascariasis. Therefore, it is very important to study the current situation of the spread of ascariasis among the population and to implement effective control and preventive measures against it.

References

1. VOZ. (2016-2020). *Ramos proqram for the control and prevention of soil-transmitted helminths infestations in the European region.*
2. Chobanov, R. A. (1985). *Epidemiological foundations for the development of a unified complex for the improvement of the population from ascariasis, trichocephalosis and enterobiasis.*
3. Salehov, A. A., Fatullayeva, N. (2018). In modern conditions, the prevalence level and epidemiological characteristics of geohelminthosis (ascariasis and trichocephalosis) among the population in Baku city and the Absheron peninsula. *Health*, 4, 140-144.
4. Salehov, A. A., Khanmirzayev, F. I (2020). Prevalence and clinical signs of ascariasis and trichocephalosis among individuals with different pathologies. *Health*, 3, 89-94.
5. Ibrahimova, M. V. (2014). Clinical and immunological features of intestinal parasitosis (ascariasis, enterobiosis, giardiasis) against the background of dysbacteriosis in children, their treatment and prevention in modern conditions. Abstract of the doctoral dissertation in medicine.
6. Salehov, A. A. (2015). Prevalence and epidemiological characteristics of larval ascariasis and toxocarosis among children. *Modern achievements of Azerbaijani medicine*, 2.
7. Salehova, G. B. (2017). Clinical-epidemiological characteristics of larval ascariasis and toxocarosis in children. Abstract of the doctoral dissertation in medicine.
8. Salekhov, A. A., Ibragimova, M. V. (2013). Kishechnie parasitozi serdi detey i effektivnost ix serodiagnostiki v Azerbaijan. *Allergology and immunology*, 14(2), 94-95.
9. Salekhov, A. A., Ibragimova, M. V, Salekhova, G. B. (2013). The spread of ascariasis is detailed, the problem is diagnosed in Lechenia and Azerbaijan. *Nauchno-prakticheskiy journal, Vestnik KAZNMU*, 4(1), 156-158.

ISSN: 2707-1146
e-ISSN: 2709-4189

10. Centers for Disease Control and Prevention (2015). *Ascariasis – Biology*. https://www.cdc.gov/parasites/ascariasis/biology.html
11. Najafov, I. H. (2014). *Parasitic diseases in the country pathology of Azerbaijan.*
12. Strunz, E. C., Addiss, D. G., Stocks, M. E., Ogden, S., Utzinger, J and Freeman, M. C. (2014). Water, sanitation, hygiene, and soil-transmitted helminth infection: a systematic review and meta-analysis. *PLoS Medicine*, 11. [PMC free article] [PubMed] [Google Scholar]
13. Vaz Nery, S., Pickering, A. J., Abate, E., Asmare, A., Barrett, L., Benjamin-Chung, J., Bundy, D., Clasen, T., Clements, A., Colford, J. M., Ercumen, A., Crowley, S., Cumming, O., Freeman, M. C., Haque, R., Mengistu, B., Oswald, W. E., Pullan, R. L., Oliveira, R. G., Einterz Owen, K and Brooker, S. J. (2019). The role of water, sanitation and hygiene interventions in reducing soil transmitted helminths: interpreting the evidence and identifying next steps. *Parasites and Vectors*, 12, 273. [PMC free article] [PubMed] [Google Scholar]
14. Jourdan, P. M., Lamberton, P., Fenwick, A and Addiss, D. G. (2018). Soil-transmitted helminth infections. *The Lancet*, 391, 252-265. [PubMed] [Google Scholar]

Received: 01.06.2024
Revised: 15.07.2024
Accepted: 05.08.2024
Published: 20.08.2024

ISSN: 2707-1146
e-ISSN: 2709-4189

CHEMISTRY

https://doi.org/10.36719/2707-1146/47/10-16

Aygun Bayramova
Institute of Space Research of Natural Resources NASA
Doctor of Philosophy in Technical
aygun.b74@mail.ru

Drying and Purification of Natural Gas on Modified Clinoptilolite Type Zeolite by Adsorption Method

Abstract

Adsorption properties of sulfurous compounds in natural gases have been studied using clinoptilolite type zeolite catalyst with rich deposits in Azerbaijan. As a result, it was determined that the use of modified clinoptilolite is the most effective based on experimental evidence for the adsorption of H_2S, COS and RSH on modified clinoptilolite and NaX zeolite. Based on H_2S and COS adsorption heats in modified clinoptilolite, the optimal temperature of regeneration was determined at 250 °C. This is the value of the rate of desorption of sulfur compounds (H_2S and COS) from NaX zeolite at 320 °C, determined in industry, in other equal conditions. Thermally modified clinoptilolite is shown to have the best absorption and protective properties.

Keywords: *sulfurous compounds, adsorbent, natural zeolites, modification, clinoptilolite, mordenite*

Introduction

Currently, there are various methods of extracting sulfur compounds (H_2S və COS) in the industry. Among them, adsorption processes occupy an important place. Synthetic and natural zeolites are most often used as adsorbents, they differ in polar molecules and have a high absorption capacity at low concentrations. The price of natural zeolites is very low, they are resistant to high temperatures and aggressive environments. Among natural zeolites, clinoptilolite is of the greatest interest.

Taking this into account, the adsorption properties of sulfur compounds contained in natural gases were studied in Azerbaijan using a clinoptilolite type zeolite catalyst with rich deposits. Of the several dozen mineral types of zeolite in Azerbaijan, only clinoptilolite, mordenite, shabazite and phillipsite are of practical importance.

For some consumers (adsorption technologies, production of catalysts, etc.) in most cases, modification of zeolites produced by solutions of acids, alkalis, salts or other substances is required. Other types of modifications are also used: phosphorus, arsenic, volatile organic compounds, quadruple chloride hydrocarbon, silica compounds, hydrogen sulfides, etc.

It should be noted that chemical methods of processing zeolites have a number of significant disadvantages. The thing is that any chemical treatment of zeolites affects many chemical elements, including those with biological value. After chemical treatment of a certain zeolite rock with a prohibited set of micro- and macroelements, the mechanism of its action is significantly disrupted. The positive side of the chemical treatment of terraformed rocks with zeolite is that, when used, it is possible to change the properties of zeolites in the desired direction. Therefore, the use of such technologies makes it possible to significantly expand the scope of application of zeolite-containing rocks.

In modern conditions, the production of zeolite products of the required quality can be achieved not only by chemical, but also by mechanical and physical action. It should be noted that the prospects for the widespread introduction of natural zeolites into the national economy are mainly related to the problems of obtaining marketable products from the mature mass of zeolite-containing date sauces that meet the requirements of consumer sectors.

ISSN: 2707-1146
e-ISSN: 2709-4189

When using zeolites in most sectors of the national economy, the following main water-alluvial ones are formed: removal of polluting additives; an increase in the amount of zeolite in the commercial product compared to the original rock; improve the performance of any class of materials.

The capabilities of most of the main products-OTI-to produce high-quality zeolite products have been investigated using enrichment methods using structural differences in particle size, density, hardness, magnetic susceptibility, wettability and other characteristics of the components being separated. In the processing of zeolites, gradient enrichment, magnetic and electrostatic separation, flotation, as well as chemical treatment aimed at changing the substance are used.

Clinoptilolite is a layered zeolite discovered by Schaller and belonging to the mordenite group (Mina, 2019). According to various researchers, the size of the access windows to the intracrystalline spaces of clinokyrolite is 3.5 – 4.4.

According to their chemical composition, three main groups of clinoptilolites can be distinguished: with a predominance of Ca^{+2} cations (Shuts, Rhodopa, Balkhash, Dzegvi, Novi-Kochb deposits); with a Na^{+} cation (Cermine deposit); with a predominance of K^{+} cations (deposits in Italy, Patagonia). At the same time, for some types of clinoptilolite, a high content of two cations was obtained, for example, for cuneiform tyrolite of the Shuts deposit-the presence of calcium and potassium cations, for cuneiform tyrolite of the Balkhyz deposit-the presence of calcium and sodium cations.

Table 1 presents the comparative mineralogical composition of zeolites, which are the most typical deposits in different countries.

Table 1.
Mineralogical composition of zeolites

Minerals	**Deposits**			
	Aydag	Dzegai	New Kohob	Bakiz
Clinoptilolite	77-85	85-95	85-95	71-76
Quartz	15-18	1,5-2,5	5,0-7,0	17-25
Calcite	1,8-2,5	0,85	0,48	1,2-3,0
Biotite and chlorite	2,0-4,0	3,0-4,0	3,5-5,0	1,5-3,5
Other minerals	2,0-2,5	1,5-3,2	0,6-2,0	2,0-3,0

Although the order of selectivity varies slightly, a similar pattern is generally preserved for Salt alloys: $Rb^{+}>Li^{+}>K^{+}>Na^{+}$ (Sharipov, 2016, p. 267-269). The indicated property of clinoptilolites makes it possible to use them as ion exchange materials in the processes of purification of tap water at industrial enterprises and other sectors of the national economy.

Granulation of small fractions in cuneiform-montmorillonite rocks allows, with the help of sorption processes, to increase the fractional yield to the required values from -5 to +3 mm, and the fractional output from -3 to +1 mm can be adjusted.

The highest concentration of a whole component-clinoptilolite-falls on the fraction p = 2.14-2.20 g/cm^3, and the maximum content is recorded in multiples of p = 2.16-2.205 g/cm^3. In the fraction P =2.205 g/cm^3 and in layers of higher density, the insignificant content of quartz is noted, which is explained by its presence in a fine compound with other minerals. Starting from a layer of P = 2.210 g/cm^3, cuneiform thyrite predominates in fractions, the content of which in the sample increases to a noticeable p = 2.230 g/cm^3. In addition, they are intensively enriched with quartz as the density of the fractions increases.

Studies point to the possibility of gravitational release of the enriched polevoshpat group of clay mineral, cuneiform concentrate and quartz fractions enriched with a heavier mineral.

ISSN: 2707-1146
e-ISSN: 2709-4189

However, the main disadvantage of this method is the use of zeolites as a means of separating the compound of organic bromoform and dimethylformamide liquids from absolute absorbable, and their further desorption is extremely difficult from a technical point of view.

Thus, achieving an efficient separation of zeolite minerals (cuneiform tyrolite), clay particles and minerals of the feldspar and quartz group significantly violates the technological properties of zeolites.

In connection with the acquisition of clinoptilolite concentrates, a gravitational magnetic plating scheme was developed. Thus, studies have proposed a laboratory scheme for the isolation of clinoptilolite concentrates for one of the types of zeolite-containing rocks of the Aydag deposit (rich in clinoptilolite and weak montmorillonite), determined that the yield of the Hashed clinoptilolite concentrate can potentially be 75-80 %, while the amount of clinoptilolite is about 90-95 %. In this case, the montmorillonite part si remains in the zeolite concentrate.

Each branch of the national economy manifests itself as an influencer on the quality of zeolite raw materials obtained by chemical, physical and complex influences. At the same time, modern technologies for processing and plating zeolite-containing rocks do not always allow obtaining zeolite products of the required quality.

Of great importance in the number of sorption-regeneration cycles, as well as in the process of functioning of natural zeolites as adsorbents of one purpose or another, there is a regeneration process. It is most profitable both economically and environmentally – do not throw away natural zeolites as long as possible and do not extend the service life. Thus, the issue of industrial application of natural zeolites as adsorbents is positively solved by an effective method of their regeneration.

In this situation, during the use of natural seolites, the recovery of the adsorbent The problem of geo-chemical barriers, the release of pollutants Cleaning of hot water, fuel and energy production waste gases It occupies an important place in you. As a rule, the use of natural seolites as adsorbents is proposed in this or other industry. It is the level of regulation that determines the quality of the sound.

The main property of clinoptilolite as an adsorbent is its ability to absorb moisture. Mu is the amount of water in the voids in the crystals. The moisture content of clay is highly dependent on its cationic form.

The increase in the atomic mass of the metal in the same valence Falling down with heat. This is due to the increase in the volume of the particles and the decrease of the free volume in the cell of the zeolite. As the charge density of the second cation decreases, the rate of hydration is related to its decrease (Mazgarov, 2015, p. 70).

Compared to synthetic zeolites of type A and X, clinoptilolite is smaller in size. It has a larger volume and is easier to water. Clinoptilolite already loses 80.3 % of its original amount of water at a temperature of 200 °C. In the same conditions, NaA and NaX lose 50 % and 57 % of water, respectively.

Clinoptilolite well adsorbs substances whose molecules are small in size (no larger than 4 Å): water, carbon dioxide, oxygen, nitrogen, etc. (Nikiforov, 2011, p. 48; Savostyanov, 2014, p. 43-48). In clinoptilolit, the adsorption isotherms of water vapor have a steep rise in the initial section, which is kharakhterik for microporous adsorbents. At a relative pressure P/Ps=0.1-0.2, the voids of the clinoptilolite are almost completely filled with water.

ISSN: 2707-1146
e-ISSN: 2709-4189

The properties of natural clinoptilolite are shown in Table 2.

Table 2.
Properties of natural clinoptilolite

Indicator	Clinoptilolite
Bulk density: g/cm^3	0.65 – 0.7
Clinoptilolite content: without less %	76 – 80
Porosity: %	29.4 – 50
Granular porosity: at least %	40
Water resistance: at least %	95
Vibration wear: without less %	1
Heat resistance: ^{0}C	650
Mechanical crushing strength of granules: at least	8 kg per pellet
Exchange capacity for NH_4: at least mg-ekv/g	0.70 – 2.5
Standard fractions: output of target fraction at least 85 %	3 – 5 mm
Moisture capacity in static conditions at relative humidity (1.0 %): at least	60 mg/sm^3
Appearance:	irregularly shaped granules
Color:	light gray, yellow gray
The dimensions of the windows, Å	4.0 – 7.2

The most common methods for cleaning natural gas from hydrogen sulfide are chemosorption processes. Aqueous solutions of alkali metal salts of organic bases – amines: carbon, phosphoric acids, amino acids are widely used as reagents in this group of processes (Seong, 2011, p. 583-590).

The regeneration of the saturated solution is carried out by boiling it in a reboiler heated by steam or flame at a temperature of 70-150 °C. Sour gases from the regeneration are sent to the production of sulfuric acid or elemental sulfur by the Klaus method. When the gas contains carbon dioxide, it is removed together with hydrogen sulfide. But the absorption rate of CO_2 is much lower than the absorption rate of H_2S. This allows, in cases where the amount of carbon dioxide in the purified gas is not regulated, to regulate its absorption in the purification process and thereby reduce energy costs. The absorption selectivity of H_2S for primary and secondary amines, which interact with CO_2 to form carbonates, is very low. This reaction belongs to the class of fast reactions. The selectivity of H_2S absorption decreases with increasing absorption temperature and irrigation density.

The degree of purification of gas from sulfurous organic compounds in the processes under consideration is generally not higher than 30 %. Mercaptans and carbon disulfide are absorbed mainly at the expense of physical solubility. The removal of carbonyl sulfide is determined by the rate of its hydrolysis in an alkaline solution and increases with the rise of the pH of the solution. The optimum processing temperature is 60-80 °C.

The ability of aqueous solutions of chemosorbents to absorb acid components practically does not depend on the partial pressure of acidic components in the gas phase, being a function of temperature and the amount of chemosorbent. For this reason, when the amount of sulfurous compounds in the purified gas increases, the energy costs of circulating the absorbent solution in the system and its regeneration increase almost proportionally. To lower the amount of hydrocarbons in sour gases, multi-stage aeration of the saturated absorbent is applied, followed by compression of the aeration gases and their return to the purification cycle, as a result of which energy costs are significantly increased.

Physical absorption processes are more economical than amines if the partial pressure of acidic components in the purified gas exceeds 4-6 atm, depending on the type of organic solvent.

Physico-chemical absorbers, consisting of a mixture of amines, physical solvents and water, are characterized by a high degree of absorption of sulfur compounds and CO_2 in the area of both high and low partial pressure. The effect of physico-chemical absorbers is based on chemosorption of CO_2 and H_2S with amines and physical solubility of sulfurous organic compounds.

However, the initial quality of zeolite-containing rocks of these deposits does not always satisfy the need for this type of raw materials in the oil and gas industry, agriculture and animal husbandry, as well as in medicine, food industry, etc. its requirements for the content of zeolites and various types of impurities for use (quartz, iron oxides, etc.).

For example, when using natural zeolites as bioactive additives, extremely stringent requirements are imposed on the iron oxides contained in them, the use of zeolites in most medical fields requires their monominerality, and the requirements for the purity of zeolite products for livestock and fish farming are tightened. The gas processing industry also strictly regulates the quality of zeolites, the main requirement is that the content of zeolite should be from 90 to 100 %.

In this regard, there is a need to develop technology for processing and enriching zeolite-containing rocks, which can provide the necessary purity of zeolites and obtain high-quality commodity products that meet the conditions of one or another branch of the national economy **(**Angelova, 2011, p. 306-311).

However, at present, the issues of deep enrichment of zeolite-containing rocks are at the initial stage of development. In industrial conditions, the preparation of zeolites for use in the national economy is limited to decomposition and threshing in several stages. Large-sized raw materials are first crushed, and then crushed in 2-3 stages.

Sometimes the primary processing scheme includes additional drying, tabletting or granulation of crushed material by crushing. A type of zeolite divided into fractions is a catysh product sent directly to consumers. In industrial use, all fractions of zeolite raw materials are applied up to 10 mkm 4 mm.

In Azerbaijan, seolite has a number of minerals, mainly clinoptilolite, mordenite, shabazite and phylipsite, which make up the practical population.

It should be noted that chemical processing methods zeolites have a number of significant drawbacks. The thing is that any chemical processing of zeolites affects many chemical elements, including biologically valuable ones. After chemical processing of a certain zeolite rock with a ban-gilt set of micro – and macroelements, the mechanism of its action is significantly distorted. The positive side of the chemical processing of zeolite-containing rocks is that during its application it is possible to change the properties of zeolites even in the required direction. Therefore, the use of such technologies can significantly expand the area of geolith-containing rocks.

In modern conditions, the production of zeolite products of the required quality can be achieved not only by chemical, but also by mechanical and physical influences.

It should be noted that the prospects for the widespread use of natural zeolites in the national economy are largely associated with the problems of purchasing products for sale from the sexual mass of zeolite-containing rocks that meet the requirements of consumer industries (Garcia-Basabe, 2010, p. 187-196).

Based on the results of experimental tests, the expediency of using modified clinoptilolite in desulfurization processes in combination with synthetic zeolites is revealed: the first layer of synthetic zeolite along the purified gas flow, the complementary layer – clinoptilolite. Since the adsorbent processing rate in complementary layers is low, replacing synthetic zeolite with clinoptilolite will not have a noticeable effect on the total sulfur capacity of the layer. On the other hand, taking into account the high thermochemical durability of clinoptilolite and its low catalytic activity in cracking reactions, the use of a combined layer in reverse-flow regeneration will allow to increase the service life of adsorbents (Rakitskaya, 2014, p. 52-58).

Currently, adsorption methods in the presence of various solid adsorbents are used to purify low-sulfur gases at high concentrations of carbon dioxide. These processes take advantage of the

high selectivity of zeolites. For example, hydrogen sulfide is better adsorbed than a mixture of nonpolar gas and liquid coal hydrogens.

The processing of low-sulfur gases at high concentrations of carbon dioxide has a great effect taking into account the properties and characteristics of the low-sulfur gases, the zeolite surface A new way of cleaning by adsorbing in water, then desorbed hydro The catalytic conversion of gen sulphide to elemental sulfur is determined.

The use of adsorption method for complex processing of low-sulfur gases, gas and sulfur It allows us to eliminate someone and leads the whole process to a period without jumping. The gas mixture and gas sulfur products of the process are cleaned of H_2S. Production waste and gas loss are almost non-existent. The use of molecular sieves will allow efficient purification in the sorption zone at a high linear gas velocity, which will allow to significantly reduce the size of adsorbers, as well as to combine the purification of gas mixtures from H_2S with deep drying (Yusubov, 2016, p. 22-23).

Synthetic zeolites are much lower than natural samples in terms of chemical stability and other useful properties. In this regard, the study of new types of mineral raw materials, that is, natural zeolites, is one of the important national economic tasks and has great economic importance (Adzhiev 2017, p. 43-48; Makhmudova, 2019, p. 159-166).

Due to the presence of industrial deposits of natural zeolite, Azerbaijan can be represented as one of the large zeolite regions of the CIS, which can provide the national economy with the necessary raw materials for decades to come.

Conclusion

Based on experimental data on adsorption of H_2S, COS and RSH in modified clinoptilolite and NaX zeolite, the concentration range of sulfur compounds in which the use of modified clinoptilolite is most effective was determined. Depending on the temperature, an increase in the adsorption capacity of modified clinoptilolite due to ethyl mercaptan was recorded, which is explained by the appearance of a sieve effect. Based on this, it was concluded that the use of modified clinoptilolite for purification of natural gases from ethylmercaptan is advisable in cases where further gas processing is carried out at high temperatures.

References

1. Meimand, M. M., Javid, N., and Malakootian, M. (2019). Adsorption of Sulfur Dioxide on Clinoptilolite. Nano Iron Oxide and Natural Clinoptilolite. *Health Scope,* 8(2). doi:10.5812/jhealthscope.69158.
2. Sharipov, K. K., Yusupov, T. A. (2016). The study of the physico-chemical properties of adsorbents in the purification of sulfur dioxide. *Young scientist*, 2, 267-269.
3. Mazgarov, A. M. (2015). *Technologies for purification of associated petroleum gas from hydrogen sulfide*. Textbook.
4. Nikiforov, I. A. (2011). *Adsorption methods in ecology*.
5. Savostyanov, A. P., Narochny, G. B., Yakovenko, R. E., and others. (2014). Development of basic technological solutions for a pilot plant for the production of synthetic hydrocarbons from natural gas. *Catalysis in industry*, 3, 43-48.
6. Seong-Ched Jang, Se-il Yang et.al. (2011). Adsorption dynamics and effeets carbon to zeolite ratio of layered beds for multicomponent gas adsorption. *Korean Journal Chemical Engineering*, 28(2), 583-590.
7. Angelova, D et al. (2011). Kinetics of oil and oil products adsorption by carbonized rice husks. *Chemical Engineering Journal,* 172, 306-311.
8. Garcia-Basabe, Y., RodriguezGznaga, I., Menorval, L., Llewellyn, Ph., Maurin, G. (2010). Step-wise dealumination of natural clinoptilolite: Structural and physicochemical haracterization. *Journal of Microporous and Mesoporous Materials*, 3(3), 187-196.

9. Rakitskaya, L., Raskolah, L. A., Kiose, T. A., Yarchuk, A. V., Korotkova, A. S. (2014). Adsorption and protective properties of modified clinoptilolite relative to sulfur dioxide. Bulletin of ONU. *Chemistry*, 19(49), 52-58.
10. Yusubov, F. V., Bayramova, A. S. (2016). Investigation of the process of adsorption purification of natural gases on CaX zeolite. *The journal Science, Technology and Education*, 6(24), 22-23.
11. Adzhiev, A. Yu., Moreva, N. P., Dolinskaya, N. I. (2017). Determination of the propensity of zeolite adsorbents of type a to coke formation during drying of hydrocarbon gases. *Scientific Journal of the Russian Gas Society*, 2, 43-48.
12. Makhmudova, L. Sh., Khadisova, Zh. T., Akhmadova, Kh., Abdulmezhidova, Z. A. (2019). Osushka i ochistka prirodnogo gaza na tseolitakh (obzor). *Fundamental'nyye i prikladnyye issledovaniya v nauke i obrazovanii sbornik statey po itogam Mezhdunarodnoy nauchno-prakticheskoy konferentsii*, 28(2), 159-166.

Received: 15.05.2024
Revised: 11.07.2024
Accepted: 03.08.2024
Published: 20.08.2024

https://doi.org/10.36719/2707-1146/47/17-22

Asmar Valiyeva
Western Caspian University
Doctor of Philosophy in Chemistry
esmer_elesgerli@mail.ru
Parviz Nadirov
Azerbaijan State Oil and Industry University
Doctor of Philosophy in Chemistry
parvizm1971@mail.ru
Jabrail Mirzai
Baku State University
Doctor of Chemical Sciences
mirzacabrayil@gmail.com

Synthesis and Characterization of Nax/Ni Zeolite Nanocatalyst and Their Application in the Process of Oxidative Dehydrogenation Propanol

Abstract

Catalyst samples were synthesized by the method of impregnation on the basis of NaX zeolite and Ni metal and their activity was studied in the oxidation process of n-propanol in the temperature range of 423-723K. It has been established that the conversion rate of alcohol and the yield of reaction products on the modified samples increase significantly compared to the original NaX sample. According to the results of the research, it was found that if the reactions of intramolecular and intermolecular dehydration of alcohol predominate at relatively low temperatures, then the reactions of its partial and complete oxidation are accelerated at high temperatures. It was determined that the method of modifying the original NaX zeolite makes it possible to optimize the phase composition of the synthesized catalyst and the size of the active component, which allows to adjust the yield of the main reaction products and reduce the temperature limit of the reaction. As a result of the study, it was found that the average size of NiO particles included in the structure of NaX zeolite is 28314 nm. This suggests that the size of NiO particles in the zeolite structure is at the nanoparticle level.

Keywords: *catalysis, zeolite, alcohol, oxidation,nanotecnology*

Introduction

As is known zeolites have almost very weak oxiding and reducing properties when they contain an alkali metal cation as the primary exchange cation. However, highly active oxidation catalysts can be obtained by introducing transition metals into their crystal lattice in various ways**.** On the other hand, recently there has been great interest in processes involving nano-sized catalytic systems. The basis of the work carried out in this direction is the development of methods for the synthesis of catalytic systems with nanostructured particles, determination of their structure and morphology, and determination of methods that allow changing the basic properties of the catalyst (Henry, 2007, p. 354; Khalaji, 2013, p. 245).

Based on the above, it can be said that, the study of zeolites containing transition metals is of great importance and relevance both in terms of the theory of catalysis and the creation of new multifunctional catalytic systems and the development of new catalytic processes.

In practice, the conversion of alcohols can be carried out using various catalysts. The traditional catalysts for this process are zeolites. In case of application of zeolites in the mentioned process, the researcher has the opportunity to preselect the structure type and pore size of the catalyst, thereby directing the process in the desired direction. The conversion of alcohols, including low molecular weight dihydric alcohols such as ethanol, n-propanol, on zeolites, is generally a complex process consisting of several stages depending on the conditions. The study of the features of this process

is one of the pressing problems of the petrochemical industry complex today (Korobitsyna et al., 2008, p. 169).

Experimental part

Taking into account the above, the conversion of n-propanol in the presence of NaX-based zeolite catalysts containing Ni-transition metal has been extensively investigated. The mentioned catalysts were obtained using the impregnation method. For this, the nitrate salt solution of the given metal was soaked onto the original zeolite (NaX) and then the mass was dried at 1000C and then heated at 3000C until the salt was completely decomposed. In the end, the resulting mass was incandesced at a temperature of 5500C for twelve hours and catalyst samples were obtained. Thus, using the impregnation method, catalysts containing 1.0 %, 2.5 %, 5.0 %, 7.5 % and 10.0 % Ni-metal were synthesized. In order to prepare the synthesized catalysts for use in the process, they were first made into pill form and then crushed into 1-2 mm particles (Gaigneaux et al., 2002, p. 354; Purnomo, Salim & Hinode, 2012).

The study of the activity of the synthesized catalysts was carried out in the process of converting n-propanol in air oxygen environment. The process was carried out in a flow-through installation equipped with a tubular reactor in the temperature range of 423-773 K. The volume of the catalyst taken for the study was 5 ml, the feed rate of the initial reaction mixture into the reactor was 2400 h-1. Alcohol-air mixture was fed into the reactor in a ratio of 1:10. The chromatographic method was used for the analysis of the initial substances and reaction products (Qia et al., 2009: 13; Suryanarayan & Grant, 1998, p. 428).

X-ray phase analysis studies of catalyst samples containing different amounts of modifiers before and after the reactions were carried out on a RIGAKU SC-70 device at an angular velocity of 10 rev/min (40 kV, 15 mA) in the angular interval of 3-60^{o} in CuK-beams to study the phase state of the impregnated compounds. Decoding of diffractograms was performed using the ICDD, PDF-2 database (Min Kim et al., 2021, p. 162; Almashhadani et al., 2017, p. 428).

Thus, the NaX structure is an excellent starting point for the developing of the group of new zeotype catalysts where one of the most important materials is Na. Many efforts have been devoted to introduce intracrystalline mesoporosity into NaX structure in order to reduce the micropore environment restrictions, e.g. modified crystallization methods (Breck, Eversole & Milton, 1956; Weisz & Frilette, 1960, p. 382) templating and demetalation (Argauer & Landolt, 1972). In group of post-synthetic methods of modification of zeolitic materials one of the most effective and most economical seems to be desilication process. The desilication is identified with the process of selective extraction of silicon from the framework in the alkaline medium. The effectiveness of Si extraction from the framework depends on a number of parameters, including the value of Si/M ratio, framework topology, type and concentration of the desilication agent, temperature and time of process.

The results obtained and their discussion

The temperature dependence of the yield of the reaction products obtained from the conversion of N-propanol on NaX+Ni catalyst samples has been extensively studied. It has been established that the conversion of alcohol is observed starting from the temperature of 523K. The maximum alcohol conversion corresponds to the NaX (+5.0 % Ni) sample and is 70.0 % (723K). The maximum yield of carbonyl compounds (acrolein + propion aldehyde) corresponds to the above-mentioned catalyst sample and temperature and is 13.0 %. The maximum yield of propene also corresponds to the NaX sample (+5.0 % Ni) and is 22.3 % at a temperature of 623K. The maximum yield of carbon dioxide, which is a product of complete oxidation of alcohol, on the specified sample is 39.7 % (723K).

In the continuation of the research, X-ray phase and EPR analysis of Ni-containing catalyst samples used in the process of n-propanol oxidation was carried out before and after the process.

Figure 1 shows roentgenograms, of NaX samples containing 5.0 and 10.0 % Ni before and after the experiment.

ISSN: 2707-1146
e-ISSN: 2709-4189

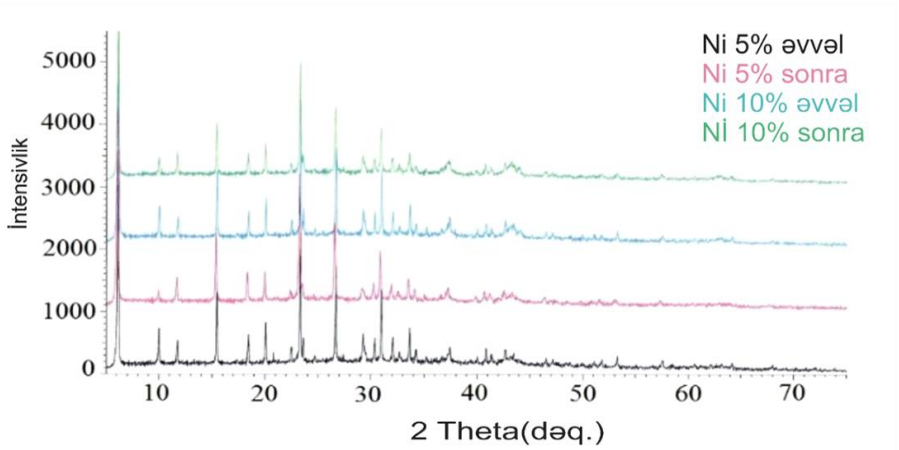

Figure 1. Radiographs of NaX (+5 % Ni), NaX (+10.0 % Ni) samples taken before and after the experiment

It was determined that the peaks of 2θ = 6.116, 10.002, 23.347, 26.669, 32.037° correspond to the standard pattern of primary NaX zeolite. The peaks of 2θ = 37.386 (111), 43.478 (200) and 63.222° (220) prove the presence of NiO particles in NaX+Ni samples. The sharpness and intensity of these peaks suggest that the NiO-nanoparticles have a high degree of crystallinity. This suggests that nickel (II) nitrate impregnated on the zeolite surface is completely decomposes into NiO nanoparticles when heated at 5500 C. Using the formula D = kλ / βcosθ, the average size of NiO crystals was determined. Here, λ is the wavelength of X-rays and is 1.54056 nm. β = FWHM and θ – diffraction angle is calculated based on the peak. And k is an empirical coefficient and is 0.9. As a result of the calculation, it was established that the average size of NiO particles included in the structure of NaX zeolite is 28314 nm. This suggests that the size of NiO particles in the zeolite structure is at the nanoparticle level.

Table 1 shows the sizes (as a result of RF analysis) and values (as a result of EPR analysis) of magnetic resonance parameters of NiO particles formed in a pure state and on the surface of NaX zeolite. As can be seen from the table results, the size of NiO nanoparticles formed on the surface of NaX zeolite is smaller than the size of pure NiO crystallite.

Table 1.
Size and value of magnetic resonance parameters of NiO crystallite formed in pure state and on the surface of NaX zeolite

Parameters	Pure NiO crystallite	NiO/NaX
Nanoparticle size (nm)	32,65	28,31
g – factor value	1,92	2,1
EPR spectrum width, ΔHpp (mT)	72,5	66,9

Figure 2 shows the EPR spectra of NaX (+1.0 % Ni) and NaX (+5.0 % Ni) samples taken before the experiment and after 6 hours of operation during the n-propanol conversion process. It üas determined that the addition of even a small amount of metallic Ni (~1 %) to the original NaX zeolite causes a noticeable change in its ESR spectrum. Against the background of a broad signal created by a large magnetic field, a convex-shaped signal with a g-factor of 2.1 and a width ΔH = 19-20 mT is observed, which corresponds to nano-sized NiO particles.

ISSN: 2707-1146
e-ISSN: 2709-4189

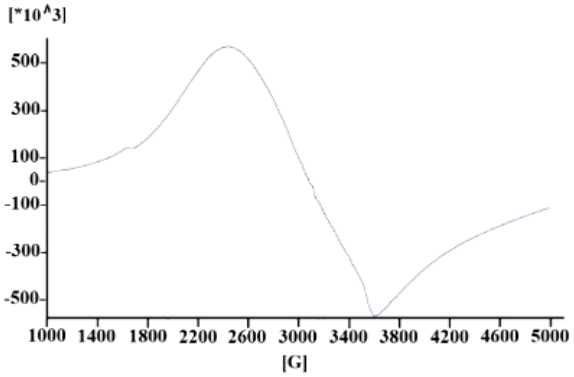

a) NaX (+1.0 % Ni), before the experiment

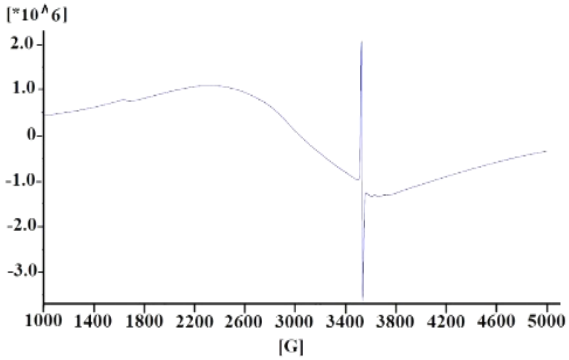

b) NaX(+1.0 % Ni), after the experiment

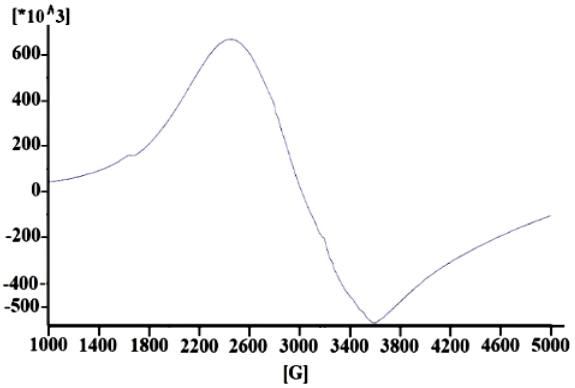

c) NaX (+5.0 % Ni), before the experiment

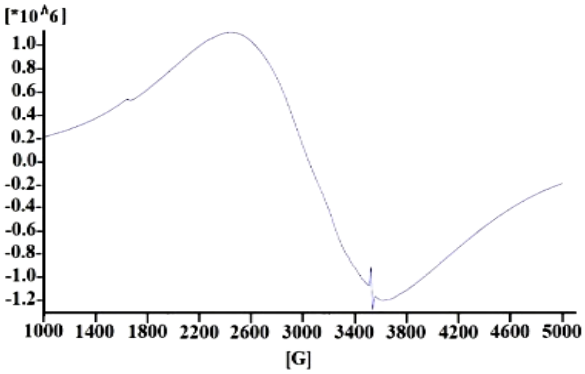

d) NaX (+5.0 % Ni), after the experiment

Figure 2. EPR spectra of NaX samples containing 1.0 % (a, b) and 5.0 % (c, d) Ni before the experiment and after 6 hours of operation in the n-propanol conversion process

It was found that when the mass amount of Ni included in the original zeolite increases up to 10.0 %, their EPR spectrum becomes complex and consists of many signals. For example, in the NaX (+5.0 % Ni) sample, the number of signals reaches six. Research has shown that the EPR spectrum of catalyst samples involved in the conversion of n-propanol undergoes a noticeable change within 6 hours. Based on the ESR spectra of the catalyst samples processed in the process, a certain amount of coke formation is observed on the surface of the catalyst. Thus, against the background of the broad signal, a narrow signal characterized by the parameters g=2.0026 and ΔH= 0.9 мТ is observed, which corresponds to coke residues with paramagnetic properties. It is assumed that the formation of coke on the surface of the catalyst creates the conditions for the reduction of nickel oxide to metallic nickel. Note that the EPR spectrum of the coked sample obtained after annealing in the presence of air at a temperature of 773 K is practically indistinguishable from the EPR spectrum of the initial catalyst sample. It is quite possible that the catalytically active centers of this reaction are nanosized particles of nickel oxide NiO, and the main participants in the redox stages of the process are Ni and NiO particles.

Catalyst samples processed for 6 hours in the n-propanol oxidation process were studied using the IR-spectroscopy method.

Figure 3 shows the IR spectra of the NaX (+2.5 % Ni) sample taken before and after processing in the mentioned process.

ISSN: 2707-1146
e-ISSN: 2709-4189

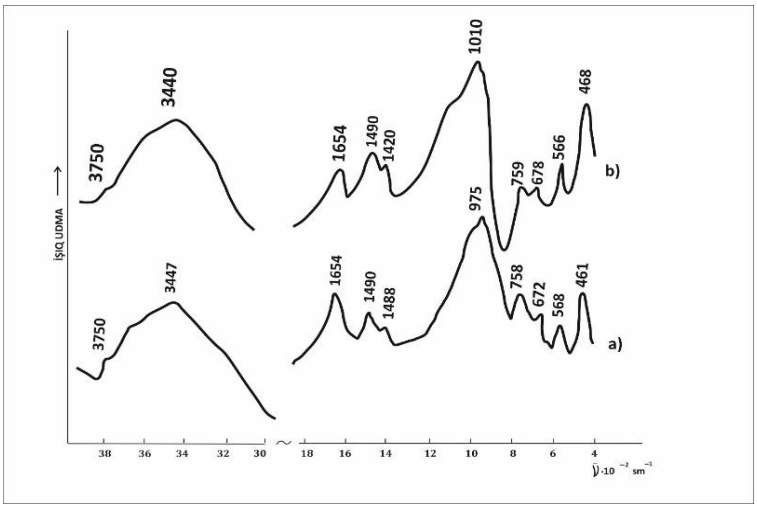

Figure 3. IR-spectra of NaX (+2.5 % Ni) catalyst before (a) and after (b) treatment in n-propanol conversion process

The comparison of the corresponding spectra shows that no significant changes of the spectral landscape occur in the vibrational regions of either the crystal lattice or water after the aforementioned catalytic process. Naturally, small shifts are observed in the maxima of some absorption bands. In addition, after the process there is an increase in the integral intensity of the absorption bands, observed at 1400-1500 cm-1 in the region of carboxylate structures (monodentant or bidentate).

Conclusion

In the process of oxidative dehydrogenation of N-propanol in the presence of nickel-containing NaX zeolite catalysts, in addition to the activity of the catalyst, its phase composition, active component distribution, magnetic and catalytic properties have also been widely studied. It has been shown that the amount of modifier in the catalyst allows to optimize its phase composition and the size of the active component, which allows to adjust the yield of the main products and reduce the reaction temperature. It has been shown that the inclusion of NiO nanoparticles in the composition of the zeolite leads to an increase in the activity of catalysts at high temperatures and significantly increases their stability. It was determined that the optimal amount of nickel in the catalyst is 5 % by mass. Thus, as a result of the process of oxidative dehydrogenation of propanol in the presence of the mentioned catalyst, the maximum yield of carbonyl compounds (acrolein + propion aldehyde) was 13.0 % (723K), and the maximum yield of carbon dioxide, which is the complete oxidation product of alcohol, was 39.7 % (723K), which is considered a fairly high result.

References

1. Henry, C. R. (2007). *Catalysis by nanoparticles. In Nanocatalysis.* Springer.
2. Khalaji, A. D. (2013). Preparation and characterization of NiO nanoparticles via solid-state thermal decomposition of nickel (II) Schiff base complexes [Ni (salophen)] and [Ni (Mesalophen)]. *Journal of Cluster Science*, 24(1), 209-215.
3. Korobitsyna, L. L., Velichkina, L. M., Vosmerikov, A. V., Radomskaya, V. I., Astapova, E. S., Ryabova, N. V., & Agapyatova, O. A. (2008). Ultra-high-silica ZSM-5 zeolites: Synthesis and properties. *Russian Journal of Inorganic Chemistry*, 53(2), 169.
4. Gaigneaux, E. M., De Vos, D. E., Jacobs, P. A., Martens, J. A., Ruiz, P., Poncelet, G., & Grange, P. (2002). *Scientific Bases for the Preparation of Heterogeneous Catalysts*. Elsevier.
5. Qiao, H., Wei, Z., Yang, H., Zhu, L., & Yan, X. (2009). Synthesis of pure Na–X and Na–A zeolite from bagasse fly ash. *Microporous and Mesoporous Materials*, 162, 6-13.
6. Purnomo, C. W., Salim, C., & Hinode, H. (2012). EPR (Electron Paramagnetic Resonance) spectroscopy of polycrystalline oxide systems. *Metal Oxide Catalysis*, 1-50.

ISSN: 2707-1146
e-ISSN: 2709-4189

7. Suryanarayana, C., Grant, N. J. N. Y. (1998). A Practical Approach Plenum Press. New York. Preparation and characterization of NiO nanoparticles by anodic arc plasma method. *Journal of Nanomaterials.*
8. Min, H. K., Kim, Y. W., Kim, C., Ibrahim, I. A. M., Han, J. W., Suh, Y. W., Jung, K. D., Park, M. B., Shin, C. H. (2022). Phase Transformation of ZrO2 by Si Incorporation and Catalytic Activity for Isopropyl Alcohol Dehydration and Dehydrogenation. *Chemical Engineering Journal*, 428. https://doi.org/10.1016/j.131766
9. Almashhadani, H., Samarasinghe, N., Fernando, S. (2017). Dehydration of n-propanol and methanol to produce etherified fuel additives. *AIMS Energy*, 5(2), 149-162.
10. Breck, D. W., Eversole, W. G., Milton, R. M. (1956). New synthetic crystalline zeolites. *Journal of the American Chemical Society*, 78, 2338-2339.
11. Breck, D. W., Eversole, W. G., Milton, R. M., Reed, T. B., Thomas, T. L. (1956). Physical and Inorganic Chemistry: Crystalline Zeolites. The Properties of a New Synthetic Zeolite. *Journal of the American Chemical Society*, 78, 5963-5972.
12. Weisz, P. B., Frilette, V. J. (1960). Intracrystalline and Molecular-Shape-Selective Catalysis by Zeolite Salts. *The Journal of Physical Chemistry*, 64, 382-382.
13. Argauer, R. J., Landolt, G. R. (1972). Crystalline zeolite ZSM-5 and method of preparing the same (U.S. 3702886 A).

Received: 22.05.2024
Revised: 10.07.2024
Accepted: 30.07.2024
Published: 20.08.2024

ISSN: 2707-1146
e-ISSN: 2709-4189

https://doi.org/10.36719/2707-1146/47/23-37

Samadagha Rizvanli
Azerbaijan State Oil and Industry University
rizvanlisemedaga170@gmail.com
Bayim Shahpalangova
Azerbaijan State Oil and Industry University
bela_53@mail.ru

Assessment of the Hazard Risk That May Arise During the Transportation of Hazardous Chemicals by Vehicle Transport

Abstract

During our modern era, there are various types and numbers of chemically dangerous objects in the territory of our Republic, and they are constantly in operation. Thus, during the operation of these objects, significant reserves of dangerous chemicals of an emergency nature are used in a certain amount. According to information, thousands of tons of hazardous chemical substances are transported from one area to another in the Republic of Azerbaijan every year. So, the vehicles carrying those types of chemically dangerous substances have to pass through areas inhabited by people. Also, in case of accidents during the transportation, there may be a large number of people in the chemical contamination zone.

As we know, as a result of the spillage of dangerous chemicals, the environment, living beings, people, and animals are damaged in a huge amount. In order to prevent this, a plan of various measures should be implemented. In this article, special parameters were mainly used in the study of the dispersion of dangerous chemicals as a result of an accident and risk assessment, which are used for the main work:

1. Toxodose of dangerous chemicals according to distance and effect.
2. The average concentration of dangerous chemical substances entering the human body by inhalation.
3. Site of accidental spillage of chemical hazardous substances.
4. Area coefficient of distribution of known types of hazardous chemicals.
5. Infiltration.

Keywords: *hazard chemicals, vehicle, risk assessment, transportation, danger, harm*

Introduction

According to world statistics, 2/3 of man-made emergencies are characterized by accidents in the field of transport. Based on the conducted research data, chemical poisoning can occur in a total area of 0.08 thousand sq. km in the territory of our Republic, and approximately 231 thousand people live in that area. It should be noted that there have been more than a hundred accidents resulting in the release of dangerous substances into the environment in such facilities, and thousands of people have been injured. The goal was to ensure safety during transportation of dangerous goods by road and reducing possible accidents during transportation of that cargo. One in three industries and other businesses operating worldwide are closely related to hazardous chemicals, which are involved in technological processes, products, raw materials or intermediates that are released in those facilities (Aleksandrovich, 2020, p. 12-17).

Research. Complex measures to eliminate the consequences of accidents during transportation of dangerous chemicals by road include the following:

- predicting the consequences of probable chemical hazardous accidents,
- detection and evaluation of the consequences of hazardous chemical accidents,
- accident-rescue and other urgent work,
- prevention of chemical poisoning,
- special cleaning of technical equipment as well as sanitary cleaning of people.

In case of evacuation of people in the zone of possible pollution due to the flow (spill) of dangerous chemicals, emergency situations occur, the persons carrying out the transportation process should predict the possible emergency events that may occur and implement a plan of preventive measures to minimize the consequences of the accident.

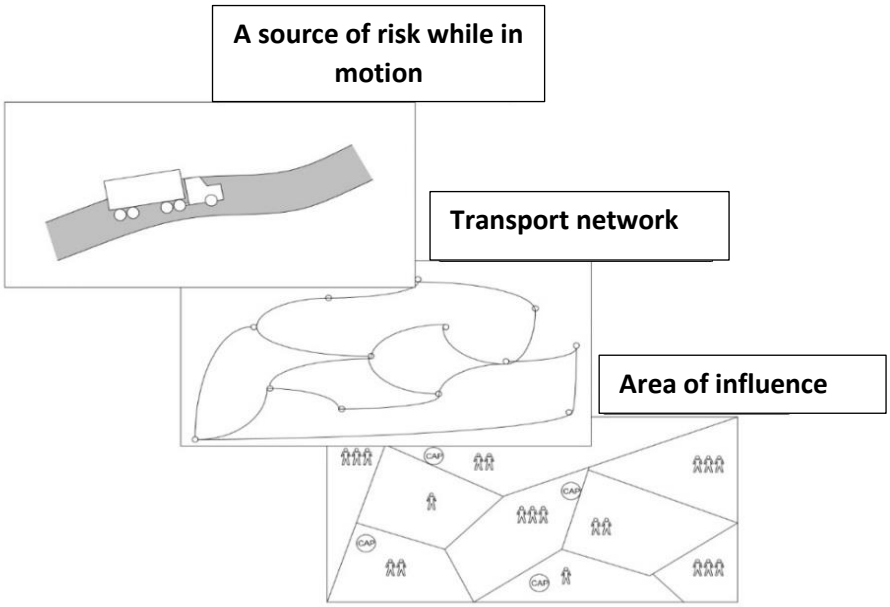

Figure 1. Interrelation between data sources for risk assessment of transportation of hazardous chemicals

The following measures should be taken to prevent accidents in the transport infrastructure and to minimize the risks of chemical hazards during the transportation of dangerous chemicals by road:

1. Research and improvement of ways to ensure the safety of the population and persons accompanying dangerous goods during accidents related to the spillage of hazardous chemicals.

2. Improvement and preparation of quick elimination methods and disinfection methods in the area of spilled dangerous substances.

All participants in the chain are responsible for the safety of transporting hazardous chemicals by road. Accidents during this can pose a significant threat to people's lives and health. They can damage infrastructure and cause environmental pollution and pollution (Gasimov, 2021, p. 54-62).

In case of an accident, dangerous chemicals are scattered beyond the capacity, that is, the toxodose can be calculated for the distance of any element of the object falling into the poisoning zone, and in this case, the risk assessment is as follows:

$$R_{toxy} = \frac{200 \cdot Q}{\upsilon \cdot k_1 \cdot (k_2 \cdot X)^{3/2}}, (\frac{mq}{l} \cdot dəq),$$

From what is shown here, X – is the distance indicator between the capacity of the object and its element, m; k_1 – the roughness coefficient on the ground surface: k_1=1 – when the ground is open; k_1=3.5 – for city-like buildings; k_2 is the coefficient of the vertical stability of the atmosphere; k_2=1 – when the ground is open; k_2=1.5 – for urban areas; k_2=2 – for forest areas; υ – is surface wind speed, m/sec; Q – is the mass of hazardous chemicals, kg. (Gasimov, Abdullayeva, 2017, p. 63-75).

Hazardous chemicals are divided into different types according to the degree of danger, they are as follows:

- object,
- local,
- regional,
- global.

ISSN: 2707-1146
e-ISSN: 2709-4189

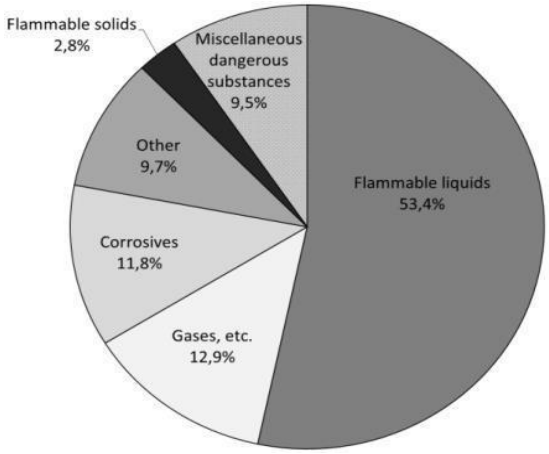

Figure 2. Case diagram of types of hazardous chemicals

Based on experience, the area of accidental substance spillage is calculated by the following formula:

$$P_{ds} = 3{,}14(3{,}018 \cdot E_y^{0{,}393} \cdot V_y^{-0{,}116} \cdot t_{yai}^{0{,}115} \cdot M_{ysə}$$

here, according to the indicators, E_y – is the volume of spilled (flowing) y-type hazardous chemicals, m^3; V_y – kinematic viscosity of dangerous chemicals of type y, m^2/s; t_{yai} – duration of diffusion of liquid, min. (Gasimov, Abdullayeva, Huseynov, 2009, p. 15-20).

Table 1. Types and effects of hazardous chemicals

Material	Energy ration	Efficiency factor
Hydrocarbons	10	0.04
Ethylene oxide	6	0.10
Vinyl chloride monomer	4.2	0.04
Acetylene oxide	6.9	0.06

When transporting hazardous chemicals, the person or persons must be aware of the high degree of danger involved in this type of activity and take all possible measures to prevent emergency situations that may cause casualties among the crew of the vehicle carrying hazardous chemicals.

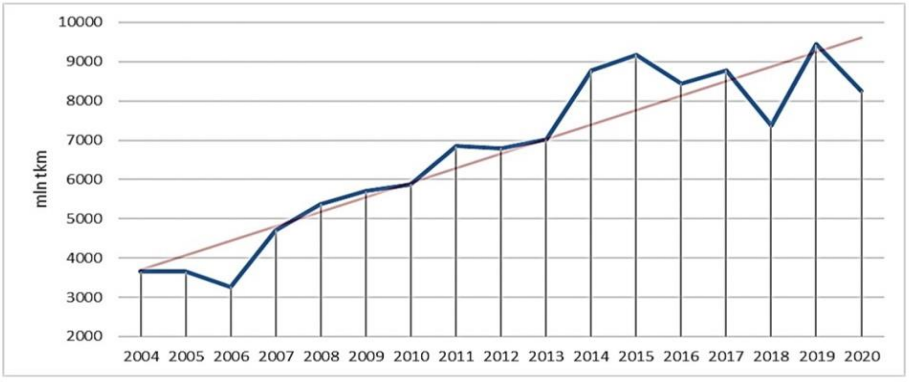

Figure 3. Dispersion distance of hazardous chemical substances during different years (2004-2020)

ISSN: 2707-1146
e-ISSN: 2709-4189

Quantitative risk during the transportation of hazardous chemicals is usually assessed as the probability of occurrence of an undesirable event (incident). In risk theory, such an indicator of the risk magnitude as mathematical expectations of the magnitude of undesirable consequences was used. It seems more rational to use this indicator for risk assessment during the transportation of dangerous chemicals and first of all to assess the danger degree of a certain cargo type. It should be noted that determining the mathematical expectation of damage in the transportation of hazardous chemical substances will require a new approach to the formation of the information base.

The amount of damage caused by the accidental release of hazardous chemicals and the quantitative risk assessment is calculated as follows:

$$R_{ziy} = \sum_{i=1}^{n} (P_i \cdot U_i)$$

here P_i – those that are likely to occur. risk events in Ch – M-S – G system; U_i – is the amount of damage during the i-th event. It should be noted that the feature of most technological processes related to the use of cars is the absence of well-defined technological operations that are stable in time and space. Under these circumstances, assessing the risk of the whole system seems to be a complex and often difficult task (Aksenov, 2020, p. 56-63).

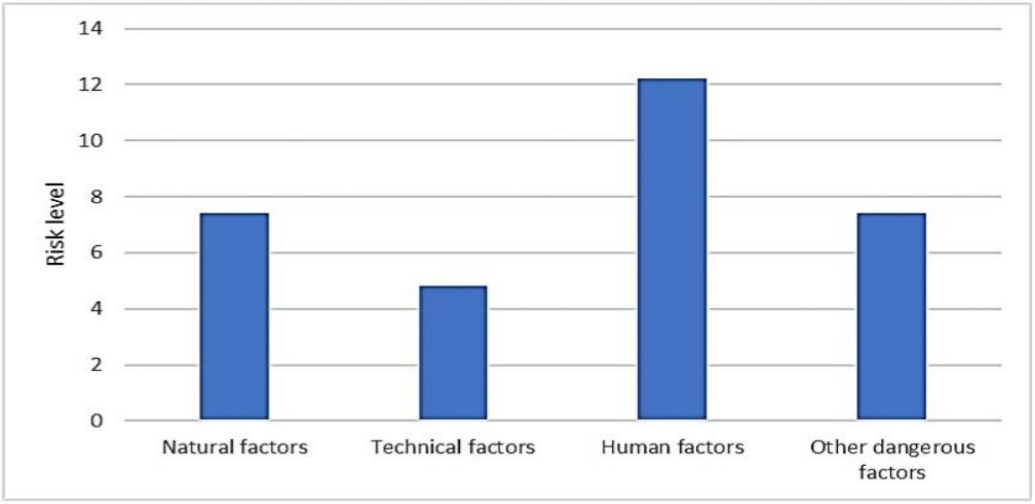

Figure 4. Levels of risks of hazardous chemical substances in hazardous areas

Accident In case of an accident during the transportation of hazardous chemicals, the characteristics of those hazardous substances differ according to the following:

- ignition,
- spontaneous combustion,
- dangerous reactions with water or other substances,
- explosiveness,
- corrosiveness,
- radioactivity,
- risk of infection (Daineka, 2023, p. 17-21).

ISSN: 2707-1146
e-ISSN: 2709-4189

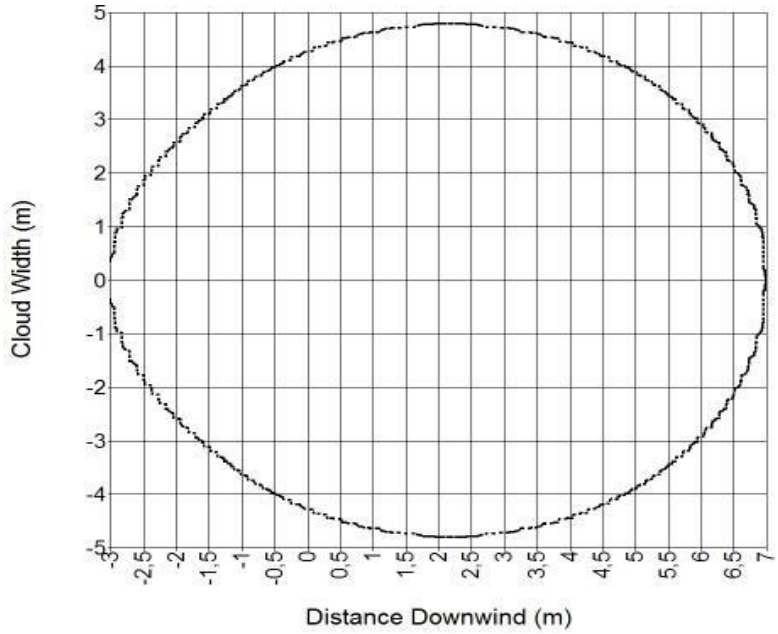

Figure 5. Evaporation of ammonia during the accident

The following parameters should be taken into account in the risk assessment during the accidental release of hazardous chemicals:

1. Meteorological conditions during the probable accident.
2. Norm rates for small pipes, large pipes and cylinders – taking into account different distribution probability of released quantities for each shipping container.
3. Day and time of the accident (affecting meteorological conditions).
4. Month of the year that affects relative accident probabilities (Rasulov, Badalova, Safarov, Ganiyeva, 2023, p. 277-278).

When planning routes for the transportation of hazardous products, the "risk factors" that must be achieved in order to achieve the goal of a route of minimal risk can be used as an expected result of an activity. With only one event (R) as a risk of potential factors, the probability of this event occurring is affected by the accident (P) that the event occurred (C). Accidental release of harmful substances is defined as a risk:

$$R = P \cdot C$$

Risk assessment during transportation of dangerous chemicals is carried out using the following formula:

$$R=\sum(P_i \cdot C_i)$$

here parameters P and C are the probability and outcome of the type i event. In general, the expression tree is as follows:

$$R=\sum(P_i \cdot C_i^{\alpha})$$

The people death risk as a result of the accidental release of dangerous chemicals is grouped as follows:

I. $R \leq 10\text{-}2$ – extremely high level.

II. $10\text{-}3 < R \leq 10\text{-}2$ – high level.

III. $10\text{-}4 < R \leq 10\text{-}3$ – medium level.

IV. $R \leq 10\text{-}4$ – low level (Surnikov, 2023, p. 385-397).

ISSN: 2707-1146
e-ISSN: 2709-4189

Before loading the vehicle, i.e. the special capacity of the car, with hazardous chemicals and sending it to the selected point, all the parameters, density, pressure, type and initial data of those substances should be checked.

When the amount of dangerous chemicals increases or decreases during the accident, the sensor is activated, a signal is issued and sent to the driver's cabin to stop the car urgently, and the signal about the accident is transmitted to the server and the data transmission system installed in the vehicle is activated.

Table 2.
Hazardous chemicals and their types

Classes	Description
I	Explosives and articles
II	Gases, flammable, non-flammable and toxic gases
III	Flammable liquids
IV	Combustible solids, self-reactive substances and solid desensitized explosives
V	Substances prone to spontaneous combustion
VI	Substances that emit flammable gases in contact with water
VII	Oxidizing agents
VIII	Organic peroxides
IX	Toxic substances
X	Infectious substances
XI	Radioactive material
XII	Corrosive substances
XIII	Various dangerous substances and objects

The width and length of the area where hazardous chemicals were spilled (flowed), taking into account their density and the height of the spillage on the bottom surface should be determined here (Javoronkov, 1985, p. 9-10).

Thus, the following are the main parameters influence of the recontamination cloud depth on a chemical waste facility and spilling (flowing) of chemicals during an accident:

- the area where the dangerous chemical substance was spilled (flowed),
- height of liquid layer (thickness of poured layer),
- degree of chemicals infiltration into the subsurface.

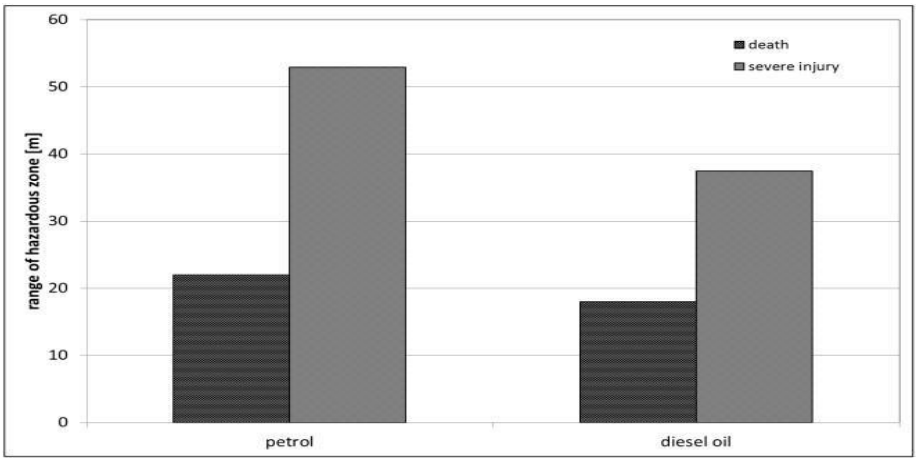

Figure 6. Danger indicators during the combustion of gasoline and diesel chemicals during an accident

ISSN: 2707-1146
e-ISSN: 2709-4189

The transport of hazardous chemicals can be defined as the elements (people, goods and infrastructure) affected during and after an accident. There are two types of risk mitigation measures:

1. On reducing the level of damage and losses and on their prevention.
2. Protection, which consists of reducing the level of danger.

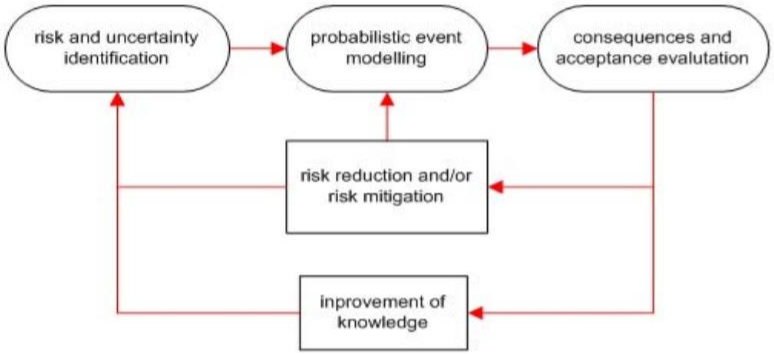

Figure 7. The main principle scheme of risk assessment

The process of optimizing the route for transporting hazardous chemicals, a cost-benefit analysis is performed that does not take into account the effects of a possible accident on the biotic and abiotic components of a specific area. These effects are associated with pollutant effects on people and energy caused by emissions of pollutants around the crashed vehicle. This pollutant activity is highly complex and stochastic, largely controlled by the meteorological conditions (mainly winds) prevailing at the time and at the site of the accident. In this case, the affected area is relatively large. Consequently, quantifying and evaluating the associated sequelae is a difficult challenge (Savchuk, Kreitor, Aksenov, 2018, p. 2-4).

According to the duration of the effectiveness of their damaging effects, hazardous substances are divided into different components:

a) fast-acting unstable dangerous chemicals (cyanic acid (HCN), ammonia (NH_3), carbon monoxide (CO));

b) slow-acting unstable ones (phosgene ($COCl_2$), nitric acid (HNO3));

c) quick-acting persistent ones (phosphorus-organic compounds ($RP(OH)_2$), aniline ($C_6H_5NH_2$);

d) slow-acting persistent ones (sulfuric acid ($H2SO_4$), dioxin (belongs to the group of the most toxic substances), etc.).

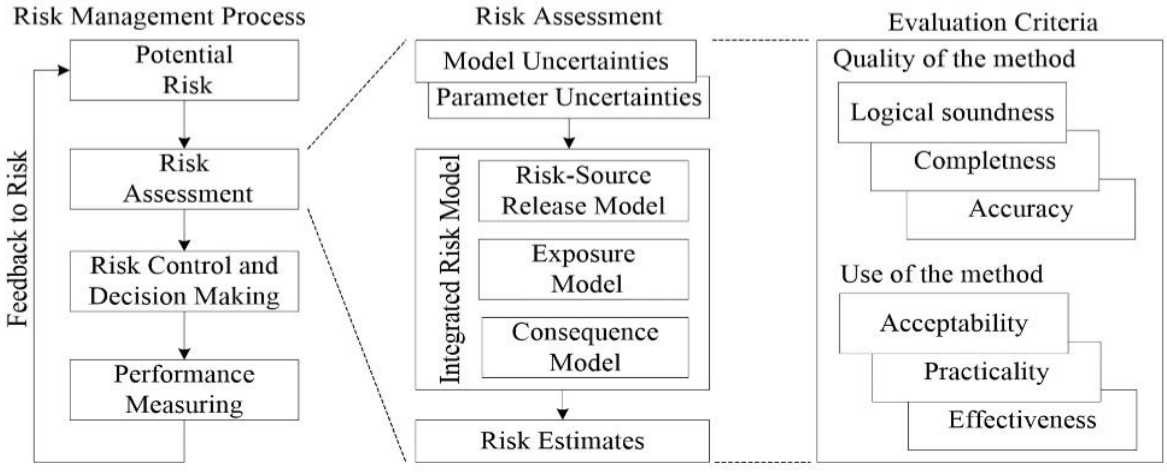

Figure 8. Evaluation criteria of risk assessment as a part of risk management process

ISSN: 2707-1146
e-ISSN: 2709-4189

The following are the main criteria used when selecting routes within the methodology:

1. Considering the current distribution of source destinations.
2. Partial use of the most used roads for the movement of vehicles for the transportation of dangerous goods.
3. Greater use of roads reserved for freight transportation.
4. Minimize the distance between the source and destination points as much as possible.
5. Reduce the size of the potentially affected area by narrowing the choice of roads under existing conditions (Ojagov, 2009, p. 377-381).

Experimental studies were conducted in order to detect the leakage rate of the spilled area and known types of hazardous chemicals to the subsurfaces. The data collected as a result of experimental studies in order to find out the area where the spill happened are shown in Figure 1. On the basis of various types of experiments, the spread area coefficient (D_{nmb}) of known types of hazardous chemical substances is determined by the following formula:

$$D_{nmb} = \frac{C_{iasds}}{C_{isctds}}$$

according to the coefficients shown here, C_{iasds} – dispersion (flow) area of b-type dangerous chemicals on m-type subsurface, m^2; C_{isctds} – is the y-type dispersion area of hazardous chemicals on an ideal smooth surface (glass), m^2.

When organizing the transportation of hazardous chemicals, the main activity is to ensure safety. The organization as a whole must be protected from various types of threats and dangerous events. Prevention of damages and losses that may occur as a result of the accidental spillage of hazardous chemicals, as well as hazard risk assessment should be conducted regularly. All environmental factors must be taken into account during risk assessment. The supply or area where the second source of danger is created must be controlled.

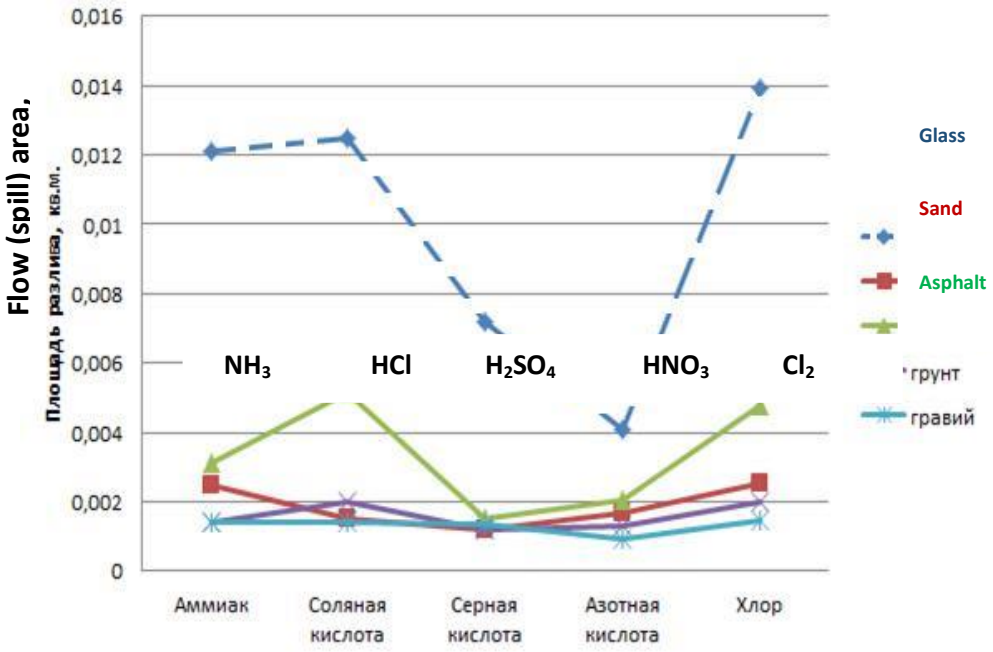

Figure 9. The main results of experimental studies to determine the area of flow (spill) of hazardous chemicals on different surfaces

Mathematical models of the optimized method for the hazard risk assessment during the substance transportation by road vehicles and the implementation of the software on electronic computers are presented. The probability of chemicals release during an accident is a result of the

ISSN: 2707-1146
e-ISSN: 2709-4189

speed of motor vehicle accidents involving hazardous materials and the probability of release of the hazardous chemical (Savchuk, Kreitor, Aksenov, 2018, p. 2-40).

So, based on the experimental data, it is possible to calculate the infiltration coefficient using the following formula (N_{in}):

$$N_{in} = \frac{S(t_e)}{S_{beg}}$$

according to the coefficients indicated here, $S(t_e)$ – the volume occupied by hazardous substances in the cylinder during the exposure period, m^3;

S_{beg} – initial volume of dangerous chemical substances in the cylinder, m^3; te is the exposure time calculated from the beginning of the experiment, min.

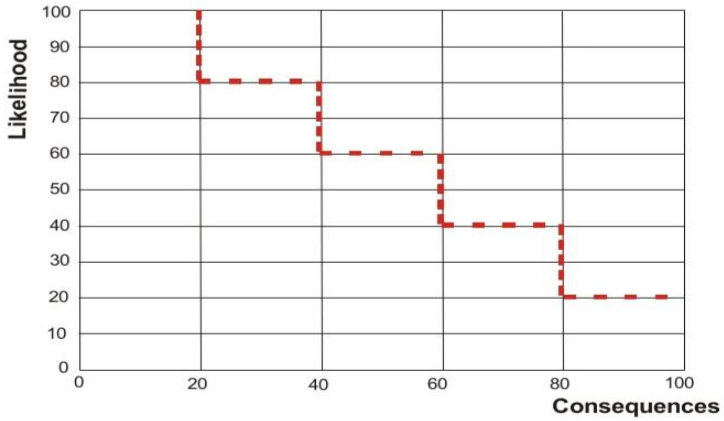

Figure 10. Risk matrix

During the conducted experiment, the rate of infiltration of dangerous substances into the deeper surfaces after partial leakage into the ground was determined. In many cases of accidents, several chemicals are transported in the same container. Therefore, it is possible for several chemicals to be released into the atmosphere at the same time, either when there are several chemicals in one spilled container, or when several containers are broken (Moroz, 2020, p. 124-135).

Industrial requirements as well as a number of human activities depend on the daily transportation of dangerous goods. The percentage of traffic accidents involving hazardous chemicals is increasing every year. The consequences of those accidents cannot be compared with simple collisions in terms of seriousness. Due to the dangerous properties of the cargo (toxicity, flammability, corrosiveness, etc.), the risks arising during transportation can extend a wide radius to the affected area in the event of an accident. The risk assessment methodology during road transportation of hazardous chemicals has been developed. Two critical factors were considered. The first is the probability of consequences (release of toxic materials, various types of fires and explosions of flammable materials) in the event of an accident, which is calculated by analyzing the consequences. The second is the consequences of the result (thermal radiation, overpressure, toxic load) and calculated by modeling.

ISSN: 2707-1146
e-ISSN: 2709-4189

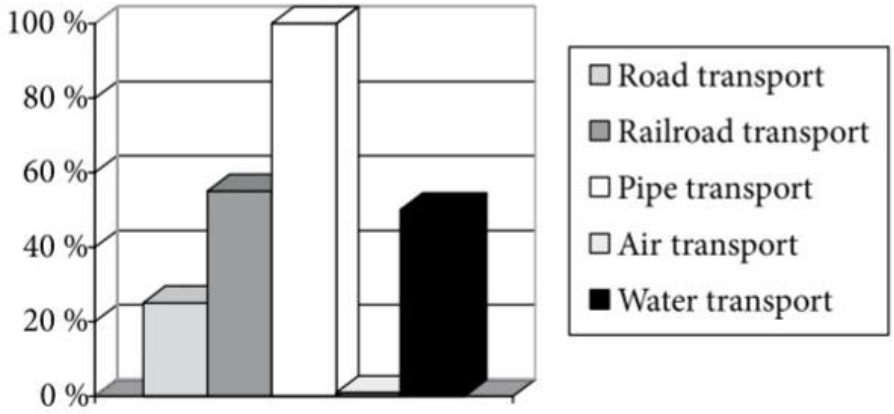

Figure 11. Statistics of vehicles causing dangerous chemical accidents

One of the important conditions is the assessment of the area width where hazardous chemicals are spilled (flowing) and its height in the braking area, which ultimately affects the depth of chemical pollution and is determined by the amount of substances flowing into this area (Smith, 2019, p. 124-135).

For transporting dangerous chemicals, the following measures should be taken into account and the hazard risk assessed:

1) the technical basis of the type of transport (for example, the basis for road transport is better than for railway transport),
2) security guarantees,
3) the length of the road,
4) shipping cost,
5) cost of cargo,
6) chemical properties and amount of material,
7) personnel training and knowledge base,
8) route,
9) climatic conditions.

Risk management process is a set of procedures that can be used in the chemicals transportation to reduce risks. The first step in the risk management process is to identify all potential risks. The next step, which is the objective of the present work, is to assess the identified risks to provide decision makers with powerful tools for the third step of the process. In the third step, decision makers must consider the results of the risk assessment before selecting appropriate and effective security control measures that lead to the necessary risk reduction. Finally, measuring the performance of proposed and implemented security controls completes the risk assessment process by providing feedback for the first step. In general, risk exists when three conditions are met. First, there must be a risk source, which can be a system, process or activity that can release the risk indicator. Second, there must be an exposure process through which people can be exposed to the released risk indicator. Third, there must be a causal process by which exposure to the risk indicator leads to undesirable consequences. The final output will be estimates of possible undesired human health outcomes, including a characterization of the probabilities and uncertainties associated with these estimates. Based on the above, a complete risk assessment consists of four interrelated but distinct steps:

- assessment of releases,
- exposure assessment,
- impact assessment and risk assessment.

ISSN: 2707-1146
e-ISSN: 2709-4189

The future, attempts will be made to incorporate these uncertainties in a more extensive uncertainty analysis using Monte Carlo techniques. The Monte Carlo analysis included not only probability distributions for a number of key variables, but also several proposed improvements to the methodology considered for the deterministic approach. Notable among these changes in approach is the recognition that vehicle accidents will result in spills of the same or different chemicals from the vehicle. The inhalation health effects of a mixture of vapors of various chemicals were included in a Monte Carlo analysis.

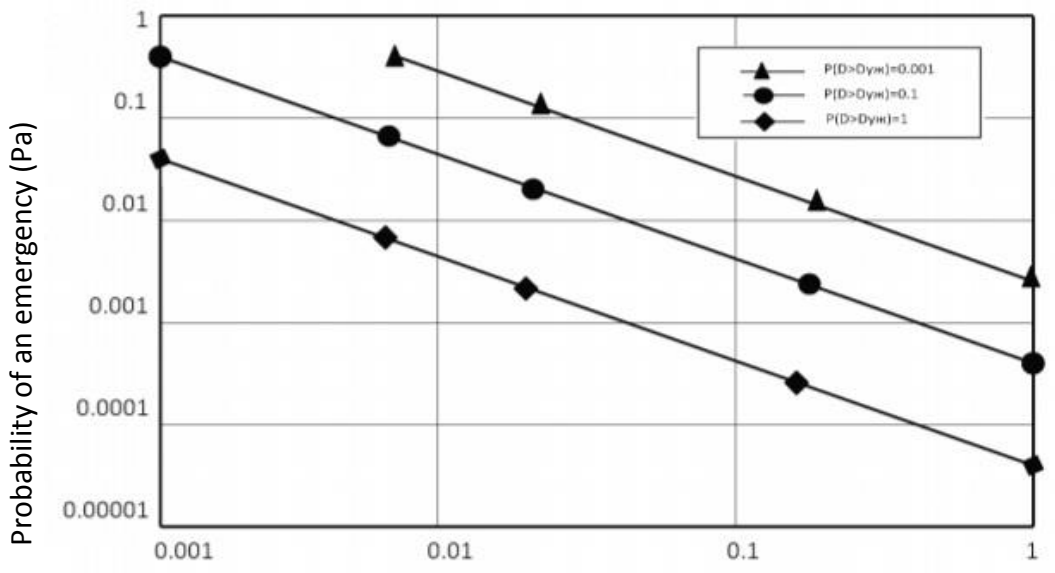

Figure 12. **Scale for assessing the adverse effects risk of hazardous substances**

Damages and losses depend on many factors, such as the amount and type of hazardous chemicals released, the extent of contamination, etc. Both dangerous goods transport risk factors are related to each other because damage will occur in an accident, but damage is not always the direct cause of the accident, so the first factor is more important and plays a bigger role in the justification. transport choice problem; but the second factor should not be forgotten, because it also plays an important role. The probability of loss factor is directly related to the loss of money, because now much attention is paid to their protection (Garcia, 2018, p. 300-308).

The risk criteria have been determined for the specified cities and are expressed as follows:

- Severe risk $F>0,1/N$
- Mild risk $F<10^{-4}/N$

Transportation of hazardous chemicals and risk assessment of stationary facilities for the population and the environment is carried out as follows:

- Severe risk $F>10^{-3}/N^2$ və ya $10\leq N\leq 10000$ fatalities
- Mild risk $F<10^{-5}/N^2$ və ya $10\leq N\leq 1000$ fatalities

ISSN: 2707-1146
e-ISSN: 2709-4189

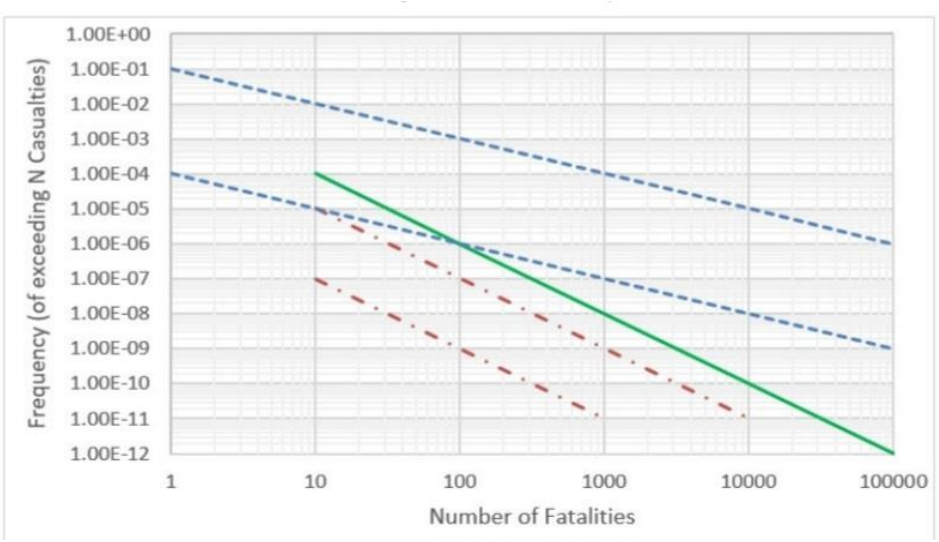

Figure 13. Public risk values for transportation of hazardous chemicals

In order to design an information system that can manage the transportation infrastructure of hazardous chemicals, it is necessary to organize a classification hierarchy that can be related to management. This classification is as follows:

- strategic level,
- tactical level,
- operational level,
- level of control real-time.

Figure 14. Risk classification

The individual risk is defined as the probability in a year that an exposed person, positioned at a precise distance to the source of risk, is hit by the undesired effects of the event. This is formally defined by the following expression:

$$I_r = P_f \cdot P_{df}$$

here P_f – is the probability of accident happening; P_{df} – is the probability of death of the individual if the accident happened.

ISSN: 2707-1146
e-ISSN: 2709-4189

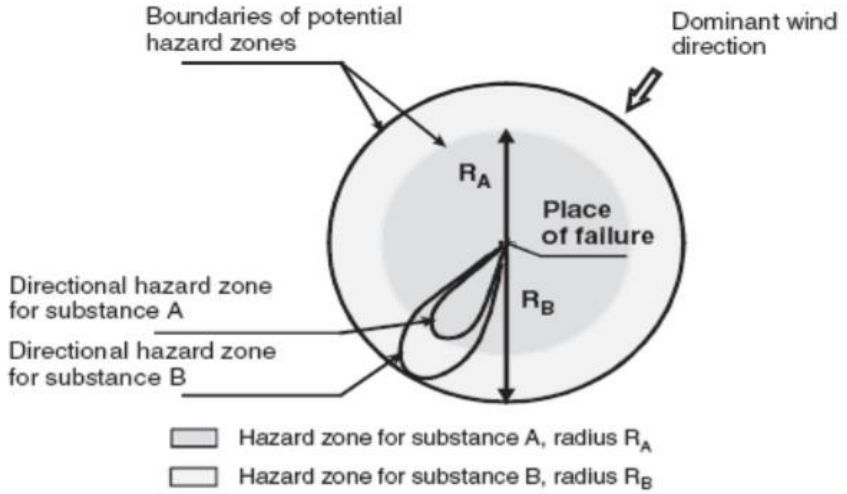

Figure 15. Potential hazard zone, defined after an accidental release of a dangerous goods into the air

The frequency of accidents during the transportation of dangerous chemicals is determined by the following expression:

$$f_i = \gamma_i \cdot L_i \cdot n_i \text{ or } \gamma_i = \gamma_0 \cdot \sum_{j=1}^{6} h_j$$

here γ_i – frequency expected on the i-esimo stretch of roa, (accidents km-1 per vehicle); L_i – road length, km; n_i – number of vehicles; γ_0 – basic frequency (accidents km-1 per vehicle); h_j – parameters of amplification / local mitigation.

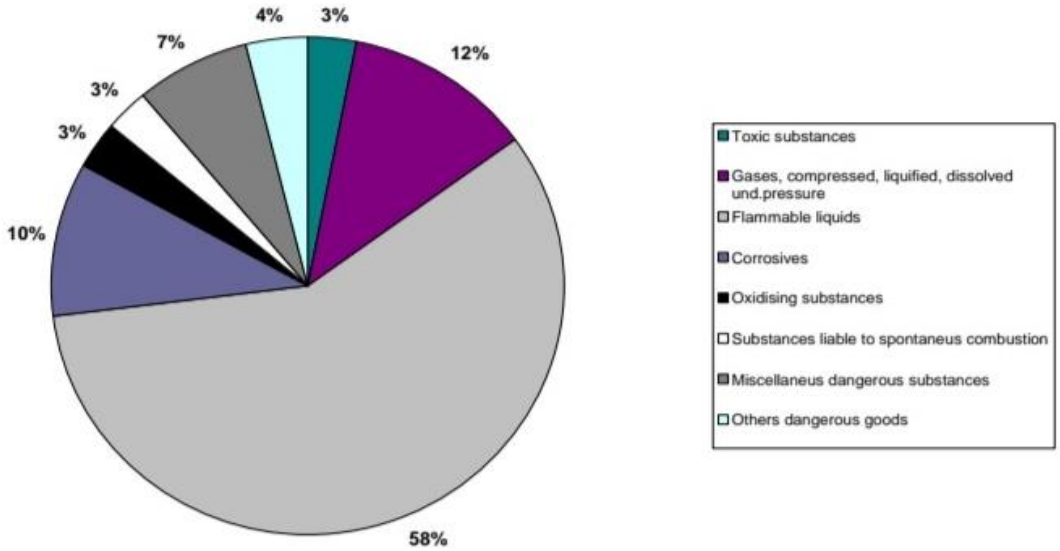

Figure 16. Dangerous goods transported by road

Conclusion

1) A digital procedure for calculating individual and public risks arising from the transportation of hazardous chemicals by road has been presented. It is designed to support decision makers in safety management and safety control activities as well as to transport toxic and flammable substances. In particular, the proposed equation for calculating the individual risk takes into account both the prevailing wind and the current seasonal condition. With regard to social risk,

population distribution modeling is described that takes into account the presence of the population in closed spaces as well as the differences between off-road and on-road populations.

2) During the study, a new man-made risk prevention system was proposed, which revised the risk assessment criteria and included the analysis of existing measures, and had a clearer formulation of the criteria and a simpler methodology of the risk calculation form. It allows employees to assess possible risks while performing work at each stage and to determine preventive measures in advance.

3) For the transportation of dangerous goods, we must consider and evaluate these key aspects:

- the technical basis of the type of transport; the length of the road;
- shipping cost;
- chemical properties of the material and its amount;
- staff training and knowledge base, route;
- climatic conditions;
- the level of probable damage.

4) Risk assessment allows carriers to choose basic transportation criteria, flexibility, and use alternatives. Using risk assessment, it is possible to reduce the probability of an accident and increase traffic safety.

5) Solving risk assessment tasks will allow finding the minimum risk using the same technical and technological means.

6) The causes of accidents are usually man-made, including transport accidents involving dangerous chemicals that expose people to risks with serious consequences. The accident risk is characterized by the local source of danger (leakage of dangerous substances or fire), the magnitude of the danger depends on the distance from the center of the accident. As a large number of people often suffer from accidents, it can be shown as both an individual and a social risk.

References

1. Alexandrovich, A. A. (2020). Chemical hazard risk assessment during road transport of hazardous chemicals. Topic and abstract of the dissertation at the Higher Attestation Commission of the Russian Federation.
2. Gasimov, C. N. (2017). *Emergencies and the environment (textbook).*
3. Gasimov, C. N., Abdullayeva, N. Z. *Dangerous factors of emergencies (teaching material).* Printing house of AzTU.
4. Gasimov, C., Abdullayev, M., Huseynov, A. (2009). *Civil defense. Synopsis of lectures (tutorial for higher schools).* Printing house of AzTU.
5. Aksenov, A. A. (2020). Ways to improve measures to ensure the safety of transportation of dangerous chemically dangerous substances by road transport in the Republic of Mordovia based on the risk assessment of chemical hazards. *"Problems of risk management in the technosphere" scientific-analytical magazine*, 1(53), 56-63.
6. Daineka, A. D. (2023). Increasing the efficiency of transportation of dangerous goods using information technologies. *Transport technic and technology,* 28(475), 17-21.
7. Rasulov, S. R., Badalova, A. N., Safarov, S. H., Ganiyeva, R. Y. (2023). *Transport ecology (textbook).* ASOSU Publication.
8. Snurnikov, A. S. (2023). Risk minimization strategies for transporting dangerous goods on highways. *Occupational safety in industry*, 52(499), 385-397.
9. Javoronkov, N. Yu. (1985). *Risk assessment of chemical hazards of substances and materials transported by water transport.*
10. Savchuk, O. N., Kreitor, V. P., Aksenov, A. A. (2018). Ways to improve the methodology of risk assessment of chemical hazards based on the transport of damage by motor vehicles. 27(10), 2-4.
11. Ojagov, H. O. (2009). *Eliminating the consequences of emergencies (textbook for higher schools).* Printing house of "TI-MEDIA" company.

12. Moroz, E. V. (2020). *Problems of legal regulation of international road transport of dangerous goods.*
13. Smith, J. (2019). *Transportation of Hazardous Materials: Risk Mitigation Strategies*. Wiley.
14. Garcia, L. (2018). *Strategies for minimizing risks in the transportation of dangerous goods.*

Received: 12.05.2024
Revised: 05.07.2024
Accepted: 20.07.2024
Published: 20.08.2024

ISSN: 2707-1146
e-ISSN: 2709-4189

https://doi.org/10.36719/2707-1146/47/38-43

Arzu Mammadova
Institute for Space Research of Natural Resources
arzu-mamedova1965@mail.ru
Durdana Aliyeva
Institute for Space Research of Natural Resources
elmitexnikisobe@mail.ru
Sevda Jalalova
Institute for Space Research of Natural Resources
sevka_b@mail.ru
Tahira Hasanova
Institute for Space Research of Natural Resources
azerbaycan9195@mail.ru

Metal-Based Matrix Materials

Abstract

One of the components of the fuel composition of dispersion nuclear fuel is a non-fissile material (matrix), which ensures its high radiation resistance. Despite the fact that dispersion nuclear fuel is used in reactors of various purposes (research, power, nuclear power plants, etc.), the operating conditions of which vary significantly, there are a number of requirements that must be taken into account when choosing the matrix material. Metals (aluminum and zirconium, as well as their alloys) have found wide application as matrix material in the production of dispersion-type fuel elements for research reactors and reactors of naval nuclear power plants (NPPs). Stainless steel matrix is used in dispersion nuclear fuel in power reactor plants.

Keywords: *metal, matrix, materials, components, composition*

Introduction

In table 1 provides data on the absorption cross-section of thermal neutrons of metals. The thermal neutron absorption cross section of alloys is defined as the sum of the products of the nuclear concentration and the absorption cross section for each component of the alloy, divided by the total number of nuclei in a gram of alloy (Degueldre, 1999, p. 274).

Table 1.
Absorption cross-sections of thermal neutrons of metals

Elements	Thermal neutron absorption cross section $10^{-24}sm^2$
Beryllium	$10 \cdot 10^{-2}$
Carbon	$3,7 \cdot 10^{-3}$
Nitrogen	1,9
Oxygen	$2,0 \cdot 10^{-4}$
Magnesium	$7,0 \cdot 10^{-2}$
Aluminum	0,24
Silicon	0,16
Zirconium	0,18
Niobium	1,16

ISSN: 2707-1146
e-ISSN: 2709-4189

Chromium	3,1
Titanium	5,8
Vanadium	5,0
Manganese	13,2
Iron	2,6
Nickel	4,6
Copper	3,8
Molybdenum	2,7
Tungsten	19,2
Tantalum	21,0

Aluminum and its alloys

Aluminum and its alloys are widely used as a matrix of dispersion fuel composition for research reactor fuel elements due to good nuclear and thermal properties, as well as excellent technological qualities. However, aluminum has low strength and unsatisfactory corrosion resistance. At the operating temperatures of most research reactors (100–150 °C), these disadvantages have little effect on the performance of fuel elements (Skorov, 1979, p. 344).

To improve the mechanical properties of aluminum, it is alloyed with magnesium, zinc, silicon, copper, silver, lithium, and gallium. The greatest effect in improving the mechanical properties of aluminum is achieved with simultaneous alloying with several elements. Aluminum alloys after heat treatment with precipitation hardening have good long-term mechanical properties (Tsykanov, 2000, p. 249).

Table 2.
Mechanical properties of some aluminum alloys before and after irradiation with a neutron flux

Alloy brand	□, *MPaB*	□0,2□, *MPa*	□ , %
	Before/after irradiation	Before/after irradiation	Before/after irradiation
AD1	95/180	47/120	38/21
SAB– 1	290/330	245/280	11/10
6061 (USA)	315/350	270/310	17,5/16

Under reactor irradiation conditions, the properties of structural materials change, and their plasticity is greatly reduced. Reactor irradiation has little effect on the mechanical properties of aluminum and its alloys. It is noteworthy that aluminum and its alloys practically do not lose plasticity when irradiated, but the strength of aluminum and alloys increases. The effect of irradiation on the mechanical properties of aluminum and its alloys is characterized by the data presented in figure 1.

ISSN: 2707-1146
e-ISSN: 2709-4189

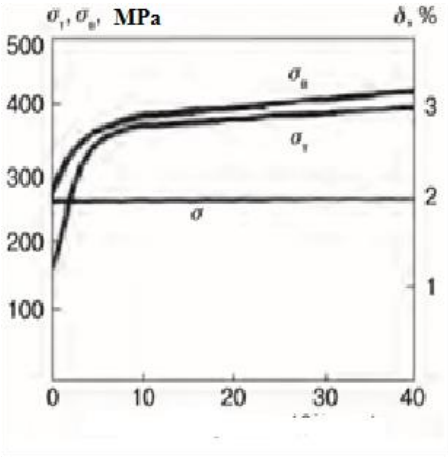

a)

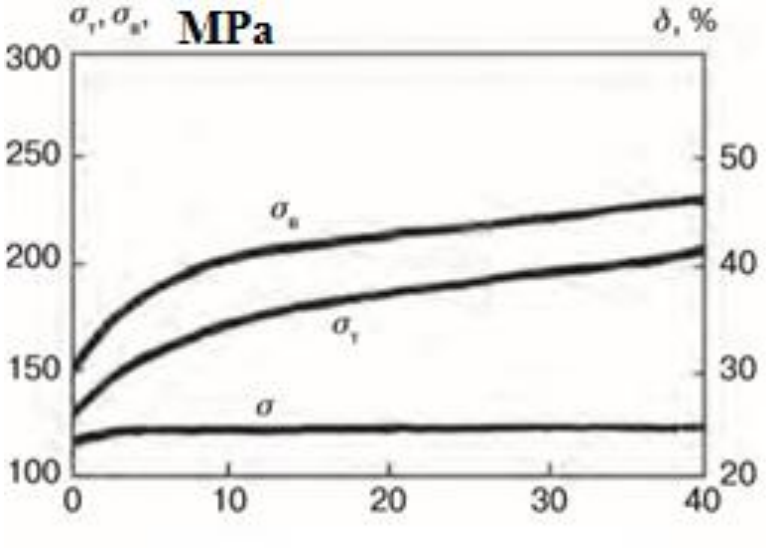

b)

Figure 1. Effect of irradiation on the mechanical properties of technical aluminum (a) and Al + 7 % Si alloy (b)

From the analysis of the presented dependencies (Figure 1) it follows that the greatest change in properties occurs up to a neutron flux of (3–5)•1021 cm–2. The available data show that technical aluminum containing iron, silicon, copper and other impurities can be successfully used as a matrix of the fuel composition of dispersion nuclear fuel up to temperatures of 100–130 °C. Technical aluminum with the addition of nickel is used as a matrix of the fuel composition of dispersion nuclear fuel in nuclear power reactors with pressurized water at temperatures up to 215–230 °C (Samoilov, 1982, p. 224).

Zirconium and its alloys

Zirconium and its alloys are widely used in nuclear power engineering due to the combination of their properties: nuclear, chemical and technological. However, these properties manifest themselves if zirconium is purified from hafnium, with which it is usually found in nature. Before use in nuclear technology, zirconium is usually subjected to iodine refining. Zirconium has found wide application as a matrix material in reactors of naval nuclear power plants (Beskorovayny, 1995: 324).

Currently, the existence of three phases of zirconium has been established: α-phase (T > 862 °C), β (T = 862–1855 °C) and unstable ω-phase (P > 6 GPa). During phase transformation, volumetric changes occur, which must be taken into account when determining the operating conditions of zirconium products (EMT, 1964, p. 127).

ISSN: 2707-1146
e-ISSN: 2709-4189

Figure 2 shows the effect of alloying elements on the strength of zirconium. The most important alloying elements used in zirconium alloys are niobium and tin.

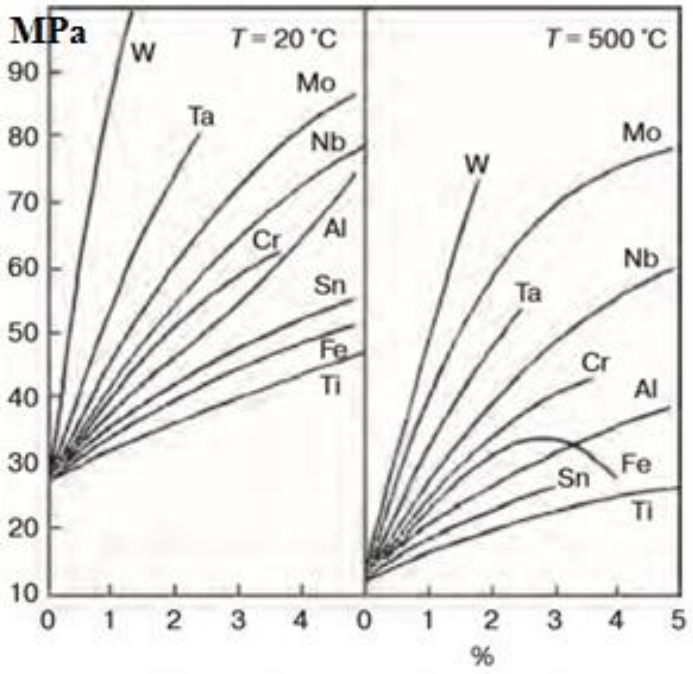

Figure 2. Effect of alloying element content on the strength of zirconium at different temperatures

As follows from the data in Figure 2, niobium, having a relatively small cross-section for capturing thermal neutrons, significantly increases the strength of zirconium both at room temperature and at 500 °C. In our country, zirconium alloys with a niobium content of 1 % (E110) and 2.5 % (E125) are mainly used. In the USA, complex alloys are used (Eidenson, 1969, p. 352).

Irradiation has a significant effect on the properties of zirconium and its alloys. When zirconium alloys are irradiated, they are strengthened with a simultaneous decrease in ductility.

Table 3 shows the data characterizing the effect of irradiation on the mechanical properties of pure zirconium. The data in Table 3 show that the change in the properties of zirconium as a result of irradiation is significant (Polmear, 2008, p. 464).

Table 3.
Effect of irradiation on the mechanical properties (at 20 °C) of zirconium annealed at 650 °C for 30 minutes

Irradiation temperature, ∘ *C*	Fast Neutron Stream 1023 neutron/m^2	□, *MPaB*		□, *MPa* 0,2		□ , %	
		Before irradiation	After	Before irradiation	After	Before irradiation	After
80	0,3	300	330	160	220	35	26
80	4,0	265	320	160	260	34	20
80	10,0	265	360	160	340	34	15
300	0,4	260	280	150	220	34	25

At a fast neutron flux of 1023 neutrons/m2, the ultimate strength increases by a maximum of 36 %, the yield strength by 112 %, and the elongation decreases by 68 %. According to, the zirconium alloy E635 is practically not subject to radiation growth at an irradiation temperature of 80 and 300 °C (Calliot, 1963, p. 1).

In nuclear technology, zirconium and its alloys are widely used as fuel element cladding materials. Information on the use of these materials as inert matrices for nuclear fuel dispersion compositions is extremely limited (Samsonov, 1978, p. 472).

Nickel

Nickel was used as a matrix for the dispersion fuel composition in the SM-2 reactor. It does not undergo allotropic transformations. The thermal conductivity of nickel is higher than that of stainless steel (CSNCT, 2001, p. 23).

At a temperature of 100 °C, its thermal conductivity is 83 W/(m•°C). A distinctive feature of nickel is the combination of high strength and elastic modulus with good plasticity (σ = 30–40 %) (SPR, 2001, p. 15).

Along with thermal conductivity, long-term strength characteristics have a significant impact on the performance of the dispersion fuel composition. Figure 3 shows the long-term strength data, and Figure 4 shows the dependence of the creep rate of nickel on stress at different temperatures (Alekseev, 2013, p. 240).

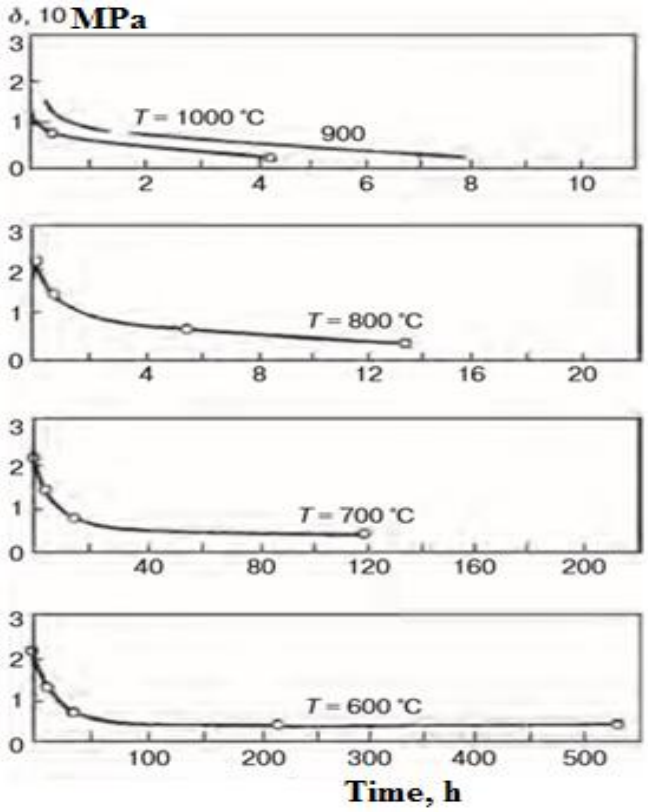

Figure 3. Long-term strength of nickel at different temperatures

Conclusion

Study of the effect of neutron irradiation in a reactor on the mechanical properties of nickel showed a sharp drop in plasticity in irradiated nickel at a temperature of 600 °C and above, while strength increases. Figure 5 shows the effect of temperature on the mechanical properties of technical nickel, unirradiated and irradiated to a neutron flux of 1.7•1020 cm–2, at a temperature of 150–200 °C. According to the data in Figure 5, up to a temperature of 400 °C, typical for research reactors, the plastic properties of nickel remain quite high.

ISSN: 2707-1146
e-ISSN: 2709-4189

References

1. Degueldre, C., and Paratte, J. (1999). *Journal of Nuclear Materials*, 274.
2. Skorov, D. M., Bychkov, Yu. F. (1979). *Reactor Materials Science.* 2nd ed. Atomizdatsh.
3. Tsykanov, V. A. (2000). *Fuel Elements for Research Reactors*. SSC RF NIIAR.
4. Samoilov, A. G., Kashtanov, A. I. (1982). *Dispersion Fuel Elements. Materials and Technology*, 1, 224.
5. Beskorovayny, N. M. (1995). *Structural materials of nuclear reactors*. Energoatomizdat.
6. Tumanov, A. G. (Ed.) (1964). Encyclopedia of modern technology: Structural materials (Vol. 2). Soviet Encyclopedia.
7. Eidenson, M. A. (1969). *Magnesium*: *Metallurgy.*
8. Polmear, Ya. (2008). *Light alloys from traditional to nanocrystals*. Tekhnosfera.
9. Calliot, R. (1963). Reasons for choosing Mg-Zr alliance to gain combustible elements. *Journal of Nuclear Materials*, 8(1), 1.
10. Samsonov, G. V. (1978). *Physical and chemical properties of oxides*. Handbook.
11. International Atomic Energy Agency. (2001). *Current status of neutron capture therapy* (IAEA-TECDOC). International Atomic Energy Agency.
12. International Atomic Energy Agency. (2001). *Strategic planning for research* (IAEA-TECDOC-2212). International Atomic Energy Agency.
13. Alekseev, S. V., Zaitsev, V. A. (2013). *Nitride fuel for nuclear power engineering*. Tekhnosfera.

Received: 02.05.2024
Revised: 16.07.2024
Accepted: 28.07.2024
Published: 20.08.2024

ISSN: 2707-1146
e-ISSN: 2709-4189

https://doi.org/10.36719/2707-1146/47/44-48

Rena Gulamova
Institute for Space Research of Natural Resources
rena145@mail.ru
Chingiz Mursaliyev
Institute for Space Research of Natural Resources
cingizmurseliyev0@gmail.com
Rena Isayeva
Institute for Space Research of Natural Resources
isayeva57@mail.ru
Imran Mammadov
Institute for Space Research of Natural Resources
baki194@mail.ru

Plasma Chemical Synthesis Research

Abstract

When using uranium – 238, thorium – 232 and plutonium – 239 isotopes, there is no need for expensive isotopic enrichment, and the use cycle of such nuclear fuel can be extended to 10-15 years. At the same time, the predicted reserves of thorium in the earth's crust are 3-5 times greater than uranium, and the use of ceramic nuclear fuel from oxide compositions based on thorium will make it possible to create ultra-small and small power plants for use in remote and hard-to-reach regions, in mines and quarries. However, ceramic nuclear fuel still has a significant drawback – low thermal conductivity. One of the promising areas for the further development of nuclear energy is the use of dispersion nuclear fuel, in which inclusions of fissile metals (uranium, thorium, plutonium) in the form of granulated oxide compositions (microspheres) are placed in a matrix with a high thermal conductivity coefficient.

Keywords: *plasma, chemical, synthesis, methods, nitrides*

Introduction

One of the most common chemical methods for obtaining highly dispersed powders of nitrides, carbides, borides and oxides is plasma-chemical synthesis. The main conditions for obtaining highly dispersed powders by this method are the reaction occurring far from equilibrium and a high rate of formation of new phase nuclei at a low rate of their growth. In real conditions of plasma-chemical synthesis, it is advisable to obtain nanoparticles by increasing the cooling rate of the plasma flow in which condensation from the gas phase occurs; due to this, the size of the resulting particles is reduced, and the growth of particles by merging during collisions is suppressed. In plasma-chemical synthesis, low-temperature (4000-8000K) nitrogen, ammonia, hydrocarbon, argon plasma of arc, glow, high- or ultra-high-frequency discharges is used; elements, their halides and other compounds are used as feedstock (Parkhomen, 1991, p. 166-170).

The characteristics of the resulting powders depend on the raw materials used, the synthesis technology and the type of reactor. Particles of plasma-chemical powders are single crystals and have sizes from 10 to 100-200 nm and more. Plasma-chemical synthesis ensures high rates of formation and condensation of the compound and is characterized by fairly high productivity (Dorzet, 1978, p. 103-110).

The main disadvantages of plasma-chemical synthesis are a wide distribution of particle sizes and, as a result, the presence of fairly large (up to 1-5 μm) particles, i.e. low selectivity of the process, as well as a high content of impurities in the powder. To date, the plasma-chemical method has been used to obtain highly dispersed powders of titanium, zirconium, hafnium, vanadium, niobium, tantalum, boron, aluminum and silicon nitrides, titanium, niobium, tantalum, tungsten, boron and silicon carbides, magnesium, yttrium and aluminum oxides (Dulnev, 1974, p. 264).

ISSN: 2707-1146
e-ISSN: 2709-4189

The plasma-chemical method is most widely used for the synthesis of nitrides of transition metals of groups I\/ and \/. The plasma temperature, reaching 10,000 K, determines the presence of ions, electrons, radicals and neutral particles in an excited state. The presence of such particles leads to high rates of interaction and rapid reactions. High temperature ensures the transition of almost all initial substances to a gaseous state with their subsequent interaction and condensation of products. Plasma-chemical synthesis includes several stages. Powders obtained by plasma-chemical synthesis have a regular shape and particle size from 10 to 100 nm and more (Misnar, 1968, p. 464).

Plasma-chemical powders of metal, boron and silicon carbides are usually obtained by the interaction of chlorides of the corresponding elements with hydrogen and methane or other hydrocarbons in argon high-frequency or arc plasma; nitrides are obtained by the interaction of chlorides with ammonia or a mixture of nitrogen and hydrogen in low-temperature microwave plasma. Using plasma-chemical synthesis, it is also possible to obtain multicomponent submicrocrystalline powders, which are mixtures of carbide and nitride, nitride and boride, nitrides of different elements, etc. Synthesis of oxides in electric arc discharge plasma is carried out by evaporation of metal with subsequent oxidation of vapors or oxidation of metal particles in oxygen-containing plasma (Polmear, 2008, p. 464).

Plasma-chemical synthesis of aluminum oxide nanoparticles with an average size of 10-30 nm is described. It follows from the results of this work that the formation of aluminum oxide nanopowders with a minimum particle size is achieved by the interaction of metal vapors with atmospheric oxygen under conditions of intense air injection, due to which a rapid decrease in temperature occurs. Plasma-chemical synthesis with the oxidation of aluminum particles in a flow of oxygen-containing plasma leads to the formation of larger oxide particles compared to the oxidation of pre-obtained metal vapor. Gas-phase synthesis using laser heating of the reacting gas mixture is quite closely related to plasma-chemical synthesis (Calliot, 1963).

The reliability and cost-effectiveness of the synthesis of nanopowders in laser-stimulated gas-phase reactions make this method quite competitive compared to other methods. Laser heating ensures controlled homogeneous nucleation and eliminates the possibility of contamination. Such a material should consist of hollow spherical molecules, the shell of which is built of graphite sheets, and 5-membered cycles should be included in the network of hexagonal rings of C60 for stability. However, no one noticed that a similar design had already been proposed in 1951 by the famous American architect (Samsonov, 1978, p. 472).

Fuller, who patented a structural basis for the construction of spherical structures - the so-called geodesic dome. Such a dome design was used, for example, in the construction of the US pavilion at the Expo 67 World Exhibition in Montreal. Fullerenes are obtained by electric arc spraying of graphite in an He atmosphere; the gas pressure is 1.33. 104 Pa. As a result of the combustion of the arc, soot is formed, which condenses on the cold surface (Alekseev, 2013, p. 240).

After evaporation of the solution, a black condensate is formed, which consists of about 10-15 % of a mixture of fullerenes. To obtain fullerenes, instead of an electric arc, electron beam evaporation and laser heating are also used. The central place among fullerenes belongs to the C molecule, which has the highest symmetry and, as a consequence, the greatest stability. In shape, the fullerene molecule resembles a football cover and has the structure of a regular truncated icosahedron (Fig. 1).

ISSN: 2707-1146
e-ISSN: 2709-4189

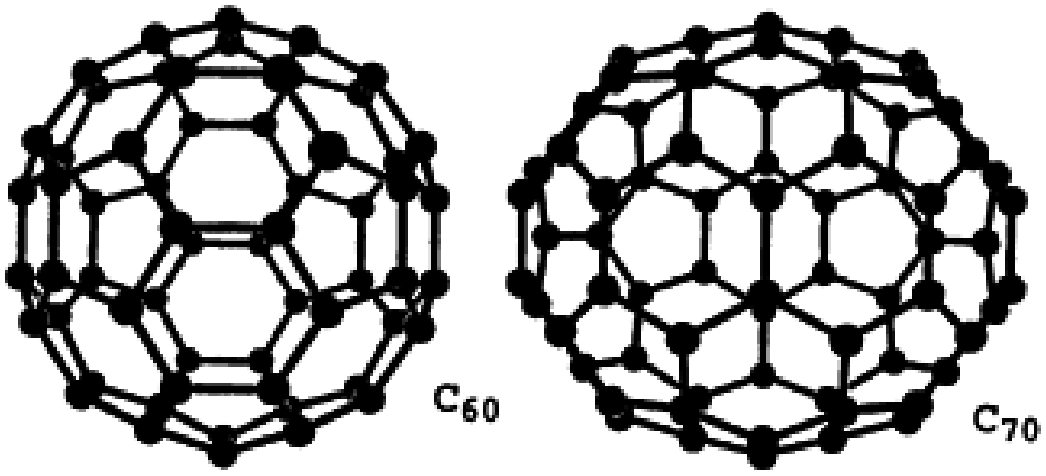

Figure 1. The structure of the most important fullerenes C60 and C70

The C60 molecule is built like a football and has a diameter of about 0.7 nm. All fullerenes contain hexagonal six-membered and pentagonal five-membered rings of carbon atoms. In the C60 fullerene molecule, the carbon atoms form a closed hollow spherical surface consisting of 5- and 6-membered rings, with each atom having a coordination number of three and located at the vertices of two hexagons and one pentagon. The diameter of the fullerene molecule is 0.72-0.75 nm. When C60 crystallizes from a solution or gas phase, molecular crystals with an FCC lattice are formed; the lattice parameter is 1.417 nm. Fullerene in the solid state is called fullerite. Fullerene (270, which has the shape of a closed spheroid, also has high stability. Fullerenes can be considered as a spherical form of graphite, since the mechanisms of interatomic bonding in fullerene and bulk graphite are very similar to a large extent (Hollek, 1988, p. 319).

In early 2001, a group of scientists discovered a new fullerene-like form in which, compared to ordinary fullerene, a fifth of the carbon atoms are replaced by nitrogen atoms (Fig. 2). If in fullerene crystals the molecules are united by weak van der Waals forces, then the presence of nitrogen atoms leads to the appearance of strong covalent bonds. For this reason, the fullerene-like crystalline material has unique very unusual properties of fullerenes.

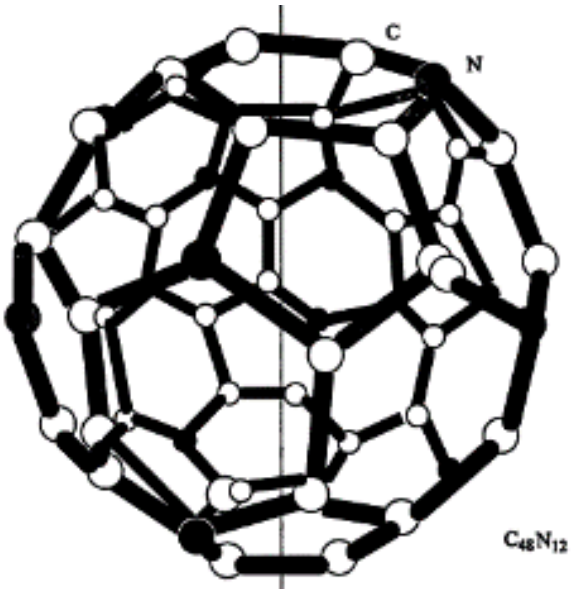

Figure 2. Fullerene structure, the solid line shows the position of the C60 symmetry axis

ISSN: 2707-1146
e-ISSN: 2709-4189

Thus, crystalline fullerenes are semiconductors and have photoconductivity, and crystals doped with alkali metal atoms.

In general, plasma-chemical synthesis with different methods of creating plasma is one of the most promising methods for obtaining various nanostructured materials.

The undoubted advantages of using plasma for plasma-chemical synthesis of oxide compositions for dispersion nuclear fuel from dispersed mixed aqueous nitrate solutions compared to the sol-gel process and technology based on separate production and mechanical mixing of metal oxides include: single-stage; high speed; the ability to actively influence the size and morphology of particles; compactness of process equipment. Figure 3 shows a diagram of plasma processing of dispersed solutions (Matzke, 1999).

The initial solution is dispersed and fed into the plasma jet. High dispersion of the droplets facilitates their faster and deeper processing. The formation of the target product can be achieved in two ways. The first is that the solution droplets evaporate completely, homogeneous chemical reactions occur in the gas phase, and when the reaction gases are cooled, nanosized particles of the target product are formed. The second way is the formation of particles due to the emergence of crystallization centers and their subsequent growth directly in a liquid drop of the initial solution, which can lead to the formation of larger particles. Mixed aqueous solutions or suspensions are used as feedstock.

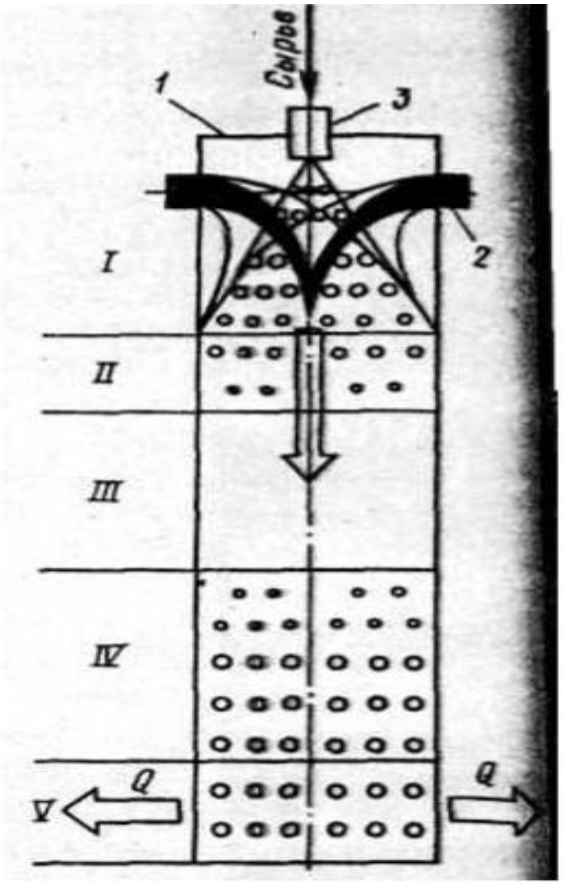

Figure 3. Scheme of plasma processing of dispersed solutions

Thermolysis of aqueous solutions of salts or suspensions is a flexible and universal method for obtaining nanosized powders of simple and complex metal oxides. Its main advantages are a large number of channels for influencing the physicochemical properties of the product, the possibility of synthesizing complex oxide compounds, as well as the high chemical activity of the resulting target products. Nitrates, sulfates, acetates, carbonates, and hydroxides of metals are used as initial compounds for the preparation of aqueous solutions and suspensions. Complex oxides are obtained

from aqueous solutions and suspensions that include compounds of several metals (CSNCT, 2001, p. 24).

However, plasma treatment of only mixed aqueous solutions and suspensions requires significant energy consumption (up to 4 MW h/t) and does not allow obtaining oxide compositions of the required stoichiometric composition in one stage without additional hydrogen reduction. Direct plasma-chemical synthesis in an air-plasma flow of complex oxide compositions (including oxides of fissile materials and a matrix of refractory metal oxides with a high thermal conductivity coefficient and low resonance absorption of neutrons) from dispersed combustible aqueous-organic nitrate solutions containing an organic component (alcohols, ketones, etc.) and having a net calorific value of at least 8.4 MJ/kg is proposed (SPR, 2001, p. 43).

Conclusion

Plasma processing of such solutions leads to a significant reduction in specific energy consumption for their processing (up to 0.1 MW h/t), will significantly increase the productivity of plasma installations, and will also provide conditions in the plasma installation reactor for direct synthesis in air plasma of nanosized complex oxide compositions with a homogeneous phase distribution, high thermal conductivity, and the required stoichiometric composition without additional hydrogen reduction.

References

1. Parkhomen, V. (1991). Plasma-chemical methods for obtaining powdered substances and their properties. *All-Union Journal of the Chemical Society named after D. I. Mendeleev*, 36, 166-170.
2. Dorzet, V. (1978). *Study of plasma processes and devices*. ITMO AN BSSR.
3. Dulnev, G. (1974). *Thermal conductivity of mixtures and composite materials: reference book.* Energy.
4. Misnar, A. (1968). *Thermal conductivity of solids, liquids, gases and their compositions: trans. from French*. Mir.
5. Polmear, J. (2008). *Light alloys from traditional to nanocrystals*. Tekhnosfera.
6. Calliot, R. (1963). Reasons for choosing Mg-Zr alloy for the gain of combustible elements. *Journal of Nuclear Materials*, 8(1), 12.
7. Samsonov, G. (1978). *Physicochemical properties of oxides: Handbook.* Metallurgy.
8. Alekseev, S. (2013). *Nitride Fuel for Nuclear Power Engineering*.
9. Hollek, H. (1988). Binary and Triple Carbide and Nitride Systems of Transition Metals: Handbook. Translated from German. edited by Yu. V. Ivenskiy, Metallurgy.
10. Matzke, H. (1999). Materials Research on Inert Matrices: a Screening Study. *Journal of Nuclear Materials*, 274(1-2), 47.
11. International Atomic Energy Agency. (2001). *Current status of neutron capture therapy* (IAEA-TECDOC-1223, p. 25). International Atomic Energy Agency.
12. International Atomic Energy Agency. (2001). *Strategic planning for research* (IAEA-TECDOC-2212, p. 52). International Atomic Energy Agency.

Received: 09.05.2024
Revised: 11.07.2024
Accepted: 30.07.2024
Published: 20.08.2024

https://doi.org/10.36719/2707-1146/47/49-53

Larisa Zakirjanova
Institute for Space Research of Natural Resources
larisa_53@mail.ru
Mirvari Jabrayilova
Institute for Space Research of Natural Resources
azerbaycan9195@mail.ru
Shahla Hajiyeva
Institute for Space Research of Natural Resources
elmitexnikisobe@mail.ru
Konul Yusupova
Institute for Space Research of Natural Resources
elxan207@gmail.com

Determination of the Chemical Composition of Oil and Gas

Abstract

Oil is a complex mixture of liquid organic substances in which various solid hydrocarbons, resinous substances and accompanying gases are dissolved. In the article various methods of separation of complex mixtures into simpler compositions were examined. The bulk of the oil components is also determined.

An important indicator in the identification of oil products is the amount of aromatic hydrocarbons in their content. In the methods used in the study of petroleum products in environmental objects, gas chromatographic analysis is preferred due to its highest selectivity, sensitivity and accessibility, using different types of detection. On the other hand, during the determination of PAHs in oils and middle distillates, in the chromatograms, the analyte appears against the background of the "naphthenic hump" and paraffins, which form fragments of molecules under electronic conditions, which overlap with each other. Fragments of molecules of substances analyzed in terms of ion mass are placed on them and their mass spectra are analyzed. When performing such analyses, it is practically impossible to identify, quantify, and accurately estimate the signal intensity of peaks associated with polycyclic condensed arenes.

Keywords: *distillation, phlegm, extraction, crystallization, molecular diffusion, adsorption, absorption, chromatography*

Introduction

Oil is a complex mixture of liquid organic substances in which various solid hydrocarbons, resinous substances and associated gases are dissolved. Separation of complex mixtures into simpler ones is called fractionation. Separation methods are based on differences in the physical, surface and chemical properties of the separated components (Syrkin, 2002, p. 92-96).

The following methods are used to separate oil into narrow homogeneous groups: distillation (atmospheric distillation and rectification, vacuum distillation and azeotropic distillation); adsorption (adsorption and chromatography); absorption (extraction) and crystallization. The most common fractionation methods are distillation. These include distillation and rectification. The essence of atmospheric distillation is that the mixture is continuously heated, with its components gradually distilled off from low-boiling to high-boiling (Ryabov, 2009, p. 17-47).

As the boiling point of the components increases, the heating temperature of the mixture being separated is also increased. By collecting fractions in predetermined temperature ranges and measuring their quantity, one can get an idea of the fractional composition of oil. The fractional composition of oil or oil products is understood to be the quantitative content of substances in oil that boil within certain temperature limits (Virzhichinskaya, 2009, p. 59-151).

Atmospheric distillation is used for rough separation into wide fractions. During factory refining of oil, the following fractions or distillates are collected:

1) gasoline (initial boiling point up to 170-200 ºC),
2) ligroin (170-200 ºC),
3) kerosene (200-270 ºC),
4) gas oil (270-350 ºC).

From these distillates, light oil products are further produced. The residue after collecting fractions up to 300-350 ºC is called fuel oil. Fuel oil is distilled into oil fractions under vacuum to prevent its thermal decomposition. Fractions are selected not by boiling point, but by viscosity. Oil distillates are divided into solar, transformer, spindle, machine, autol, and cylinder distillates as viscosity increases. The residue after distillation of fuel oil is called tar or semi-tar depending on viscosity (Ghosal, 2016, p. 13-69).

In accordance with the elemental composition, the bulk of oil components are hydrocarbons (RH). The gasoline fraction contains practically only three classes of hydrocarbons: alkanes, cycloalkanes, and benzene arenes. Bi- and tricyclic hydrocarbons make up a significant share in the kerosene and gas oil fractions. There are no unsaturated hydrocarbons with unsaturated bonds in crude oils. In addition to RH, heteroatomic organic compounds are present in the low-molecular part of the oil: oxygen (phenols), sulfur (sulfides, mercaptans), and sometimes nitrogen (amines) (Sorial, 2018, p. 1-17).

Their quantity is small in the low-boiling part of oil, they are mainly concentrated in fractions boiling above 350C (fuel oil). Azeotropic distillation also belongs to distillation methods. Mixtures of two mutually soluble liquids are called azeotropic, the boiling point of which is either lower than the boiling point of the low-boiling component, or higher than the boiling point of the high-boiling component (Gou, 2020, p. 1-13).

The essence of azeotropic distillation is as follows: a third, water-soluble, non-hydrocarbon component is added to the mixture being separated. In the presence of this substance, the initial components of the azeotrope change their vapor pressures differently when heated, i.e. have different boiling points. If the third component is close in volatility to the mixture being separated, then it forms an azeotrope with one of the components of the mixture (azeotropic distillation) (Guo, 2019, p. 297).

If the volatility of the third component is low, then it remains in the liquid phase and retains one of the substances being separated (extractive distillation). Molecular diffusion is used to separate the highest boiling substances. The method is based on the difference in molecular weights and depends on the relative evaporation rate of the molecules (Gupte, 2020, p. 127-149).

Adsorption methods. The essence of the method is that individual components of the mixture can be selectively and sequentially sorbed on one or another sorbent (absorber) and thus separated from the overall mixture. Then these components are desorbed unchanged in the form of individual fractions and can be studied separately. Desorption occurs in the reverse order of adsorption.

Chromatography. Adsorption chromatography is the process of separating substances on solid adsorbents by color. There are the following types of chromatographic analysis methods: gas-adsorption, liquid-adsorption, gas-liquid. Gas-adsorption chromatography is used to analyze gases and is based on the adsorption of gas components of a mixture on solid absorbers. Liquid adsorption chromatography is a method for separating liquid mixtures using solid adsorbents (silica gel).

Absorption. The essence of the method lies in the volumetric absorption of gases or vapors by a liquid (absorbent), leading to the formation of a solution. Absorption is used to separate gases. To isolate a component, a solution of the absorbent (absorbent) with the gas dissolved in it is sent for desorption.

Extraction is the process of extracting individual components from the feedstock by treating it with a selectively acting solvent (extractant). As a result of extraction, two immiscible phases are formed: an extract and a raffinate. The extract contains a solvent and highly soluble raw material components.

ISSN: 2707-1146
e-ISSN: 2709-4189

Crystallization. This method is used to separate substances with high melting points, i.e. solid hydrocarbons soluble in oil. Crystallization is carried out by freezing from solutions in a suitable solvent. The solvent must also be a precipitant for the substances separated by crystallization. It must dissolve high-melting components significantly worse than low-melting ones.

Determination and sampling of aromatic hydrocarbons in petroleum products by sulfation method

To separate aromatic hydrocarbons from oil products, let's consider the sulfation method. A rapid method for determining the amount of aromatic hydrocarbons in gasoline fractions is the sulfation method. When a hydrocarbon mixture is affected by sulfuric acid (concentration below 100 %) in the absence of alkenes, only arenes react with the formation of aromatic monosulfonic acids (Gupte, 2016, p. 363-378).

In this case, polysulfonic acids are not formed. In order to determine the content of arenes, the reaction of distillates with sulfuric acid is carried out at room temperature. Usually, the structure of the sulfuric acid formed corresponds to the structure of the arene. But in some cases, the reaction is complex and is accompanied by isomerization, disproportionation; this is mainly observed in polyalkylated arenes.

Arenes of petroleum distillates form water-soluble sulfuric acids. The solubility of sulfuric acids in petroleum distillates depends on the molecular weight and structure of the acids. Sulfuric acids formed from short side-chain arenes contained in the low-boiling fractions are insoluble in the distillate. They are all monobasic acids, and the difference between their properties is determined only by the structure of the side chain (Haleyur, 2019, p. 49-58).

Distillate-soluble sulfuric acids are derivatives of polycyclic arenes with fairly long side chains; dissolved in sulfuric acid, they completely pass into an acid layer where sulfuric acid is abundant. Sulfuric acids from long side-chain arenes are readily soluble in distillation. They can be isolated from treated distillates by adding ethyl alcohol.

The concentration of sulfuric acid is an important factor. A weak acid practically does not react with arenes. Fuming acid, on the other hand, can cause side reactions such as oxidation. In addition, fuming acid also affects other hydrocarbons – it causes dehydrogenation of six-membered naphthenes and reacts with isoparaffins.

Necessary equipment and materials: sulfator; sheath with drawn end; 98 % sulfuric acid; 10 % sodium hydroxide solution; calcium chloride; 1-2 l capacity separating funnel; apparatus for distillation with heated water vapor; concentrated sulfuric acid (monohydrate).

Work performance methodology. A well-washed and dried sulfator is fixed vertically on a tripod, the tap is closed, and using a funnel with an elongated end, 98 % sulfuric acid is carefully poured up to the "0" mark (so as not to spread along the walls of the sulfator). The acid is allowed to drain from the walls and its level is accurately recorded on the sulfator scale (Johnsen, 2007, p. 533-543).

After that, in the same way, 10 ml of the studied gasoline fraction is poured into the sulfator and its level is fixed. The sulfator is tightly closed with a plug, removed from the tripod, and the contents are carefully poured into the upper circular part, where it is shaken well for 1 minute, from time to time the tap should be opened a little to release the gases formed. After mixing, the sulfator is installed vertically on a tripod and the mixture should be kept for 1 hour. After this period, the volume of gasoline is recorded. The determination should be repeated twice, and the algebraic average of the results of both experiments is calculated. The volume share of aromatic hydrocarbons in the studied A0 fraction, in %, is found by a. the following formula:

$$A0= (V1-V2)/ 100V1 \quad (2.1)$$

where V1 – the volume of gasoline taken for sulfation; V2- is the volume of gasoline after sulfation. After measuring the volume of gasoline remaining after sulfation, the sulfuric acid gasoline layer is drained and the gasoline is washed in a sulfator with water, then with 10 % sodium hydroxide solution, then again with water until neutral, then dry. Transferred to a test tube and

dehydrated with calcium chloride. Dehydrated gasoline is taken to determine the second aniline point. In order to isolate aromatic hydrocarbons from the oil product, 200 ml of the studied fraction (heavy gasoline) boiling in the range of 150-200 ºC is introduced into the separatory funnel and 400 ml of sulfuric acid is carefully added. It is mixed and shaken in a separatory funnel for 0.5-1 hour. After precipitation, the lower (sulfuric acid) layer is carefully added to a 1.5 L round bottom flask and water (about 300 mL) is carefully added to prevent foaming during distillation. The flask is placed in the superheated steam distillation apparatus and the contents of the flask are exposed to the superheated steam. In this case, the mixture is decomposed by the formation of sulfuric acid and free hydrocarbon, steam distilled and collected in the receiver. The separated hydrocarbons are washed with water and soda solution, dehydrated over calcium chloride, and then collected in a column apparatus.

Determination of aromatic hydrocarbons in petroleum products by the method of aniline point determination

Equipment, reagents and materials: 15 ml test tube; a glass with a capacity of 750-1000 ml made of heat-resistant glass; long-handled thermometer, division degree 0.05; freshly distilled pure aniline (t.); 2 ml pipette; burettes with a graduation of 0.1 ml.

Work performance methodology. Method of equal volumes 2 ml of aniline and the gasoline fraction under study are placed in a clean and dry test bottle, tightly closed with a stopper with a thermometer and a stirrer inserted in it, and attached to a coupling immersed in a water bath. The product and aniline are obtained with 2 ml pipettes or burettes with a graduation of 0.1 ml.

The thermometer is placed so that the mercury ball is at the level of the dividing line between the layers of aniline and the product. The temperature of the water bath is slowly raised and the aniline product is continuously stirred with a stirrer. The temperature of complete mixing of liquids is noted (the solution becomes transparent). The heating is stopped and the water is expected to cool down slowly. When turbidity appears in the test tube, indicating the beginning of phase separation, the solution is stirred again with a stirrer.

At first the blur disappears with stirring, but then comes a moment of non-disappearing blur. The point of aniline is the highest temperature at which the turbidity does not disappear after mixing. The complete mixing and cloud point temperatures should not differ by more than 0.1 °C. Determination of AN is repeated with a new sample of the investigated fraction. In parallel experiments, the discrepancy between AN should not exceed 0.2 ºC (12).

Conclusion

Maximum aniline points method. 2 ml of the studied fraction is placed in a 1.6 ml aniline test bottle and the temperature of complete dissolution is determined as described above. After that, another 0.2 ml of aniline is added to the mixture and the dissolution temperature is set again. It is usually higher than the first case. Aniline is added in increments of 0.2 ml until its decrease is noted after a certain maximum of the dissolution temperature. The maximum AN is recorded; it corresponds to the true value of the test product in aniline.

When there is a sufficient amount of material for each destination, new portions of the oil product and aniline should be taken.

References

1. Syrkin, A. M., Movsumzade, E. M. (2002). *Fundamentals of oil and gas chemistry*. USTU.
2. Ryabov, V. D. (2009). *Chemistry of oil and gas*. FORUM.
3. Virzhichinskaya, S. V., Digurov, N. G., Siyushin, S. A. (2009). *Chemistry and Technology of oil and gas.* FORUM.
4. Ghosal, D., Ghosh, S., Dutta, T. K. (2016). Current state of knowledge in microbial degradation of polycyclic aromatic hydrocarbons. *Microbiol*, 1369.
5. Sorial, G. A., Ghasemi, S., and Bazyari, M. (2018). Treatment technologies for PAH-contaminated sites: a critical review. *Environ. Monit. Assess*, 1-17.

ISSN: 2707-1146
e-ISSN: 2709-4189

6. Gou, Y., Zhao, Q., Yang, S., Qiao, P., Cheng, Y., Song, Y. (2020). Enhanced degradation of polycyclic aromatic hydrocarbons in aged subsurface soil using integrated persulfate oxidation and anoxic biodegradation. *Chem. Eng*., 1-13.
7. Guo, Y., Rene, E. R., Wang, J., and Ma, W. (2019). Biodegradation of polyaromatic hydrocarbons and the influence of environmental factors during the cocomposting of sewage sludge and green forest waste. *Bioresour. Technol*., 297.
8. Gupta, S., and Pathak, B. (2020). *Mycoremediation of polycyclic aromatic hydrocarbons. Abatement of Environmental Pollutants*. Elsevier.
9. Gupte, A., Tripathi, A., Patel, H., Rudakiya, D., and Gupte, S. (2016). Bioremediation of polycyclic aromatic hydrocarbon: a perspective. *Biotechnol,* 363-378.
10. Haleyur, N., Shahsavari, E., Jain, S. S., Koshlaf, E., Ravindran, V. B., Morrison, P. D. (2019). Influence of bioaugmentation and biostimulation on PAH degradation in aged contaminated soils: response and dynamics of the bacterial community. *Environ*., 49-58.
11. Johnsen, A. R., and Karlson, U. (2007). Diffuse PAH contamination of surface soils: environmental occurrence, bioavailability, and microbial degradation. *Appl. Microbiol. Biotechnol.*, 533-543.
12. Analytical equipment for determining the composition of hydrocarbon raw materials and their processed products. www.nordwestlab.ru.

Received: 22.05.2024
Revised: 20.07.2024
Accepted: 03.08.2024
Published: 20.08.2024

ISSN: 2707-1146
e-ISSN: 2709-4189

https://doi.org/10.36719/2707-1146/47/54-58

Irina Vishnepolskaya
Institute for Space Research of Natural Resources
vishnepolira@mail.ru
Eldar Aliyev
Institute for Space Research of Natural Resources
aliyev57@mail.ru
Hagigat Isgandarova
Institute for Space Research of Natural Resources
azerbaycan9195@mail.ru
Kanan Mustafa
Institute for Space Research of Natural Resources
kenan_m66@bk.ru

Chemical Nature of Magnetic Properties of Substances

Abstract

Using the example of the mineral magnetite, which is the main component of magnetic volcanic sand, a quantum-chemical analysis of the nature of paramagnetic properties was carried out using the molecular orbital method. Magnetic properties are among the most important characteristics of substances, and magnetic interaction is one of the fundamental forces in the universe. Understanding the chemical nature of magnetic properties allows not only to effectively use materials with magnetic properties, but also to create new materials with the desired characteristics. The magnetic properties of substances depend on their structure and elemental composition, since each charged particle inside the substance has its own magnetic moment-spin.

Keywords: *chemical, nature, magnetic, properties, substances*

Introduction

In technology, substances are divided into paramagnets, diamagnets, ferromagnets, antiferromagnets and ferrimagnets. Ferrimagnets are the most complex in structure – these are crystalline substances whose magnetic structure is represented by several sublattices with signs of spontaneous magnetic ordering, while each individual part has a non-zero resulting magnetic moment (Kurnikov, 2005, p. 120).

Based on this, the purpose of this work was to study the magnetic nature of magnetic sand from Sakhalin Island. The selected average sample weighing 114 grams was sifted through a large sieve to remove large debris, then separated into magnetic and non-magnetic components in the magnetic field of a strong neodymium magnet. It was found that the magnetic part makes up 93,86 %, the main composition of which is represented by a mixed iron oxide – Fe_3O_4. This chemical compound is also interesting because it has a crystalline structure in the lattice nodes of which iron and oxygen alternate, with divalent and trivalent iron – $FeO \cdot Fe_2O_3$. Thus, one stoichiometric unit of the substance contains 24 % Fe (II), 48 % Fe (III) and 28 % O, that is, almost a quarter of the substance is represented by an atom in an intermediate oxidation state, another quarter – in a lower oxidation state and almost half in a state of a higher oxidation state (Kharlamov, 2003, p. 82-85).

The group of magnetic materials primarily includes elements of the iron triad: iron, cobalt and nickel. The chemical properties of these elements are determined by their position in the periodic table. Atoms of Fe, Co and Ni have two 4s-electrons and 6, 7 and 8 electrons in the 3d-sublevel, respectively. For example, in Fe4s2 3d6, filling the 3d-cells with electrons affects the decrease in oxidation states when moving from Fe to Ni. The maximum oxidation state is +6 for iron, +4 for cobalt and +3 for nickel. Most often, iron exhibits oxidation states of +2 and +3, nickel +2, cobalt +3 in simple compounds and +3- in complex compounds (Went, 1952, p. 194).

Obviously, not all electrons of the unfilled 3d-sublevel participate in valence bonds. Formation of complex compounds is typical for Fe, Co and Ni. Pure metals of the iron family are strong and

ISSN: 2707-1146
e-ISSN: 2709-4189

ductile. The standard electrode potentials for Fe, Co and Ni are -0.441, -0.277 and -0.250 V, respectively. Diluted hydrochloric, sulfuric and nitric acids dissolve these metals, converting them into E2+ ions. When interacting with hydrochloric and sulfuric acids, the metals displace hydrogen, and the reaction with nitric acid proceeds according to the equation (Gutfleisch, 2011, p. 821-842).

$4Fe + 10HNO_3 = 4Fe(NO_3)_2 + NH_4NO_3 + 3H_2O$

More concentrated HNO3 and H2SO4, when heated, oxidize iron to Fe (III) (NO or O2 are released), for example:

$Fe + 4HNO_3 = Fe(NO_3)_3 + NO + 2H_2O$

Very concentrated H2SO4 and HNO3 at room and lower temperatures passivate these metals, forming oxide films on their surface. In alkaline solutions, all three metals are quite corrosion-resistant. They do not react with water under normal conditions, but at red-hot temperatures, iron interacts with water vapor:

$3Fe + 4H_2O = Fe_3O_4 + 4H_2$

At room temperature in air, nickel oxidizes slowly, cobalt and iron faster. When heated, they burn, forming the oxides Fe2O3, CoO and NiO. Iron also forms the oxides FeO, Fe3O4, FeO3 and FeO4. The last two are very unstable. FeO4 is obtained as a solution in CCl4 by extracting the tetroxide by CCl4 extraction from alkaline aqueous solutions formed during the anodic oxidation of iron:

$Fe + 8OH^- - 8\bar{e} = FeO_4 + 4H_2O$

Solutions of FeO4 and CCl4 decompose under normal conditions:

$4FeO_4 = 2Fe_2O_3 + 5O_2$

When Fe2O3 is fused into KOH and KNO3, dark red ferrites (VI) are formed:

$Fe_2O_3 + 4KOH + 3KNO_3 = 2K_2FeO_4 + KNO_2 + 2H_2O$

In terms of their oxidizing capacity, they are superior to such an oxidizing agent as KMnO4 (E = 1.9 V > E = 1.51 V).

Cobalt forms oxides CoO, CoO2 and Co3O4. The most stable of them is CoO. Nickel forms oxides NiO and Ni2O3. Of the hydroxides, E(OH)2 and E(OH)3 are of greatest importance. Co(OH)3 and Fe(OH)3 have some signs of amphotericity (5).

The formulas of such oxides as FeO, CoO and NiO are quite arbitrary, since, as a rule, they have a non-stoichiometric composition. For example, a study of the composition of wustite FeO showed that it has vacancies in the iron sublattice, and its composition should be expressed by the formula $Fe1 - xO$. The composition of wustite under standard conditions is close to $Fe0.95O$. With an increase in the value of X, the picometry density decreases (Robert, 2012, p. 1191-1334).

To maintain electroneutrality, it is necessary that there are two Fe3+ ions in the lattice for each Fe2+ vacancy. These more highly charged ions can be considered as holes, since at a low activation energy, electrons from neighboring Fe2+ ions can move to them, and the position of the Fe3+ ions is not localized. This positive charge diffuses throughout the crystal, which is characteristic of a hole. The same kind of hole semiconductors are $Co1 - xO$, $Ni1 - xO$, etc.

Fe (OH)2 hydroxide is a stronger base than Fe (OH)3, iron (II) salts have a more ionic character than iron (III) salts. The latter are more noticeably hydrolyzed than Fe (II) salts (Smith, 1962, p.25).

Fe (OH)2 is easily oxidized in the cold by atmospheric oxygen:

$4Fe(OH)_2 + 2H_2O + O_2 = 4Fe(OH)_3$

Ni(OH)3 is obtained by the action of strong oxidizing agents on $Ni(OH)_2$*:*

$2Ni(OH)_2 + Cl_2 + 2NaOH = 2Ni(OH)_3 + 2NaCl.$

The interaction of hydrochloric acid with Ni(OH)3 and Fe(OH)3 proceeds as follows:

$Fe(OH)_3 + 3HCl = FeCl_3 + 3H_2O$

$2Ni(OH)_3 + 6HCl = 2NiCl_2 + Cl_2 + 6H_2O$

Nickel (II) salts are green; cobalt (II) salts are blue, and their solutions and crystal hydrates are pink; iron (III) salts are brown. Iron, cobalt and nickel absorb hydrogen, but do not form specific compounds with it (Vladimirovich, 2001, p. 23).

ISSN: 2707-1146
e-ISSN: 2709-4189

Their nitrides are unstable, but when formed on the surface of steel products when saturated with nitrogen in an ammonia atmosphere, they make these products more corrosion-resistant and harder (Abbas, 2015, p. 187-191).

Iron, cobalt and nickel form carbides of the E3C type. Sulfides of the ES type are obtained by the action of ammonium sulfide $(NH_4)_2S$ on salt solutions and by dry means. Iron forms stable cyanides:

$$FeCl_2 + 2KCN = Fe\ (CN)_2 + 2KCl.$$

Fe (CN)3 is obtained in a similar manner. When these cyanides are treated with an excess of KCN, the complex salts potassium hexacyanoferrate (II)K4 [Fe (CN)6] – yellow blood salt and hexacyanoferrate (III)K3 [Fe (CN)6] – red blood salt are obtained. These salts are specific reagents for Fe3+ and Fe2+ ions:

$$4Fe^{3+} + 3\ [Fe\ (CN)_6]^{4-} = Fe_4\ [Fe\ (CN)_6]_3$$
$$3Fe^{2+} + 2\ [Fe\ (CN)_6]^{3-} = Fe_3\ [Fe\ (CN)_6]_2$$

This reaction is very sensitive and is used to detect the Fe3+ ion.

A sensitive reaction to Ni2+ ions is the interaction with dimethylglyoxime (Chugaev's reagent), as a result of which the solution turns bright pink (Kanagesan, 2014, p. 815).

It is known that some substances in a magnetic field become magnetized, i.e. they themselves become sources of a magnetic field. Therefore, the magnetic field in a substance is the result of adding up the fields created by current-carrying conductors (macrocurrents) and a magnetized environment (Meng, 2015, p. 407-411).

The reason for magnetization is that in all substances there are electric currents that close within each atom or molecule (microcurrents or molecular currents). Fig. 3.1 shows a model of molecular currents in a uniformly magnetized magnet and the corresponding surface current.

The existence of microcurrents (molecular currents) in a substance is explained by the fact that each electron rotates around the nucleus at a fairly high speed. Its location and speed at a given moment in time cannot be determined with sufficient accuracy. This means that a rotating electron represents a certain equivalent circular current that has a magnetic moment. To calculate this moment, we assume that the orbit is a circle with radius r, along which the electron moves with a constant speed vo.

The gyromagnetic ratio was determined experimentally in 1915 by Einstein and Haas. In the experiments of Einstein and Haas, an iron rod suspended on a thin elastic thread was placed inside a solenoid (Fig. 3.3). A mirror was attached to the elastic thread, onto which a beam of light was directed. When a direct electric current was passed through the solenoid, a magnetic field was created that magnetized the iron rod. As a result, the rod began to rotate, and the direction of rotation of the rod changed with a change in the current in the solenoid (the magnetic field inside the solenoid). The mirror began to rotate simultaneously with the rod. When the system rotates, the reflected beam shifts along a scale installed to increase sensitivity at a sufficiently large distance. When the mirror is rotated by an angle, the beam deflects by a double angle of 2. The occurrence of rotation during magnetization is called the magnetomechanical effect. The occurrence of the magnetomechanical effect can be explained by the following reasoning. In an unmagnetized rod, the electron orbits have an arbitrary orientation, so their total mechanical angular momentum is 0. When the rod is magnetized, the planes of the molecular currents become parallel, which leads to the occurrence of a total angular momentum.

All substances in nature are magnetic, i.e. they have certain magnetic properties and interact with an external magnetic field in a certain way. The magnetic properties of a substance depend on the magnetic properties of isolated elementary particles, the structure of atoms and molecules, and their groups (12).

The magnetic properties of an atom are mainly determined by the magnetic properties of electrons. The magnetism of other particles is relatively small. Thus, the magnetic moment of an

ISSN: 2707-1146
e-ISSN: 2709-4189

atomic nucleus is approximately a thousand times smaller than the magnetic moment of the electron shell of an atom. The magnetic moment of an electron arises as a result of the electron's orbital motion (orbital moment) and the presence of spin (spin moment). The magnetic moment of a multi-electron atom is the sum of the magnetic moments of all electrons, including both orbital and spin moments. Each electron makes an independent vector contribution to the total magnetic moment of the atom. According to modern concepts of magnetism, the following main types of magnetic states of matter are distinguished: diamagnetism, paramagnetism, ferromagnetism, antiferromagnetism and ferrimagnetism (uncompensated antiferromagnetism). Substances in which these phenomena are manifested are called, respectively: diamagnets, paramagnets, ferromagnets, antiferromagnets and ferrimagnets. The schematic arrangement of the moments of electrons of atoms of substances with different magnetic properties is illustrated in fig. 1.

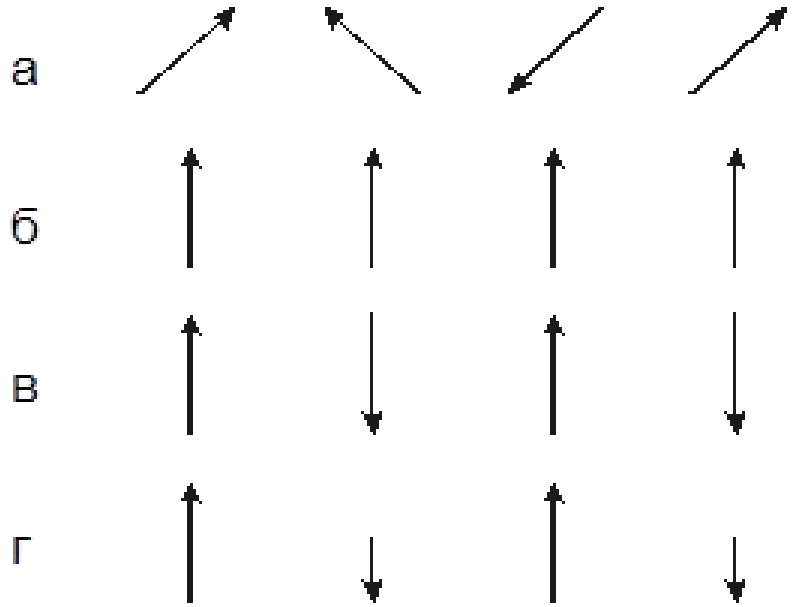

Figure 1. The schematic arrangement of the moments of electrons of atoms of substances

The main magnetic quantities include: magnetization M, A/m, M = k, where k is the magnetic susceptibility, is the magnetic field strength, A/m.

Conclusion

Particularly interesting compounds are the carbonyls of metals of this family. Iron atoms have four free places for electrons in the 3d sublevel and six places in the 4p sublevel. Under a pressure of 107 Pa and at 200 °C, liquid iron pentacarbonyl is quickly formed: Fe + 5CO = Fe (CO)5, in which carbon atoms are electron donors, iron atoms are acceptors of five pairs of electrons. For such an interaction, a rearrangement of electrons in the 3d sublevel is necessary, requiring some activation energy. Nickel atoms can accept only 8 electrons in the same sublevels, so a carbonyl of the composition $Ni(CO)_4$ is formed. At 250 °C, iron carbonyl decomposes, which is used to obtain the purest iron for electrical and radio engineering purposes. Nickel carbonyl decomposes at 200 °C, and cobalt tetracarbonyl is even less stable.

References

1. Kurnikov, Yu. (2005). Magnetic sand: a new look at the prospects for practical use. *Geology and useful minerals of the world ocean* (pp. 111-120).
2. Kharlamov, V. (2003). Unit for obtaining building materials from dumps of mining and processing plants of the KMA. *Bulletin of the Belgorod State Technical University named after V. G. Shukhov*, 3, 82-85.

ISSN: 2707-1146
e-ISSN: 2709-4189

3. Went, J. (1952). Ferroxdure, a class of new permanent magnet materials. *Philips techn. Rev*., 13, 194.
4. Gutfleisch, O. (2011). Magnetic Materials and Devices for the 21st Century: Stronger, Lighter, and More Energy Efficient. *Adv. Mater*., 23, 821-842.
5. Ofitsial'nyy sayt gruppy kompaniy «Severo-Zapadnaya Laboratoriya». http://www.ferrite.ru i.r.
6. Brusentsov, E. A., Minayev, A. M. (2002). *Fundamentals of Physics and Technology of Oxide Semiconductors*. TSTU Publishing House.
7. Robert, C. (2012). Hexagonal ferrites: A review of the synthesis, properties and applications of hexaferrite ceramics. *Progress in Materials Science*, 1191-1334.
8. Smith, J. (1962). Ferrites. Publishing House of Foreign Literature. Vladimirovich K. S. dissertation "Study of the formation of the magnetic structure of hexaferrites with isovalent and non-isovalent substitutions".
9. Abbas, W. I., Ahmad, M., Kanwal, G., Murtaza, I., Ali, M., Azhar Khan, M., Niaz Akhtar, M. Ahmad. (2015). Structural and magnetic behavior of Pr-substituted M-type hexagonal ferrites synthesized by sol-gel autocombustion for a variety of applications. *Journal of Magnetism and Magnetic Materials*, 374, 187-191.
10. Kanagesan, S. (2014). Influence of Zn-Nb on the Magnetic Properties of Barium Hexaferrite. *J. Supercond. Nov. Magn*, 27, 811-815.
11. Meng, P. (2015). Wideband and enhanced microwave absorption performance of doped barium ferrite. JMMM, 407-411.
12. http://msk.edu.ua/

Received: 16.05.2024
Revised: 13.07.2024
Accepted: 09.08.2024
Published: 20.08.2024

ISSN: 2707-1146
e-ISSN: 2709-4189

https://doi.org/10.36719/2707-1146/47/59-73

Cyrus Raza Mirza
University of Hail
crazamirza@gmail.com

The Optimization and Mechanism of Textile Dye Adsorption on the Surface of Pine Sawdust Biomass: Thermodynamic, Isotherm and Kinetic Studies

Abstract

Due to increasing problems of freshwater availability and wastewater treatment and management, there is a dire need to control water pollution. A major portion of wastewater is produced through dye contamination from textile industries. In this study, efforts were made to evaluate the renewable, environment-friendly, and biomass-based adsorbent for the effective removal of dyes from aqueous solution. Pine sawdust biomass samples were subjected to adsorption under different parametric studies to optimize the adsorption process efficiency. The maximum adsorption efficiency was observed around 50-60 % under different working conditions. This study demonstrates that the non-linear versions of the PSO and IPD kinetic models were better than the linear forms from the perspective of the dye adsorption mechanism. Comparably, the nonlinear fitting of the Freundlich model yielded lower χ^2 values and higher R^2 values than the linear fitting. Positive Gibbs free energy values imply that the adsorption is non-spontaneous and thermodynamically unfavorable at the investigated temperatures. The thermodynamic study shows that the adsorption of BBY onto the PSD adsorbent is an exothermic process.

Keywords: *sawdust adsorbent, textile dye, adsorption, linear, nonlinear fitting*

Introduction

Dye-contaminated water is becoming a huge threat to aquatic life survival and freshwater scarcity. Due to the rapid growth of art and fashion trends, there are numerous dyes used at the industrial level in the printing of cloth, from where a huge amount of dye-contaminated wastewater is produced every day (Tkaczyk et al., 2020).

Currently, there is insufficient installed technology for the treatment of such contaminated water which is discharged and mixed with freshwater resources such as lakes, rivers, and sea (Gadir et al., 2020). Treating this kind of wastewater is not an easy task because of the very fine particle size of dyes which cannot be filtered using ordinary membranes and the filtration process (Radjenovic & Sedlak, 2015). Biological process could be a suitable alternative (Grady et al., 2011). but the huge amount of wastewater produced cannot be cleaned every day because of the slow process efficiency of the biological process (Babuponnusami et al., 2023). Chemical processes are efficient processes that can meet the requirement of treating such a significant amount of wastewater (Shannon et al., 2008).

Chemical processes are of many subdivided methods, but the main two categories can be divided into two processes: adsorption and photocatalytic degradation which may be the economical way of treatment at the industrial level (Jo, Prajitno, Zeb, Kim, 2017; Solayman et al., 2023). The photocatalytic process is efficient in terms of cleaning the water from dyes, but it produces a lot of unknown organic free radicals which could perform serval reactions with the other species present in the environment. Free radical accumulation and the production of secondary pollutants are more dangerous for human health and the ecosystem (Zeb et al., 2017; Khan et al., 2023).

So, the adsorption of such dye molecules over the surface of the suitable adsorbent and then their desorption under controlled conditions for their proper disposal off may be the future technology. Another aspect of the absorption of dyes over suitable adsorbent from dye-contaminated industrial effluent could provide the baseline to reuse the wasted dyes (Solayman et al., 2023)

ISSN: 2707-1146
e-ISSN: 2709-4189

There are various types of adsorbents (Shahbaz et al., 2019; Aljohani et al., 2023) in use such as metal oxide, metal nanoparticles, single atoms, bimetallic catalysts, organic-inorganic hybrid (Zeb et al., 2022; Mohan et al., 2023) and several biomass-based renewable and environmentally friendly materials (Hafiza et al., 2023; Siddigi et al., 2022) which may be used as adsorbent material for the effective adsorption of dyes. In biomaterials graphene, graphitic materials, metal-doped graphene, non-metal atom dopes graphene, raw biomass, physical and chemical processed biomass, coal char (Asif et al., 2023; Agarwala, Mulky, 2023). and biochar could be used as an effective material for adsorption (Ravindiran et al., 2023; Hassan et al., 2023; Asif et al., 2024; Khan et al., 2024).

In this study, pine sawdust (PSD) was subjected to the adsorption of Bismarck brown dye from an aqueous solution. Before that many studies have been reported to evaluate the biochar produced after the pyrolysis of organic materials (Zeb et al., 2017; Asif et al., 2023), although this is a good approach there are huge changes during the pyrolysis which depends on the pyrolysis condition and reproducibility is very difficult. Here in this study raw biomass showed an adsorption efficiency of 50-60 % under various industrial relevant conditions, showing potential for commercialization for industrial wastewater treatment.

Material and Methodology

Pretreatment of Pine Sawdust

Pine sawdust (PSD) was used which was obtained from the nearby carpenter shop. The acquired sawdust was washed and then grounded using a disk mill, to get a 40-mesh size (420 μm) using an automatic sieve shaker. This type of particle size is well applied for adsorption purposes. The ground sawdust was left overnight in the oven at 80 ˚C using a muffle furnace and the moisture contents were removed completely (Nair et al., 2023).

Preparation of BBY Stock Solution

The 1000 mg/L BBY dye concentration stock solution was produced by dissolving 1 gm analytical grade (Merck) for both dyes in 1000 mL of deionized water. Solutions with lower dye concentrations were made through appropriate dilutions using deionized water (Eq. 1).

$$C_1V_1 = C_2V_2 \qquad \text{(Eq. 1)}$$

Whereas C1 and C_2 are the concentrations of stock and the required solutions respectively. V_1 and V_2 are the volumes of stock solution and the required volume for dilution respectively.

Preparation of 0.1M HCl and 0.1M NaOH solution

In this experiment, the adsorbent is tested on different pH to check the adsorbent's performance for adsorption. The experiments are conducted on different acid and base pH adjusted through acid and base solutions that are HCl and NaOH respectively. For this 0.1 molar HCl and 0.1 molar NaOH were prepared by adding 0.8 mL HCl into 100 mL of deionized water providing 0.1 molar of HCl. Likewise, 0.1 molar of NaOH solutions were obtained by adding 400 mg of analytical grade NaOH in 100 mL of deionized water (Tabish).

Batch adsorption experiments

The Kinetics batch experiment was conducted with 0.05 g of *PSD* (raw, physically modified, and chemically modified) by attachment with 50 mL of BBY and MG dye (concentration ranging from 25-150 mg/L) in Erlenmeyer flasks. The pH was not adjusted initially, and it was 6.5 for MG and for BBY adjusted at 4 pH which was determined by the PHS-38W microprocessor pH/temperature meter. After preparation, the solution was kept in a shaking incubator (wise cube WIS-20) and was used to shake the flask for 120 mins at 150 rpm at room temperature which is 30 ^{o}C ± 1. The adsorbed dye was then measured through a T80+UV/VIS Spectrometer at 616 nm for MG and 416 for BBY. The values were then used to estimate the concentrations. All the experiments were carried out in triplicates. The amount of dye adsorbed on the adsorbent was calculated using the following equation (Kalengyo et al., 2023):

Percentage removal was calculated by the following equation:

$$S(\%) = \left(\frac{Ci - Cf}{C_i}\right) \times 100 \qquad \text{(Eq. 2)}$$

ISSN: 2707-1146
e-ISSN: 2709-4189

Where S % is the removal percentage, C_i and C_f were the initial and final concentrations (mg L^{-1}).

$$qe = \left(C_i - C_f\right) \frac{V}{M} \quad \text{(Eq. 3)}$$

Here q_e is the equilibrium concentration of dye (mg g^{-1}), C_i and C_f are the initial and final dye concentrations (mg L^{-1}), V is the solution volume (L) used and M is the adsorbent mass (g).

Equilibrium time

The experiment was conducted at several contact times, 5 to 300 mins, and the sample was taken twenty minutes apart each (i.e. 2, 5, 10, 20, 40, 60, 80, 100, and 120), while other parameters were kept constant. Equilibrium time is important to find out the time in which the equilibrium for adsorption occurs.

Initial dye concentration

The experiment was carried out by varying the dye concentration, *i.e.*, from 25 mg L^{-1} to 200 mg L^{-1} 25, 50, 70, 100, 150, and 200 mg/L.

Particle size

Experiments were carried out to study the impact of different particle sizes, ranging from mesh size 40 to 140 (400 to 105 μm) i.e. 40, 60, 80, 100, 120, and 140.

Adsorbent dose

The adsorbent dose experiment was examined from 25 mg to 300 mg, *i.e.* 25, 50, 75, 100, 150, 200, 250, and 300 mg L^{-1}.

Temperature

Adsorption capacities of adsorbents were studied at different temperatures ranging from 30 to 50 °C, at the intervals of 5 °C i.e. 30, 40, and 50 °C.

pH

pH is the most influential parameter in adsorption studies as it affects the adsorption capacity of the adsorbent. The experiment was carried out at different pH values pH 4-10 for BBY.

Kinetic Analysis

Adsorption capacity was determined as follows:

$$q_t = \frac{(C_o - C_t)}{m} * V \quad (1)$$

Where V (mL) denotes the volume of the dye solution and m (g) represents the mass of the adsorbent. C_o represents the initial concentration (mg/L) of the dye and C_t is the concentration of dye at time t (mg/L).

The percentage removal is calculated using Equation 2.

$$\%\ Removal = \frac{(C_o - C_t)}{C_o} * 100 \quad (2)$$

PSO and Intraparticle diffusion models

Linear and non-linear kinetic models curve fitting and error function analysis

The adsorption kinetics modeling explains the rate of adsorption of adsorbate from liquid to solid phase. RB5 dynamical adsorption data was fitted into linear and non-linear equations of pseudo-second order (PSO) (Equations 4 and 5) and intra-particle diffusion (IPD) (Equation 6) models. The possible adsorption process for RB5 once in contact with TSB adsorbent in solution: (i) movement of RB5 molecules from bulk solution to the external boundary film adjacent to TSB adsorbent; attachment of dye molecules to the binding sites of TSB which is a rapid step and may include the physical adsorption or chemical (whether weak or strong) and/or both; (iii) RB5 diffusivity into the inner sites of TSB.

PSO kinetic model (Ho et al., 1999) assumes adsorption over the complete contact time range expressed in differential form as under;

$$\frac{dq_t}{dt} = k_2(q_e - q_t)^2 \quad (3)$$

Integrating Eq. 24 while applying boundary conditions (t=0, q_t =0, t=t and $q_e = q_t$)

$$q_t = \frac{q_e^2 k_2 t}{q_e k_2 t + 1} \quad (4)$$

ISSN: 2707-1146
e-ISSN: 2709-4189

Linearizing

$$\frac{t}{q_t} = \frac{1}{K_2 q_e^2} + \frac{1}{q_e} t \quad (5)$$

Intraparticle diffusion (IPD) model

$$q_t = K_{pi} t^{\frac{1}{2}} + C_i \quad (6)$$

The calculated values of kinetic model parameters, constants, and R^2 are listed in Table 2.

Isotherms analysis

To analyze the underlying adsorption mechanism, linear and nonlinear forms of Langmuir and Freundlich isotherms were fitted to equilibrium data collected by varying initial concentrations of BBY dye, i.e., 25, 50, 75, 100, and 200 mg/L.

Langmuir determines the chemisorptive interaction between adsorbate and adsorbent and indicates monolayer formation. Both linear (equation 3) and non-linear (equation 4) forms are given as:

$$\frac{1}{q_e} = \left(\frac{1}{K_L q_{max}}\right)\frac{1}{C_e} + \frac{1}{q_{max}} \quad (7)$$

$$q_e = \frac{q_{max} K_L C_e}{1 + K_L C_e} \quad (8)$$

Where C_e represents the concentration at equilibrium ($mg.g^{-1}$), q_{max} denotes the maximum adsorption capacity of adsorbent ($mg.g^{-1}$) and K_L stands for the Langmuir constant, which is used to determine the maximum energy of adsorption related to the area occupied by the adsorbent.

The Freundlich isotherm was used to verify the nature of the multilayer adsorption of MG as well as the heterogeneity of the studied adsorbent. Linear (Equation 5) and non-linear (Equation 6) forms of this model are generally expressed as.

$$ln q_e = ln K_F + \frac{1}{n} ln C_e \quad (9)$$

$$q_e = K_F C_e^{1/n} \quad (10)$$

Where, C_e represents the concentration at equilibrium, while q_e denotes the amount of adsorbate per unit mass of the adsorbent ($mg.g^{-1}$), K_F is the adsorption capacity and 1/n indicates the adsorption intensity. The error distribution, i.e., Chi-square (χ^2) error, between experimental and linear model predicted values q_{cal} were minimized by reducing the error function using solver add-in Microsoft Excel.

The chi-square (χ^2) error function equation used for this function is as follows:

$$\chi^2 = \sum_{i=1}^{n} \frac{(q_{e\,exp} - q_{e\,cal})^2}{q_{e\,cal}} \quad (11)$$

$$\text{Coefficient of determination } (R^2) = \frac{\Sigma\left(q_{t_{cal}} - \bar{q}_{t_{exp}}\right)^2}{\Sigma\left(q_{t_{cal}} - \bar{q}_{t_{exp}}\right)^2 + \Sigma\left(q_{t_{cal}} - q_{t_{exp}}\right)^2} \quad (12)$$

Thermodynamic Analysis

The BBY adsorption by PSD with temperature was explained further by thermodynamic parameters, i.e., changes in Gibbs free energy (*ΔG*), entropy (*ΔS*), and enthalpy (*ΔH*). To dimensionless equilibrium constant (K_d, L/g), K_d was multiplied by solution (water) density ($\rho w \approx$ 1000 g/mL) (Tran). The above thermodynamic parameters were estimated using slop and intercept of Van't Hoff plot ($\ln K_d$ versus l/T) with the help of the following equations:

$$l_n\, K_d(\rho_w) = \frac{q_e}{c_e} \quad (13)$$

$$ln\, K_d(\rho_w) = \frac{\Delta S}{R} - \frac{\Delta H}{RT} \quad (14)$$

$$\Delta G = \Delta H - T\Delta S \quad (15)$$

ISSN: 2707-1146
e-ISSN: 2709-4189

Results and Discussion

Discussion on Dye Removal by PSD Adsorbent

The set of graphs provides a thorough examination of the PSD adsorbent's dye removal effectiveness and adsorption capacity across a range of circumstances, including pH, contact time, initial dye concentration, and adsorbent dose

Effect of Contact Time

Graph (a) shows the connection between adsorption capacity and dye removal effectiveness as well as contact time. Within the first 50 minutes, the dye clearance % rises quickly, suggesting a high initial adsorption rate since there are plenty of active sites. Following this time frame, the removal rate steadily declines and reaches about 35 % after 300 minutes. With most of the active sites occupied, this plateau indicates that the adsorption process has nearly reached equilibrium. Similarly, the adsorption capacity exhibits an initial rapid increase before stabilizing at approximately 15 mg/g, indicating the equilibrium state. A slow approach to equilibrium is typical of many adsorbents, after the initial fast adsorption phase (Yadav et al., 2022).

Effect of Initial Dye Concentration

Different starting dye concentrations (C_0) have an impact on dye removal and adsorption capability, as shown in Graph (b). As the concentration rises, the clearance % first rises and peaks at around 70 mg/L before slightly declining. This pattern implies that larger dye concentrations at first give a stronger mass transfer driving force, which improves adsorption. Saturation of the active sites causes the clearance efficiency to decrease at very high concentrations. As dye concentrations rise, on the other hand, the adsorption capacity increases and reaches a maximum of about 55 mg/g at 200 mg/L. While the effectiveness in terms of % removal declines at high dye concentrations, this suggests that the PSD adsorbent has a large capacity for dye uptake (Gupta et al., 2011).

(a) Effect of Adsorbent Dose

The adsorbent dose has an impact on both adsorption capacity and dye removal, as seen in graph (c). At 5 g/L, the dye removal percentage reaches a maximum of around 55% as it increases with the adsorbent dosage. The increased availability of adsorption sites with larger adsorbent amounts is the cause of this growth. Nevertheless, there is a trend toward a diminishing adsorption capacity (mg/g) as the adsorbent dose increases. According to this inverse connection, while the amount of adsorbents increases overall dye removal, the amount of dye absorbed per unit weight of the adsorbent decreases. This is probably because higher dosages of adsorbent particles aggregate, which reduces the surface area available for adsorption (Kara et al., 2007).

(b) Effect of pH

Graph (d) shows how pH affects adsorption capacity and the effectiveness of color removal. When the pH rises from acidic to alkaline, both metrics exhibit a noticeable decrease. The pH of 2 yields the maximum dye removal % and adsorption capacity, suggesting that acidic environments are the optimal conditions for the PSD adsorbent to function. Surface charges of the adsorbent and the dye's ionization state are responsible for the decline in performance at higher pH values. Adsorption efficiency is increased in acidic environments by the positive charge on the adsorbent surface, which increases the attraction of negatively charged dye molecules. Reduced dye adsorption occurs in alkaline settings due to electrostatic repulsion caused by the negative charge on the adsorbent surface (Yadav et al., 2022).

The PSD adsorbent exhibits efficacious dye removal properties, whereby its performance is contingent upon contact time, initial dye concentration, adsorbent dosage, and pH. Lower pH, higher starting dye concentration, proper contact time, and regulated adsorbent dosage are ideal for achieving maximum dye removal and adsorption capacity. These results offer insightful information for maximizing PSD adsorbent utilization in real-world dye removal applications.

ISSN: 2707-1146
e-ISSN: 2709-4189

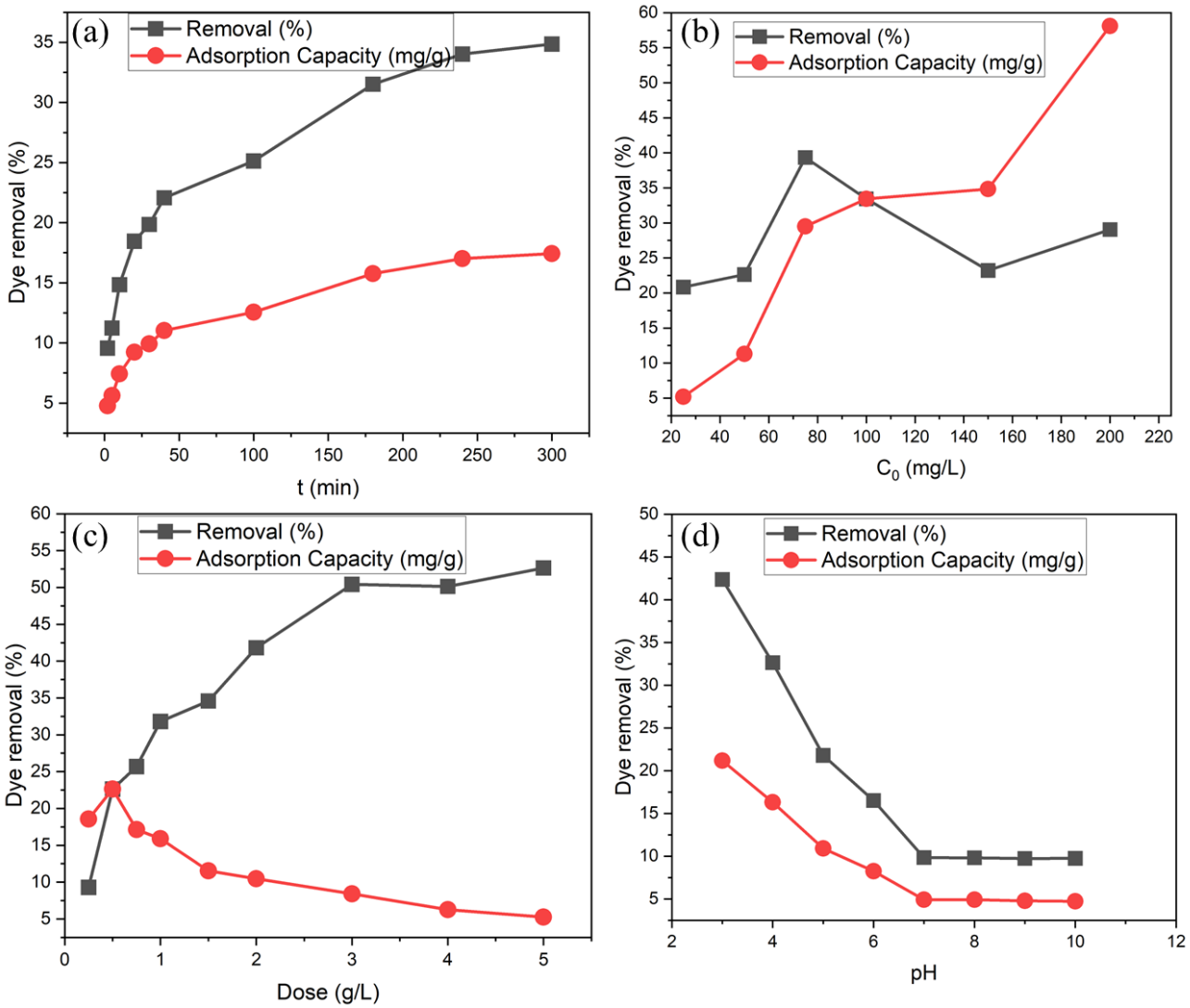

Figure 1. Evaluation of the prepared bio-adsorbent with BBY dye under different parameters (a) Effect of time (b) Effect of initial dye concentration (c) Effect of dose of the adsorbent (d) Effect of pH

Effect of Temperature

Figure 2. (a) illustrates the connection between temperature (T), adsorption capacity, and dye removal efficiency. At 30 °C, the proportion of dye removed climbs to around 22 %; at 50 °C, it reaches about 30 %. This temperature increase is consistent. This pattern suggests that higher temperatures improve the adsorption process. This is probably because the dye molecules have more kinetic energy, which makes it easier for them to move and interact with the adsorbent surface. Higher temperatures may also cause the adsorbent's pores to enlarge, creating more active sites for the adsorption of dyes. Additionally, there is a positive association between temperature and adsorption capacity, which increases from roughly 15 mg/g at 30 °C to 25 mg/g at 50 °C. This improvement shows that the adsorption process is endothermic, meaning that the dye molecules and PSD adsorbent interact better at higher temperatures (Senthil Kumar et al., 2014).

Effect of Particle Size

Particle size has an impact on both adsorption capacity and dye removal efficiency, as shown in Figure 2. (b). The dye removal percentage increases dramatically as the particle size drops from 400 µm to 100 µm, reaching a maximum of approximately 55 % at the smallest particle size. The reason behind this increase is that smaller particles have more surface area available for adsorption, which means that there are more active sites for dye molecules to stick.

ISSN: 2707-1146
e-ISSN: 2709-4189

In a similar vein, the adsorption capacity increases marginally as the particle size decreases, going from roughly 15 mg/g at 400 µm to about 25 mg/g at 100 µm. By improving the surface area-to-volume ratio, the adsorbent may absorb more dye molecules per unit weight because of the reduced particle size.

Higher temperatures and smaller particle sizes show enhanced dye removal efficiency and adsorption capacity of the PSD adsorbent. While the rise in smaller particle sizes emphasizes the significance of surface area in adsorption efficiency, the temperature-dependent increase in adsorption points to an endothermic adsorption process. These results highlight the possibility of maximizing PSD adsorbent performance in dye removal applications by improving adsorption conditions, such as temperature control and particle size reduction (Kara et al., 2007).

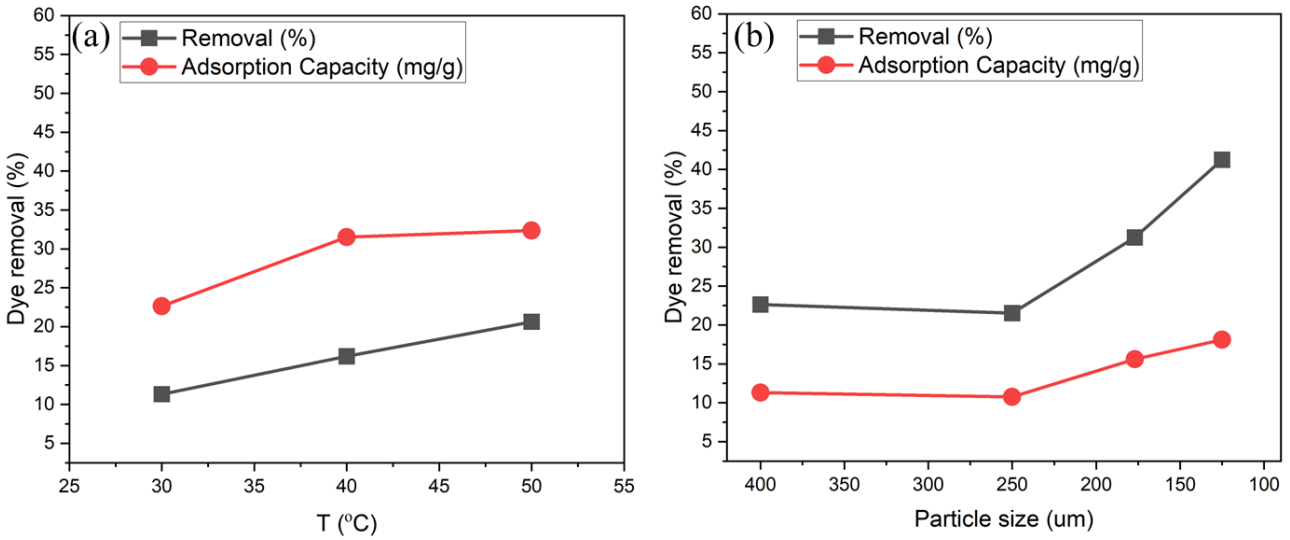

Figure 2. Evaluation of the prepared bio-adsorbent with BBY dye under different parameters (a) Effect of Temperature(b) Effect of particle size of the PSD adsorbent

Kinetic models

Intraparticle diffusion (IPD) and pseudo-second order (PSO) kinetic models were employed to kinetics experimental data for the investigation of the rate of adsorption of dye on the adsorbent. These models have been extensively applied to explain the adsorption mechanism of pollutants from wastewater. The IPD model accounts for the pore and surface diffusion mechanisms which are greatly influenced by the porosity and the nature of the contaminant transport pathway.

In this (equation 6), I (mg g^{-1}) is the intercept and k_{diff} is the intraparticle diffusion rate constant (mg g^{-1} $min^{-1/2}$). The values of q_t were found to be linearly correlated with values of $t^{1/2}$ and the rate constant k_p was directly evaluated from the slope of the regression line. The linear form of the Pseudo second-order kinetic model can be expressed as:

Here in this equation, 5 q_e represents the equilibrium amount of the adsorbate absorbed in mg/g of the absorbent, q_t denotes the quantity adsorbed in mg/g of the adsorbate at time t, and k2 (min^{-1}) stands for the pseudo-second-order rate constant. IPD and PSO order plots are shown in figure 3a and 3b respectively. It can be seen from figure 3a that at a dye concentration of 30 mg/L, the model showed a poor fit with a correlation coefficient (R^2) of 0.6899. In contrast, at 100 mg/L, a higher R^2 value of 0.9048 was observed, suggesting a more significant role of intraparticle diffusion in the adsorption mechanism at higher dye concentrations similarly figure 3b depicts that when dye concentration is 30 mg/L, the Pseudo-second order model exhibited a R^2 value of 0.9741, and at 100 mg/L, R^2 value of 0.9809. Compared to the intraparticle diffusion model, the Pseudo-second order model demonstrates a better fit for the adsorption process at both concentrations, indicating that the adsorption kinetics are more accurately described by the Pseudo-second order mode.

ISSN: 2707-1146
e-ISSN: 2709-4189

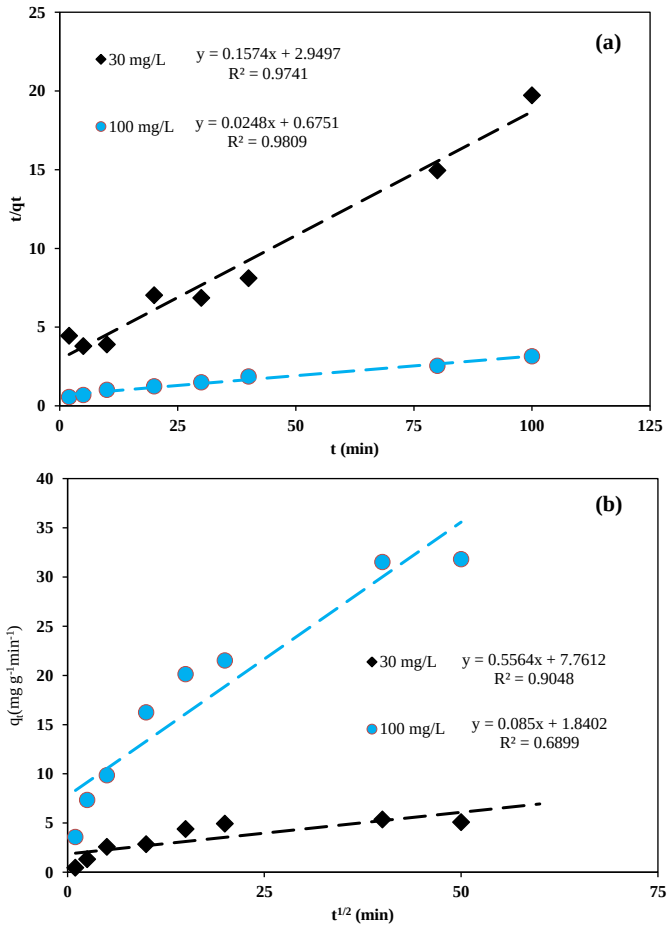

Figure 3. Kinetic modeling of the dye adsorption on PSD adsorbent (a) intraparticle diffusion model and (b) Pseudo second order kinetic model. Comparison of linear and Nonlinear fitting of IPD and PSO model

The kinetic parameters for BBY adsorption onto PSD adsorbent biomass were analyzed using both linear and nonlinear fitting for the PSO and IPD models. The linearized form of both models is provided in equation 6 and equation 5. The nonlinear form of the PSO model is as follows:

When using the linear form, experimental adsorption kinetics must be converted to a linear format for linear least-squares regression to estimate model parameters. It has been noted that changing non-linear equations to linear forms can unintentionally change how errors are measured in the model parameters. The kinetic parameters obtained from the linear and nonlinear fittings (figures 4a and 4b) are listed in table 1. It can be seen from table 1 that nonlinear fitting for the PSO model indicated better agreement with experimental data, evidenced by its lower χ^2 value (0.31 and 0.83 for 30 and 100 mg/L) and higher accuracy in qe cal. values compared to linear fitting. The R^2 values were high for both fittings, indicating good fitness. In the case of the IPD model, nonlinear fitting demonstrated higher performance with higher R^2 values (0.9877 and 0.9802 for 30 and 100 mg/L respectively) and lower χ^2 values, suggesting that nonlinear fitting provides a more accurate representation of the BBY removal kinetics. Thus, nonlinear fitting is the better approach for both models based on these parameters. As evidenced by figure 4 and figure 5, q nonlinear is closer to q experimental these results demonstrate that non-linear fitting will be more appropriate than linear fitting to obtain the kinetic parameters.

ISSN: 2707-1146
e-ISSN: 2709-4189

Table 1.
Non-linear kinetic model parameters for BBY adsorption onto PSD adsorbent biomass

Kinetic models	Parameters	Initial MG Dye Concentration (mg/L)			
		Linear analysis		Nonlinear analysis	
		30	100	30	100
	$q_{e\ exp}$ (mg/g)	5.35	31.38	5.35	31.38
PSO	$q_{e\ cal}$ (mg/g)	6.35	40.32	6.62	39.77
	k_2 (g/m.min)	0.008	0.0009	0.0075	0.0009
	χ^2	0.32	0.89	0.31	0.83
	R^2	0.9741	0.9809		
IPD	I	1.84	7.76	2	5.2
	K_{diff} (mg/g.min)	0.04	0.28	0.2	2.33
	χ^2	11.62	50.42	10.64	10.33
	R^2	0.6899	0.9048	0.9877	0.9802

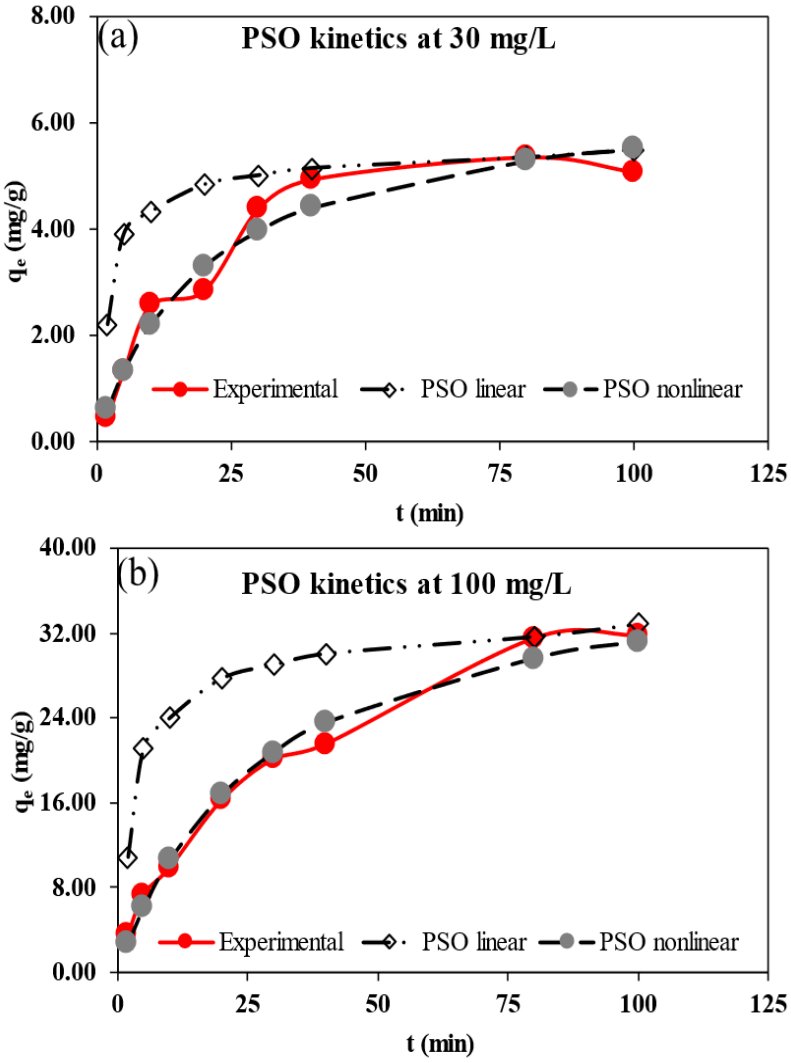

Figure 4. Comparison of predicted linear and nonlinear fitting of PSO under different initial dye concentrations, with experimental values (a) PSO kinetic modeling of 30 mg/L and (b) PSO kinetic modeling at 100 mg/L

ISSN: 2707-1146
e-ISSN: 2709-4189

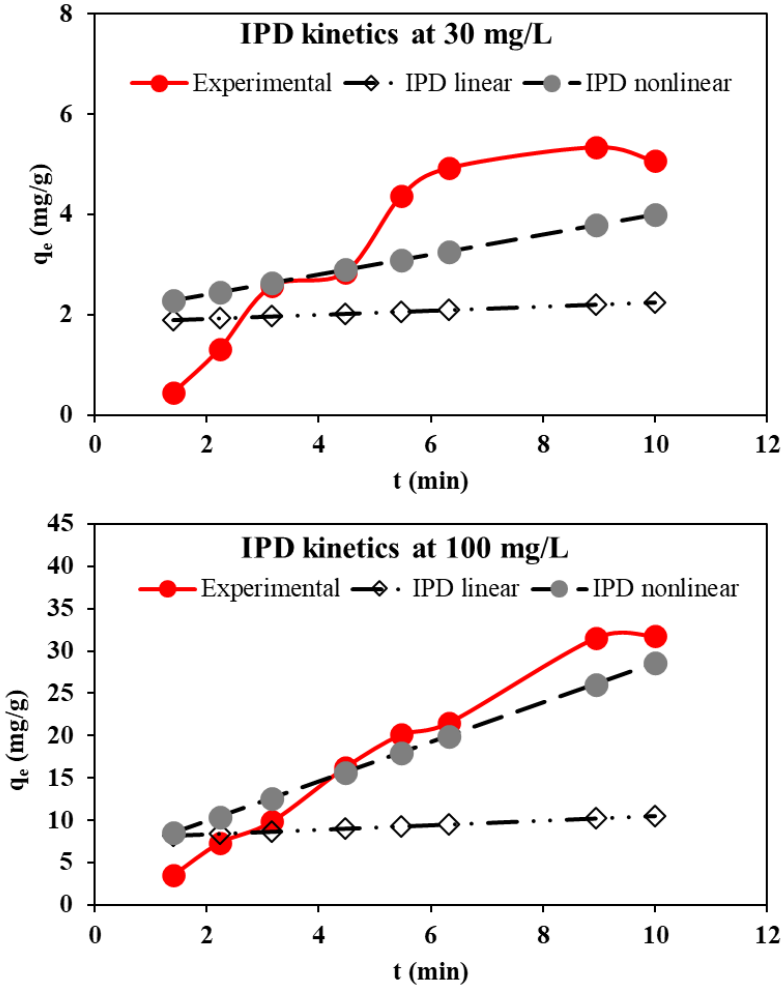

Figure 5. Comparison of predicted linear and nonlinear fitting of IPD under different initial dye concentrations, with experimental values (a) IPD kinetic modeling of 30 mg/L and (b) IPD kinetic modeling at 100 mg/L

Thermodynamic Analysis

The effect of different temperatures on adsorbent was studied and removal of BBY is displayed in Figure. 6a. The temperature varied at 300, 305, 310, 315 320, and 325. K The removal of BBY onto the adsorbent did not increase with a rise in temperature from the thermodynamic parameters including a change in enthalpy (ΔH) and entropy (ΔS) were computed using the Van't Hoff equation as under:

$$lnK_d = \frac{\Delta S}{R} - \frac{\Delta H}{RT} \quad (4)$$

Change in Gibbs free energy (ΔG) was determined using the equation. 16.

$$\Delta G = \Delta H - T\Delta S \quad (5)$$

The thermodynamic parameters in Table 2 for BBY elimination using BD adsorbent give information about the nature of the adsorption process. The negative values of enthalpy change (ΔH) and entropy change (ΔS) indicate that the process is exothermic. The positive Gibbs free energy change (ΔG) values indicate non-spontaneous adsorption at increased temperatures. The positive ΔG values also indicate that the adsorption process is not thermodynamically favorable under the current conditions.

ISSN: 2707-1146
e-ISSN: 2709-4189

Table 2.
Thermodynamics parameters calculated for BBY adsorption onto PSD adsorbent

ΔH (kJ/mol)	ΔS (J/mol.k)	ΔG (kJ/mol)			R^2
		303.15 K	313.15 K	323.15 K	
35.69	0.17	-14.34	-15.17	-15.99	0.9972

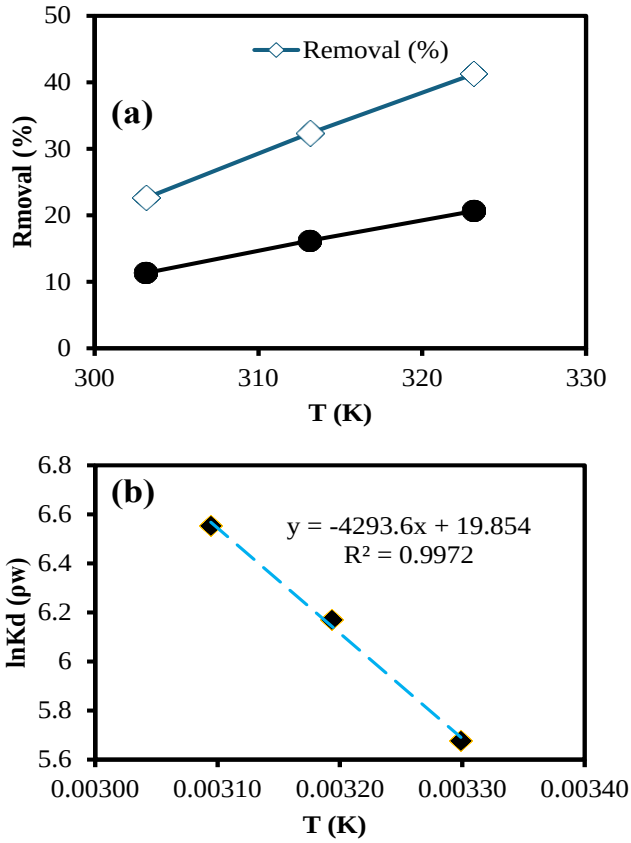

Figure 6. Effect of process parameters on BBY dye adsorption
a) Temperature, b) Van't Hoff plot

Adsorption Isotherms

By fitting the adsorption experimental data to different isotherm models, we can identify the most appropriate model that describes the adsorption behavior and gain an understanding of the driving forces behind the process. The equilibrium data of BBY on adsorbent was evaluated using linearized and nonlinearized forms of Freundlich and Langmuir isotherm models**.**

Here, KL represents the Langmuir isotherm constant, Ce is the adsorbate's concentration (mg/L), and Linear (equation 8) and non-linear forms of Freundlich isotherm are generally expressed as.

Here K_F is the adsorption capacity (mg/g), adsorption intensity is represented by 1/n, qe is the adsorbate uptake (mg/g), and Ce is the equilibrium concentration of dye in solution (mg/L). Table 3 displays all estimated parameters of linear and nonlinear fitting of Langmuir and Freundlich Isotherm models. The Langmuir model's linear fitting had a higher R^2 value of 0.9373 but a lower χ^2 value compared to its nonlinear fitting, which had a lower R^2 of 0.6154 but a higher χ^2 value. Similarly, the Freundlich model's nonlinear fitting showed higher R^2 and lower χ^2 values than its linear fitting. Overall, nonlinear fitting produced a better fit for both models.

ISSN: 2707-1146
e-ISSN: 2709-4189

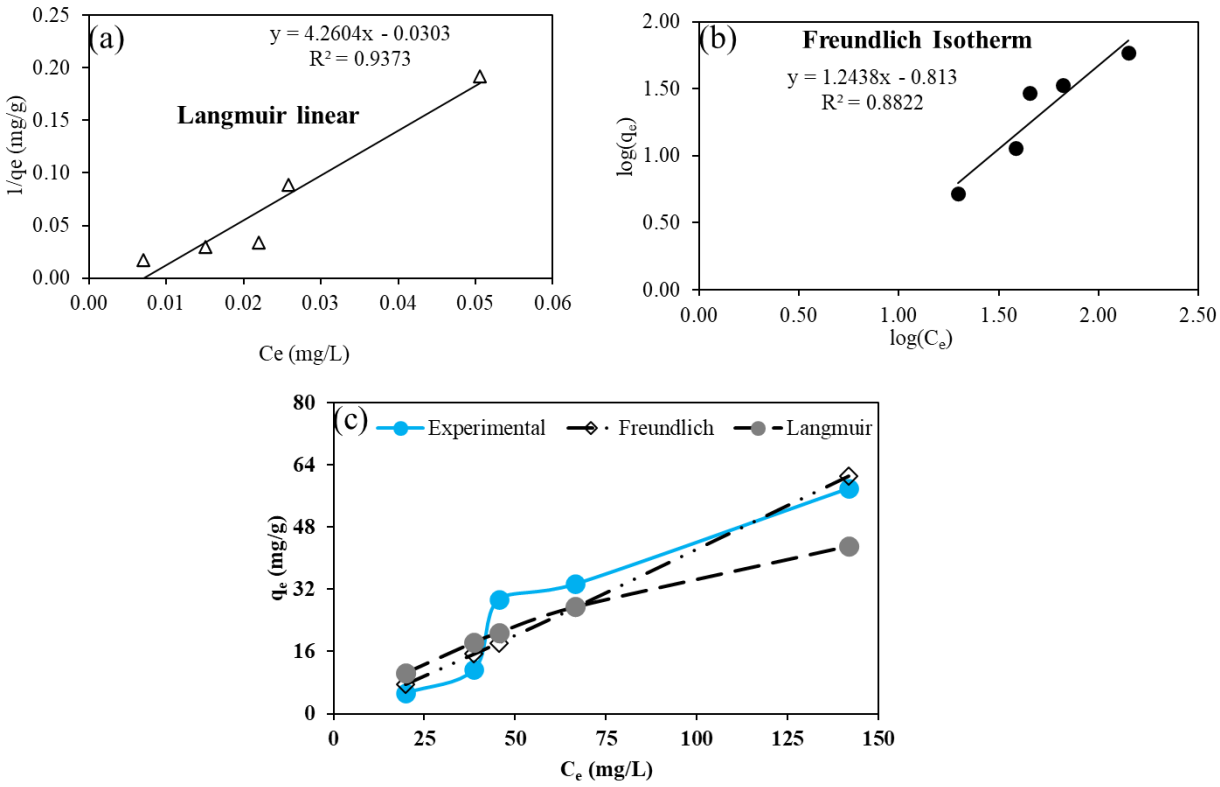

Figure 7. Isotherms Analysis (a) Langmuir isotherm analysis (b) Freundlich isotherm analysis (c) comparison of Experimental and Freundlich and Langmuir isotherm

Table 3.
Comparison of Isotherm Parameters: Linear vs. Non-Linear Fitting for the removal BBY dye by PSD biomass adsorbent

Isotherms	Parameters	Values	
	q_{exp}	58.12	
		Linear fitting	**Non-linear fitting**
Langmuir	q_{max}	33.00	86.62
	R^2	0.9373	0.6154
	X^2	72.21	25.82
Freundlich	K_f	6.50	0.31
	n	0.80	0.94
	R^2	0.88	0.9005
	X^2	17.32	7.98

Conclusion

This study aimed to explore the adsorption behavior of BBY dye on the surface of a powdered PSD biomass sample. Dye adsorption efficiency was optimized through the treatment of PSD biomass with dye solution under different working parameters such as equilibrium time, initial dye concentration, adsorbent dose, temperature, pH, and under different particle sizes of the biomass sample. The maximum dye adsorption efficiency was found to be around 50-60 % under different working conditions. This study shows that the non-linear forms of the PSO and IPD kinetic models were superior to the linear forms. Similarly, the Freundlich model's nonlinear fitting showed higher R^2 and lower χ^2 values than its linear fitting. The thermodynamic analysis reveals that the adsorption of BBY onto the PSD adsorbent is an exothermic process, and the positive Gibbs free

energy values suggest that the adsorption is non-spontaneous and thermodynamically unfavorable at the studied temperatures.

References

1. Tkaczyk, A., Mitrowska, K., Posyniak, A. (2020). Synthetic organic dyes as contaminants of the aquatic environment and their implications for ecosystems. *A review, Science of the total environment*, 717, 137222.
2. Gadir, M., Drechsel, P., Jiménez Cisneros, B., Kim, Y., Pramanik, A., Mehta, P., Olaniyan, O. (2020). Global and regional potential of wastewater as a water, nutrient and energy source. *Natural resources forum*, 40-51. Wiley Online Library.
3. Radjenovic, J., Sedlak, D. L. (2015). Challenges and opportunities for electrochemical processes as next-generation technologies for the treatment of contaminated water. *Environmental science & technology*, 49, 11292-11302.
4. Grady, C. L., Daigger, G. T., Love, N. G., Filipe, C. D. (2011). *Biological wastewater treatment.* CRC press.
5. Babuponnusami, A., Sinha, S., Ashokan, H., Paul, M. V., Hariharan, S. P., Arun, J., Gopinath, K., Le, Q. H., Pugazhendhi, A. (2023). Advanced oxidation process (AOP) combined biological process for wastewater treatment. A review on advancements, feasibility and practicability of combined techniques. *Environmental research*, 116944.
6. Shannon, M. A., Bohn, P. W., Elimelech, M., Georgiadis, J. G., Marinas, B. J., Mayes, A. M. (2008). Science and technology for water purification in the coming decades. *Nature*, 452, 301-310.
7. Jo, H., Prajitno, H., Zeb, H., Kim, J. (2017). Upgrading low-boiling-fraction fast pyrolysis bio-oil using supercritical alcohol: Understanding alcohol participation, chemical composition, and energy efficiency. *Energy Conversion and Management*, 148, 197-209.
8. Solayman, H., Hossen, M. A., Abd Aziz, A., Yahya, N. Y., Leong, K. H., Sim, L. C., Monir, M. U. K. (2023). Performance evaluation of dye wastewater treatment technologies: A review. *Journal of Environmental Chemical Engineering*, 11, 109610.
9. Zeb, H., Park, J., Riaz, A., Ryu, C., Kim, J. (2017). High-yield bio-oil production from macroalgae (Saccharina japonica) in supercritical ethanol and its combustion behavior. *Chemical Engineering Journal*, 327, 79-90.
10. Khan, M. D., Singh, A., Khan, M. Z., Tabraiz, S., Sheikh, J. (2023). Current perspectives, recent advancements, and efficiencies of various dye-containing wastewater treatment technologies. *Journal of Water Process Engineering*, 53, 103579.
11. Shahbaz, M., Yusup, S., Al-Ansari, T., Inayat, A., Inayat, M., Zeb, H., Alnarabiji, M. S. (2019). Characterization and reactivity study of coal bottom ash for utilization in biomass gasification as an adsorbent/catalyst for cleaner fuel production. *Energy & Fuels*, 33, 11318-11327.
12. Aljohani, M. M., Al-Gahtani, S. D., Alshareef, M., El-Desouky, M. G., El-Bindary, A. A., El-Metwaly, N. M., El-Bindary, M. A. (2023). Highly efficient adsorption and removal bio-staining dye from industrial wastewater onto mesoporous Ag-MOFs. *Process Safety and Environmental Protection*, 172, 395-407.
13. Zeb, H., & Riaz, A. (2022). Introduction to Organic–Inorganic Nanohybrids. *In hybrid Nanomaterials: Biomedical, Environmental and Energy Applications* (p. 1-27). Springer.
14. Mohan, K., Rajan, D. K., Rajarajeswaran, J., Divya, D., Ganesan, A. R. (2023). Recent trends on chitosan based hybrid materials for wastewater treatment. *A review, Current Opinion in Environmental Science & Health*, 33, 100473.
15. Hafiza, S., Riaz, A., Arshad, Z., Zahra, S. T., Akhtar, J., Kanwal, S., Zeb, H., Kim, J. (2023). Effect of pyrolysis temperature on the physiochemical properties of biochars produced from raw and fermented rice husks. *Korean Journal of Chemical Engineering*, 40, 1986-1992.
16. Siddigi, M. H., Liu, X. M., Hussain, M. A., Gureshi, T., Tabish, A. N., Lateef, H. U., Zeb, H., Faroog, M., Nawaz, S. (2022). Evaluation of physiochemical, thermal and kinetic properties of wheat straw by demineralising with leaching reagents for energy applications. *Energy*, 238.

17. Asif, M., Hussain, M. A., Riaz, A., Mujahid, R., Akram, M. S., Haider, B., Kanwal, S., Zeb, H. (2023). A physical coal cleaning approach for clean energy production from low grade Lakhra coal of Pakistan using diester table. *Journal of the Pakistan Institute of Chemical Engineers,* 51.
18. Agarwala, R., Mulky, L. (2023). Adsorption of dyes from wastewater: A comprehensive review. *ChemBioEng Reviews*, 10, 326-335.
19. Ravindiran, G., Sundaram, H., Rajendran, E. M., Ramasamy, S., Nabil, A. Z., Ahmed, B. (2023). Removal of azo dyes from synthetic wastewater using biochar derived from sewage sludge to prevent groundwater contamination. *Urban Climate*, 49, 101502.
20. Hassan, A. M. M., Asif, M., Al-Mansur, M. A., Uddin, M. R., Alsufyani, S. J., Yasmin, F., Khandaker, M. U. (2023). Characterization of municipal solid waste for effective utilization as an alternative source for clean energy production. J*ournal of Radiation Research and Applied Sciences,* 16.
21. Asif, M., Shafiq, M., Imtiaz, F., Ahmed, S., Alazba, A. A., Hussain, H. N., Butt, F. N., Zainab, S. A., Khan, M. K., Bilal, M. (2024). Photocatalytic Degradation of Methyl Orange from Aqueous Solution Using ZnO by Response Surface Methodology. *Topics in Catalysis*, 1-9.
22. Khan, M. S., Asif, M. I., Asif, M., Khan, M. R., Mustafa, G., Adeel, M. (2024). Nanomaterials for the Catalytic Degradation and Detection of Microplastics. *A Review, Topics in Catalysis*, 1-18.
23. Zeb, H., Choi, J., Kim, Y., Kim, J. (2017). A new role of supercritical ethanol in macroalgae liquefaction (Saccharina japonica): Understanding ethanol participation, yield, and energy efficiency. *Energy,* 118, 116-126.
24. Asif, M., Bibi, S. S., Ahmed, S., Irshad, M., Hussain, M. S., Zeb, H., Khan, M. K., Kim, J. (2023). Recent advances in green hydrogen production, storage and commercial-scale use via catalytic ammonia cracking. *Chemical Engineering Journal*.
25. Nair, V. K., Selvaraju, K., Samuchiwal, S., Naaz, F., Malik, A., Ghosh, P. (2023). Phycoremediation of synthetic dyes laden textile wastewater and recovery of bio-based pigments from residual biomass: an approach towards sustainable wastewater management, *Processes,* 11, 1793.
26. Tabish, A. N., Kazmi, M., Hussain, M. A., Farhat, I., Irfan, M., Zeb, H., Rafique, U., Ali, H., Saddigi, M. H., Akram, M. S. Biomass waste valorization by acidic and basic leaching process for thermochemical applications. *Waste and Biomass Valorization*, 1-11.
27. Kalengyo, R. B., Ibrahim, M. G., Fujii, M., Nasr, M. (2023). Utilizing orange peel waste biomass in textile wastewater treatment and its recyclability for dual biogas and biochar production: a techno-economic sustainable approach. *Biomass Conversion and Biorefinery,* 1-14.
28. Ho, Y. S., McKay, G. (1999). Pseudo-second order model for sorption processes. *Process Biochemistry,* 34, 451-465.
29. Tran, H. N. (2022). Improper estimation of thermodynamic parameters in adsorption studies with distribution coefficient KD (qe/C e) or Freundlich constant (KF): Considerations from the derivation of dimensionless thermodynamic equilibrium constant and suggestions. *Adsorption Science & Technology*.
30. Yadav, B. S., Dasgupta, S. (2022). Effect of time, pH, and temperature on kinetics for adsorption of methyl orange dye into the modified nitrate intercalated MgAl LDH adsorbent. *Inorganic Chemistry Communications*, 137.
31. Gupta, V. K., Jain, R., Nayak, A., Agarwal, S., Shrivastava, M. (2011). Removal of the hazardous dye − Tartrazine by photodegradation on titanium dioxide surface. *Materials science and engineering: C*, 31, 1062-1067.
32. Kara, S., Aydiner, C., Demirbas, E., Kobya, M., Dizge, N. (2007). Modeling the effects of adsorbent dose and particle size on the adsorption of reactive textile dyes by fly ash. *Desalination,* 212, 282-293.

ISSN: 2707-1146
e-ISSN: 2709-4189

33. Senthil Kumar, P., Fernand, P. S. A., Ahmed, R. T., Srinath, R., Priyadharshini, M., Vignesh, A., Thanjiappan, A. (2014). Effect of temperature on the adsorption of methylene blue dye onto sulfuric acid–treated orange peel. Chemical Engineering Communications, 201, pp. 1526-1547.

Received: 01.05.2024
Revised: 11.07.2024
Accepted: 30.07.2024
Published: 20.08.2024

ISSN: 2707-1146
e-ISSN: 2709-4189

BIOLOGICAL SCIENCES AND AGRARIAN SCIENCES

https://doi.org/10.36719/2707-1146/47/74-78

Elza Hasanli
Azerbaijan State Agricultural University
elza.gasanly@mail.ru

Causes Degradation of Summer Pastures and Ways to Solve Them

Abstract

Degradation of lands (and pastures) is the deterioration of the properties, fertility and productivity of lands as a result of economic activity. Summer pastures are usually represented by cereals and cereal-wormwood types. The vegetation of summer pastures develops more slowly than on spring pastures and reaches its maximum development in the early summer. Summer pastures are most productive and their feed is more nutritious in the first half of summer (May-June). By mid-summer, the vegetation on the pastures dries up and in the second half of summer, cattle use the dried feed mass to a large extent. The productivity of summer pastures is usually high and averages 3.1 c/ha of dry matter, or 1.8 c/ha of feed units (Dobrovolsky, 1997, p. 313-321). Summer pastures in the mountainous areas and winter pastures in the plains ofAzerbaijan are rich in biodiversity. Summer mountain pastures are complex coupled ecological and human systems. They provide vital forage for livestock during summer, and their traditional use is decisive for the maintenance of biodiversity, ecosystem services, and open landscapes, which benefit local populations and tourists.

Keywords: *efficiency increase, grazing rate, biodiversity, degradation, erosion, flooding, resalinization*

Introduction

Pastures are divided into spring, autumn, summer, winter, and distant pastures. Pastures are an important economic driver for many countries and define local culture.

Livestock productivity strongly depends on the productivity of pastures and, in general, on perennial forage grasses. Affects and carries risks: heat waves, spring frosts, floods, mudflows, etc. (Balamirzoyev, 2008, p. 15). Desertification of lands, in particular pastures, is an acute problem in our republic. The destruction of pastures is the main consequence of changing environmental conditions and irrational human economic activities. It manifests itself in the loss of valuable forage plant species from the grass stand and their replacement by weeds, inedible and annual species.

Pasture degradation is a decrease in the level of plant diversity in pastures, the disappearance of beneficial flora and the appearance of thorny and poisonous plants that are not edible for livestock. As a result, pastures become unsuitable for agricultural use (Bogolyubov, 2013, p. 5-10). Animal grazing has a strong impact on pastures – on their soil and plant cover, water regime and microclimate, fauna and microflora.

If pastures are used incorrectly, valuable plants are eaten away and replaced by poorly eaten grasses, low-growing animals, and low-yielding plants. This leads to a deterioration in the quality of the grass stand.

As a result of free (unregulated) grazing of soil by animals, soil compaction increases, its water-air regime is disrupted, and microbiological activity decreases.

First of all, excessive grazing of animals and an increase in livestock numbers. Shepherds use the same pastures every year for grazing, which is why the plants cannot recover by the next year, and this, naturally, leads to their complete destruction (Ogarkov, 2019, p. 59). Camel thorns and harmala, unsuitable for food, begin to take their place. An increase in livestock numbers leads to increased pressure on pastures. Let's say you previously grazed 20 sheep in a certain area, then, after a few years, the flock grows, and you already graze 100 sheep in this area.

Currently, for example, our pasture loads are 4-5 times higher than normal. The next factor is anthropogenic. Thisis human extraction of mineral resources, the organization of various expeditions, the continuous movement of vehicles to deposits, the construction of facilities, which also leads to a decrease in pasture areas (Volkov, 2016, p. 57-56).

Despite the fact that summer and winter pastures are of great fodder importance in the development of animal husbandry, those pastures have been grazed almost unsystematically for a long time, and poor attention is paid to improvement works. Currently, excessive herds of cattle and sheep are kept in the pastures. This causes trampling of pastures and erosion processes on the slopes. Therefore, the vegetation groups of the grasslands are gradually changing. Instead of valuable fodder plants, plants of less importance for fodder begin to develop.

It is necessary to implement a number of cultural-technical, agrotechnical and reclamation measures in order to adapt the productivity of natural fodder areas to the potential opportunities of the area, to meet the demand for livestock feed. Taking into account the exceptional role of pastures and meadows in the development of animal husbandry, in order to ensure their preservation and increase in productivity, they should be constantly cared for, and less productive areas should be improved and managed continuously. Surface improvement should be carried out in all pasture areas to improve the forage quality and productivity of pastures. Thanks to such a measure, on the one hand, valuable fodder grasses are preserved in the pasture, and on the other hand, the botanical composition of the pasture is enriched with valuable fodder plants.

The system of surface improvement measures includes measures such as fertilizing, harrowing the soil surface, fighting poisonous and harmful plants, cleaning the pasture from stones, leveling the field and sowing valuable grass seeds on the surface of the grass cover.

As a result of the application of fertilizers, the productivity of each hectare of pastures can be increased by 40-50 %.

One of the important measures in the improvement of pastures is cleaning the pasture from stones and unnecessary residues. At this time, it is necessary to collect the stones in the pastures or pour them into ditches and ravines, cover them with soil as much as possible and sprinkle grass seeds. On eroded steep slopes, it is necessary to collect the stones in rows 5-10 meters apart from each other in the direction of the width of the slope and sow grass seeds in the areas between the rows. Such a measure prevents the process of erosion and increases the utilization ratio of the lands under pasture. As a result of the implementation of such measures in pastures, productivity can be increased by 1-1.5 centners. Wet and swampy areas can also be found in the grasslands of our republic. Such areas occur both in summer and in winter pastures located in the Kura-Araz plain. It is necessary to dry up and make it useful by carrying out melioration measures in these areas. Due to such dried areas, the forage area can be expanded, albeit in a small amount.

Substantial improvement

Substantial improvement is one of the most important measures in pastures for effective use of pasture lands, increasing productivity, and meeting livestock feed requirements. Substantial improvement is being done on less productive degraded grasslands.

During major improvement, the natural turf layer is completely plowed and seeds of valuable forage plants are sown. Sowing in winter pastures should be carried out in the fall under conditions of irrigation and irrigation.

During the fundamental improvement of the pastures, special attention should be paid to the preparation of the soil for sowing. Cultivation systems designed according to soil-climate conditions and terrain should be used in soil preparation (Poluektov, 2009).

In ground improvement, sowing a mixture of seeds of not one but several perennial grasses and semi-shrub grasses works best. When using one or more grass mixtures, in addition to receiving a high-quality fodder product, the use of the pasture is long-term. The sowing of grass mixtures has a ositive effect on the development of the grass cover at the same level and on the improvement of the agrochemical properties of the soil. Mixed sowing also plays a positive role in the prevention of the erosion process in pasture lands.

Improvement of pastures and meadows

The process of desertification in ecological terms is one of the reasons for the loss of biodiversity, loss of biomass and productivity, and in socio-economic terms this process is the main reason and mechanism for the loss of fertile lands, generates economic and political instability in the affected regions, leads to a drop in income and living standards of the population, a decrease in the number of jobs, which ultimately leads to migration of the population. The 'silent death' of vast grasslands threatens the climate, food and the well-being of billions: The degradation of the planet's vast, often vast, natural grasslands and other rangelands through overuse, misuse, climate change and loss of biodiversity poses a serious threat to human food security and the well-being or survival of billions of people (Dobrovolsky, 2002, p. 656).

Pasture degradation manifests itself in various forms, including reduced soil fertility, erosion, salinization and soil compaction. This leads to serious consequences such as drought, changes in precipitation and loss of biodiversity.

Summer mountain pastures are complex systems in which the human and ecological dimensions are closely linked. Composed of a mosaic of grazed ecosystems that forms a functional agricultural management entity, they are managed by human actors (eg herders, farmers, and park managers) within an environment made up of the geographical context, economic opportunities, and social network (Khitrov, 1998, p. 20-26).

In many places, sheep farming is the main source of income. However, uncontrolled livestock grazing, caused by the influence of climate change, leads to active soil degradation and desertification, every year of pastures in the Greater Caucasus. According to experts, the unsystematic exploitation of summer pastures led to the fact that after 50 years they simply disappeared. There are several direct and indirect drivers of land degradation. Main factors land degradation in summer pasture unsustainable agricultural practices, expanding agricultural production on vulnerable and marginal lands, inadequate maintenance of irrigation and drainage networks, overgrazing of pastures, and land conversion, urbanization and extractive industries.

Timely action to halt, reduce and prevent land degradation makes proven economic sense and will lead to, among other things, improved food and water security, increased employment, improved gender equality, significant contributions to climate change adaptation and mitigation, and the prevention of conflict and migration. The main factors of land degradation are unsustainable land use, including over-cultivation on mountain slopes, water and wind erosion, excessivegrazing and mining operations (Gerasimova, Karavayeva, 2000, p. 356).

First of all, you need to use pastures correctly. Use the so-called driven method. That is, graze cattle in one area for three or four days, then move to another, so that the cattle do not eat the roots of the plants. This way the first area will have time to recover. Pastures, meadows, forests are overloaded with herds of animals. It should be noted that the development of numerous farmers and other farms engaged in animal husbandry is mainly accompanied by the uncontrolled and excessive exploitation of pastures, rural meadows, forest lands and reserves belonging to the state land fund. According to experts, by developing animal husbandry in the country in more advanced ways, productivity can be increased, protection of summer and winter pastures and hayfields can be strengthened, the efficiency of their use can be increased, and biodiversity can be preserved. Since 2004, the "State Program on effective use of summer and winter pastures and hayfields and prevention of desertification in Azerbaijan" has been approved. It is also noted here that the structure of the fodder necessary to ensure the development of animal husbandry in the country does not comply with the norms, and the predominance of natural fodder in its composition leads to overloading of pastures and meadows, as well as forests with herds of animals. This, in turn, leads to the degradation of foothill slopes, water-retaining forest areas, the intensification of destructive floods, and the gradual depletion of underground and surface water resources. As it is known, pastures and meadows are state-owned land in Azerbaijan. However, due to the fact that the users of these areas do not take the necessary measures to restore soil fertility from time to time and do not follow agrotechnical rules in their operation, as well as do not fully comply with the requirements

of existing standards and regulations in the field of soil protection, soil erosion, salinization, man-made exposure to violations, etc. things happen (Zalibekov, 2010).

Conclusion

When people talk about using pastures, people communicate meaning constructed within social interaction and interaction with the environment The results of this study suggest that past practices and value systems play an important role in people's descriptive comments about today's land use system (Dobrovolsky, 2002). On the one hand, the Soviet the practice of "pasture management", which involved temporary overuse resources, but also their possible restoration in as a result of the introduction of large factors of production, shaped the point of view of people in terms of domination over nature. On the other hand, assigning responsibility for pastures on specialists only strengthened the opinion of local users that they are powerless to directly influence for resources. Consequently, many of them preferred remain simple observers, with their own indicators and approaches to assessing the quality of pastures. The subsequent separation of local livestock farmers from pastures was reinforced by a system that limited its criteria for assessing the quality of work to reproductive standards and physical condition of animals.

To solve problems related to degradation, you must follow this point:

1. Integrate climate change mitigation and adaptation strategies into sustainable rangeland management plans to increase carbon sequestration and storage while enhancing the resilience of pastoral and pastoral communities.
2. Avoid or reduce rangeland conversion and other land-use changes that reduce the diversity and multifunctionality of rangelands, particularly on indigenous and community lands.
3. Adopt and support pastoral policies and practices that help mitigate the impacts of climate change, overgrazing, soil erosion, invasive species, drought and wildfires.
4. Promote policies that support participatory processes and responsive management and governance systems to improve the services that rangelands and pastoralists provide to societies (Sulin, 2015, p. 320).

For the rapid restoration of degraded mountain forage lands and increasing soil fertility, it is of great importance to create a species structure of grass with a powerful root system of loose-bush grasses and leguminous grasses, which contribute to the creation of a fine-clumped soil structure and the ecological sustainability of agroecosystems.Therefore, the development and creation of a seeder for targeted seeding of grass mixtures in solving the problem that has arisen is relevant The quality of the livestock was and is an indicator of successful work and, therefore, successful use of pastures. This point of view is also reflected in today's approach to quality, which accepts the reduced number of livestock in as an indicator of pasture richness. The primacy of livestock quality over pasture quality in people's consciousness is also associated with the new meaning that is attributed to live stock today (12).

References

1. Dobrovolsky, G. V. (1997). The quiet crisis of the planet. *Bulletin of the Russian Academy of Sciences*, 4, 313-321.
2. Balamirzoyev, M. A. (2008). *The potential of soil resources in ensuring food security of the Republic of Dagestan*. Caspian Institute of Biological Resources DNC RAS.
3. Bogolyubov, S. A. (2013). Combination of public and private ways of regulating land management. *Agrarian and land law*, 5(101), 4-10.
4. Ogarkov, A. P. (2019). Remarks on the draft federal law "On land-device". *Land management, cadastre and land monitoring*, 4(171), 89.
5. Volkov, S. N. (2016). Land resources as a key factor in ensuring food security and the main measures for organizing their rational use. Moscow Economic Journal, 4, 57-67.
6. Poluektov, E. V. (2009). *Soil science: A course of lectures*.
7. Dobrovolsky, G. V. (2002). *Degradation and protection of soils*. Publishing House of Moscow State University.

8. Khitrov, N. B. (1998). Degradation of soil and soil cover: concepts and approaches to obtaining estimates. *Anthropogenic degradation of soil cover and measures to prevent it: Tez. dokl. Vseros. conf*. (Vol. 1, pp. 20-26). Moscow.
9. Gerasimova, M. I., Karavayeva, N. A., Targulyan, V. O. (2000). Soil degradation: methodology and mapping capabilities. *Soil science*, 3, 358.
10. Zalibekov, Z. G. (2010). *Soils of Dagestan*. Institution of the Russian Academy of Sciences, the Caspian Institute of Biology resources of the DNC RAS.
11. Sulin, M. A., Shishov, D. A. (2015). *Fundamentals of land relations and land management: Textbook.* Pro-spect of science.
12. Land Code of the Russian Federation of October 25, 2001. (2002). LLC "VTTRAM".

Received: 18.05.2024
Revised: 21.07.2024
Accepted: 05.08.2024
Published: 20.08.2024

CONTENTS

MEDICINE AND PHARMACEUTICAL SCIENCES

CHEMISTRY

BIOLOGICAL SCIENCES AND AGRARIAN SCIENCES

Signed: 14.08.2024
Online publication: 20.08.2024
Format: 60/84, 1/8
Stock issuance: 10 p.s.
Order: 787

It has been published on https://aem.az
Adress: Baku city, Matbuat Avenue, 529,
"Azerbaijan" Publishing House, 6th floor.
Phone: +994 50 209 59 68
+994 55 209 59 68
+994 12 510 63 99
e-mail: info@aem.az